Optimising Technical Aspects of Lung Radiotherapy Treatment Planning

A thesis submitted to the University of Manchester for the degree of Doctor of Clinical Science in the Faculty of Biology Medicine and Health

2022

Zoe C. Walker

School of Medical Sciences

Table of Contents

Word Count: 26032

List of Figures

List of Tables

1 Abstract

Purpose

To assess technical aspects of lung radiotherapy planning that could be optimised for treatment and develop ways of using them to improve the planning process in a clinical setting, with a particular focus on robust optimisation.

Methods

An assessment of auto-contouring using DLCExpert was made for organs at risk (OARs) on lung computed-tomography (CT) scans. A comparison of 3D and 4D CT tumour outlining for lung radiotherapy was conducted for 29 lung tumours. A dosimetric analysis was carried out for 20 of the patients by re-optimising the 4D outlined plans to a new 3D planning target volume (PTV). 3D and 4D robust optimisation methods using the treatment planning system RayStation were compared to a margin-based planning approach for 14 patients with lung cancer receiving stereotactic ablative radiotherapy (SABR). Doses to the gross tumour volume (GTV) across breathing phases and OAR doses were compared. A method of extracting breathing traces from a lung 4D cone-beam CT (4DCBCT) was also developed and tested. A thorax phantom was programmed with breathing traces and used to measure doses for robustly-optimised plans.

Results

The analysis for lung contouring using DLCExpert showed excellent agreement for lungs and heart with comparable values to the literature. The tumour outlining study showed that GTV_{4D} and PTV_{4D} were significantly smaller ($p<0.05$) than their respective 3D volumes. 4D plans produced lower OARs doses that were statistically significant ($p<0.05$) for heart (average), cord (1cc) and lungs (volumes ≥10Gy and ≥5Gy). The 3D robust optimisation produced plans that were comparable to the margin-based plans with doses for lung (volume ≥20Gy) found to be significantly lower ($p<0.05$). 4D robust optimisation using GTV D99 doses from the clinical plan gave higher OAR doses than the margin-based plans. 4D optimisation using the PTV prescription gave similar OAR doses to the margin-based plans with a statistically significantly lower dose to 0.5cc of normal lung ($p<0.05$). Some GTV doses had less variance over the phases than for the margin-based plans. The method of extracting traces was better than a centroid method for 4DCT but was not adequate for 4DCBCT.

Conclusions

4DCT outlining allows for smaller PTVs and reduces OAR doses. Auto-contouring may provide a time-saving benefit. Robust optimisation can produce plans with less GTV variance over the breathing phase and some lower doses to OARs using certain methods.

2 Declaration

No portion of the work referred to in the thesis has been submitted in support of an application for another degree or qualification of this or any other university or other institute of learning.

3 Copyright Statement

i. The author of this thesis (including any appendices and/or schedules to this thesis) owns certain copyright or related rights in it (the "Copyright") and s/he has given the University of Manchester certain rights to use such Copyright, including for administrative purposes.

ii. Copies of this thesis, either in full or in extracts and whether in hard or electronic copy, may be made only in accordance with the Copyright, Designs and Patents Act 1988 (as amended) and regulations issued under it or, where appropriate, in accordance with licensing agreements which the University has from time to time. This page must form part of any such copies made.

iii. The ownership of certain Copyright, patents, designs, trademarks and other intellectual property (the "Intellectual Property") and any reproductions of copyright works in the thesis, for example graphs and tables ("Reproductions"), which may be described in this thesis, may not be owned by the author and may be owned by third parties. Such Intellectual Property and Reproductions cannot and must not be made available for use without the prior written permission of the owner(s) of the relevant Intellectual Property and/or Reproductions.

iv. Further information on the conditions under which disclosure, publication and commercialisation of this thesis, the Copyright and any Intellectual Property and/or Reproductions described in it may take place is available in the University IP Policy (see http://documents.manchester.ac.uk/DocuInfo.aspx?DocID=24420), in any relevant Thesis restriction declarations deposited in the University Library, the University Library's regulations (see http://www.library.manchester.ac.uk/about/regulations/) and in the University's policy on Presentation of Theses.

4 Dedication and Acknowledgements

I would like to thank Jane Rogers and Robert Chuter for their help and guidance during my project work. I am also very grateful to everybody who has given up their time to produce outlines or plans.

I dedicate this thesis to my husband, Simon, for his amazing support throughout HSST.

5 Preface

The author works as a state registered Senior Clinical Scientist at University Hospitals Coventry and Warwickshire NHS Trust specialising in radiotherapy imaging. The author completes small research studies as part of their work which has resulted in conference presentations or posters. Larger research projects have also been completed as part of an MPhys and MSc as detailed below.

MSc in Medical Physics dissertation: *The effect on pass rates of gamma index tests on clinical fluence map displacements*

MPhys: *Detecting small Kuiper Belt Objects*

6 Journal Format

This thesis is presented in journal format as the main areas of the work could logically be divided into sections which are related and are being prepared for journal submission. This also allows the work to be published and to add to the research in this area. Each chapter has an individual reference list with references from other sections provided at the end of the thesis. The thesis contains 4 papers which are all linked by the theme of lung radiotherapy planning. Papers 1, 2 and 4 are in publishable format with the intention of publishing in the near future. Paper 1 has been presented as an oral presentation at the Mirada User Group Meeting 2020. Paper 2 has been presented as a poster at the UK Imaging and Oncology Congress (UKIO 2020). Paper 4 has been presented as an oral presentation at UKIO 2020, the Medical Physics and Engineering Conference 2020 and the European RayStation User Group Meeting 2020. Paper 1 has an additional section on lung contouring which is part of the thesis work but will be removed for publication. The papers included are listed below.

Paper 1- Different Approaches to Measuring the Effectiveness of Deep Learning Contouring Implementation in Clinical Settings

Paper 2- Evaluation of 3D and 4D Tumour Volumes for Lung Treatment Planning

Paper 3- Extraction of Breathing Traces from 4D Cone-Beam CT

Paper 4- Robust Optimisation for Lung SABR Planning

7 Introduction

Lung cancer is responsible for 18% of cancer deaths and was the leading cause of cancer death in 2020[1,2]. The overall 5-year survival for lung cancer is low, with only 10 to 20% of patients surviving 5 years after diagnosis through 2010 to 2014[1]. Approximately 80% of lung cancer patients will receive radiotherapy at some point during their treatment[3]. Therefore, it is important to optimise the radiotherapy planning process to achieve the best possible treatment outcome.

Lung radiotherapy planning provides extra challenges due to the motion within the lung and technologies are constantly evolving which can improve the process. Delineation of structures plays an important part in all radiotherapy planning and artificial intelligence has recently been implemented in commercial software to improve this. 4DCT and 4D cone-beam CT (4DCBCT) are now available. 4DCT can be used for outlining the tumour and OARs for treatment and 4DCBCT used for matching on treatment to provide more accurate tumour coverage. Robust optimisation is now commercially available and this can be used to improve tumour coverage across all parts of the breathing cycle (breathing phases).

The work in this thesis aims to assess these technical aspects of lung radiotherapy planning that could be optimised for treatment and develop ways of using them to improve the planning process, with a particular focus on robust optimisation.

All text has been written by the author. The co-author contributions are listed below.

Paper 1- Different Approaches to Measuring the Effectiveness of Deep Learning Contouring Implementation in Clinical Settings

The study design was decided upon at each centre in collaboration with Mirada (Mirada Medical Ltd, Oxford, UK). Zoe Walker chose the unpaired study design for Coventry and collected and collated the data for Coventry. The outlines were created by dosimetrists. The co-authors have collected the data from the others centres. Zoe Walker has performed statistical analysis on the data from all sites and produced the tables and figures and the text for each section. Statistical advice was provided from Peter Kimani. The co-authors have provided guidance on analysis of the results and have helped to review the paper.

Paper 2- Evaluation of 3D and 4D Tumour Volumes for Lung Treatment Planning

Zoe Walker designed the study with guidance from Raj Shrimali and Jo Hamilton. Outlines were provided by clinicians and 5 re-plans were carried out by dosimetrists and 15 by Zoe Walker. All other work was carried out by Zoe Walker. Statistical advice was provided from Peter Kimani. Jane Rogers, Raj Shrimali and Rob Chuter have helped to review the paper.

Paper 3- Extracting Breathing Traces from Cone-Beam CT

All work has been carried out by Zoe Walker. Weibing Xu provided assistance on scripting in RayStation. Robert Chuter and Jane Rogers have helped to review the paper.

Paper 4- Robust Optimisation for Lung SABR Planning

All work has been carried out by Zoe Walker. Gareth Baugh and Bonnie Godyn provided guidance on robust optimisation in RayStation. Robert Chuter and Jane Rogers have helped to review the paper.

8 Literature Review

8.1 Introduction

To ensure an adequate dose is delivered to the tumour whilst sparing the organs at risk (OARs), the doses delivered from radiotherapy need to be as accurate as possible. Optimisation of the treatment plan requires accurate outlining of the tumour and OARs. There are now commercial methods available such as atlas-based auto-contouring and deep learning contouring (DLC) to improve the time taken and consistency of OAR delineation. The outlining of lung tumours also requires methods to provide accurate delineation throughout the breathing cycle such as the use of 4DCT.

Aspects such as patient setup, organ motion and anatomical change can cause delivered dose distributions to be different from those planned. Planning target volumes (PTVs) are normally used to account for uncertainties, but there remain inherent inaccuracies in these as estimates of systematic and random errors have to be made such as patient setup uncertainty, contouring uncertainty and delivery uncertainty. More recently, robust optimisation has become available in commercial treatment planning systems which may be able to solve some of the limitations of using a PTV.

The aim of this chapter is to review the literature on robust optimisation in radiotherapy treatment planning with a particular focus on lung tumour planning using the RayStation treatment planning system (RayStation, RaySearch Laboratories, Stockholm, Sweden). Outlining for lung planning and on-treatment imaging for lungs will also be discussed.

8.2 Outlining in Radiotherapy

8.2.1 Outlining Methods

In order to optimise a radiotherapy treatment plan, outlines of the tumour volume and OARs are required. Highly conformal dose distributions can be created, giving a high dose to the target whilst sparing normal tissue. Hence it is imperative to ensure the structures are accurately delineated. This is of particular importance for stereotactic ablative radiotherapy (SABR) where there are steep dose gradients[4]. Structures can be outlined manually but this is time consuming, especially for areas where there are several complex contours such as head and neck[5]. Manual contouring is also user dependent[6]. It has been shown that differences in outlines between observers lead to significant differences in lung SABR plans[7].

An alternative to manual outlining is to use atlas-based auto-contouring. This is available in commercial treatment planning systems for OARs and uses a library of images which have been contoured. The atlas image is registered to the patient image and the contours transformed onto the patient scan using deformable registration[8]. Atlas-contouring has been shown to reduce contouring time and improve consistency for sites such as head and neck, prostate, rectum, endometrium and lung.[9–15] However, atlases are limited by the deformation between scans[16], the limited range of patients within an atlas[17] and can be time-consuming to run.

Recently, artificial intelligence techniques in the form of deep learning have been developed for auto-contouring, using neural networks to train on large datasets of contoured images[18].

van Dijk *et al.*, (2020)[19] compared DLC, to manual and atlas-based contouring for 22 OARs of 104 head and neck cancer patient CT scans using the software by Mirada Medical (Mirada Medical Ltd, Oxford, UK). The study found that DLC significantly improved the contouring time taken for the majority of the contours with timing including editing of the DLC contours. The qualitative assessment showed that DLC gave significantly better contours than atlas-based contouring for the majority of the OARs assessed. Users also showed preference of DLC contours over atlas-based contours. However, manual contours were still preferred over DLC contours.

Wong *et al*., (2020)[20] compared manual contouring to DLC for 60 central nervous system, 52 head and neck and 50 prostate CT scans using the software Limbus Contour (Limbus AI, Canada). The study found a time saving using DLC for all sites but did not time the editing of DLC contours. Qualitative assessment showed that the DLC accuracy was comparable to inter-observer variability when OARs were contoured by experts.

Lustberg *et al.* (2018)[21] compared manual, atlas-based and DLC for OARs on 20 lung CT scans using the DLCExpert software. The study found there was an overall time saving using atlas-based contouring and DLC compared to manual contouring with a larger difference seen for DLC. The time saving was significant for all OARs compared to manual contouring except for the left lung and oesophagus contoured with the atlas method. Although there was no significant difference in dice coefficient scores for atlas-based contouring and DLC, subjective scoring was better for DLC.

8.2.2 Lung Tumour Outlining

Lung outlining poses a further outlining challenge as there is breathing motion to consider. A 4DCT is commonly used for outlining a lung tumour as it allows the tumour motion to be captured. One method of outlining using a 4DCT is the internal target volume (ITV) approach. This involves binning the 4DCT into phases and outlining a GTV on each of these. The GTVs are then combined to produce an ITV[22]. Alternatively, an ITV may be outlined directly using the maximum intensity projection (MIP) created from the 4DCT[23].

Motion compensated reconstructions can also be created from 4DCT scans for outlining. For example, Wolthaus *et al*. (2006)[24] presented the concept of the mid-ventilation CT (MidV) where the scan represents moving structures close to their time-weighted average position. It was found that the treatment volume using this scan for outlining was reduced by up to 50% compared to a free-breathing scan. It has also been shown that using motion compensated CT for lung OAR contouring can reduce inter-observer and intra-observer error[25].

If a 4DCT is not used then larger PTV margins need to be added to account for the tumour motion. There are a few small-scale studies comparing PTVs created using a 4DCT (PTV_{4D}) and PTVs created using a 3DCT (PTV_{3D}). The majority of these papers compare outlines but do not compare dosimetric consequences[26–29].

Callahan *et al*., (2014)[30] compared PTVs using a 3D positron emission tomography/CT (PET/CT) and 4D PET/CT for 29 patients with lung cancer in free-breathing. Several PTV_{3D} and PTV_{4D} volumes were created using margins of 5 mm, 10 mm and 15 mm and an asymmetrical margin. Plans were created on the set of $PTVs_{3D}$ and transferred onto the 4D scan to assess any geometric misses. It was found that PTV_{3D} margins could not be reduced from 15 mm as this would increase the chance of geometric miss due to respiratory motion. The paper provided a good assessment of PTV margins, but did not assess any differences in doses to OARs.

Wang *et al*., (2009)[31] compared 3 PTVs generated for 10 SABR lung cancer patients using CT scans. An ITV was created from the MIP and a 3 mm PTV margin added to create a PTV_{4D}. An ITV was also created from a free-breathing CT and end-exhale and end-inspiration breath-hold scans. A 3 mm margin was added to create a PTV (PTV_{3DCT}). A 5

mm anterior-posterior, left-right margin and a 10 mm superior-inferior were also added to a free-breathing GTV to create a conventional 3D PTV (PTV_{CONV}). Treatment plans were created based on PTV_{4D} and adapted to create plans based on the other 2 PTVs. The effect of the PTV was also assessed using the daily pre-treatment images. The study found that PTV_{4D} was significantly smaller compared to the other PTVs and planning using this gave a daily target coverage equivalent to the other plans. Using PTV_{CONV} significantly increased dose to normal lung tissue compared to the other methods. Although the paper provides a dosimetric assessment, doses to specific OARs were not assessed and this is a small-scale study only for patients receiving SABR.

Hof *et al.*, (2009)[32] evaluated 3D and 4D PTVs for 14 SABR lung cancer patients. PTV_{4D} was created by outlining an ITV over the breathing phases and expanding by 3 mm isotropically. The PTV_{3D} was created by expanding a GTV from a free-breathing CT by the motion measured on the 4DCT in each direction and then adding a 3 mm isotropic margin. Plans were created for each PTV. The authors found that PTV_{4D} was significantly smaller than PTV_{3D} and using PTV_{4D} significantly reduced the mean lung dose. This study again did not assess other OARs and the PTV_{3D} incorporated the 4DCT scan so was not an independent assessment of a 3D scan compared to a 4D scan.

The only study found providing a dosimetric assessment for non-SABR lung patients using CT was Bai *et al.*, (2014)[33]. PTV_{3D} and PTV_{4D} were compared for 10 patients with peripheral non-small cell lung cancer (NSCLC). The PTV_{4D} was created by outlining a GTV on each phase, expanding these by 7 mm isotropically to create a clinical target volume (CTV) and expanding the CTV by 5 mm isotropically to create a PTV. The PTV_{3D} was created by expanding the CTV on the 20% by motion observed with the patient on a simulator following their 4D scan. The diaphragm, lung and GTV motion were used. Plans were created for both PTVs. As with the other studies, it was found that planning to a PTV_{4D} significantly decreased dose to normal lung tissue. In addition, the authors found reduction in the heart and spinal cord doses but these were not significant. Although this study provides more analysis of doses to OARs it is again a small-scale study.

The literature suggests that using a 4DCT can create smaller PTVs and spare normal lung tissue. However, there are problems with using PTV margins for lung treatment planning and this is discussed further in the next section.

8.3 Problems with Planning Target Volumes in Lung Plans

Traditionally in radiotherapy treatment planning, a PTV method is used to incorporate uncertainties such as interfraction and intrafraction motion, organ motion delineation and setup uncertainties[34]. This method has been defined and recommended by the International Commission on Radiation Units and Measurements (ICRU)[35,36]. For lung cancers, the tumour motion can be evaluated using 4DCT but a PTV margin is still required to account for the other uncertainties. Radiotherapy for lung tumours is now commonly planned using intensity modulated radiation therapy (IMRT) or volumetric modulated arc therapy (VMAT), where optimisation is used to try to conform dose to the target whilst minimising dose to the OARs[37]. One problem with this method is the breathing pattern during treatment may not match that from the 4DCT and this has been shown to cause under-dosing of the tumour[38]. However, if all possible different breathing scenarios were accounted for this would increase the dose to normal tissue[39]. A breath-hold technique could be used which has been shown to be feasible for patients with lung cancer,[40,41] but there is also evidence within studies that not all patients can tolerate this and patients often require training in order to implement the technique[42–44]. In addition, the technique is slower than conventional delivery due to the beam being paused to allow the patient to recover between breath-holds[45]. Abdominal compression,[46,47] tracking[48] and gating[49] have also been investigated.

Although these methods can be used to quantify or minimise tumour motion, a PTV margin still needs to be added to account for the other uncertainties such as interfraction motion, intrafraction motion and setup uncertainties. There are inherent inaccuracies from using these in lung planning as dose optimisation will occur over large amounts of air which has a lower density to the tumour volume. Literature shows that a high fluence delivery is needed to deliver dose to this tissue due to the lack of electronic equilibrium[50]. In addition, if a patient is treated in free-breathing then the tumour could be at any point within the PTV, hence the delivered dose would be different to the plan.

A potential method to overcome the density issue is to override the electron density of the PTV. Although results suggest that this provides a more accurate dose distribution and reduced monitor units compared to using no electron density override, there is variation as to the best density to use for any override[51–53]. Only one paper was found[54], that used the RayStation dose calculation algorithm with a density override for lung plans and the authors found that this resulted in unsatisfactory target coverage.

Another solution is to use robust optimisation within a planning system which optimises the dose for variation of patient position in addition to the clinical goals[55]. This is discussed further in section 8.4.

8.4 Robust Optimisation Techniques

There were two main methods for robust optimisation of a radiotherapy treatment plan found within the literature. The first is stochastic programming (also known as expected value optimisation or probabilistic planning) where each uncertainty has an importance weight or a probability of occurring. The probabilities are also known as probability density functions (PDFs). The optimiser then minimises an objective function over all uncertainties with more weight given to more likely scenarios[56]. There are several examples of this method within the literature[57–59]. The second method for robust optimisation is minimax optimisation which will be explained below.

The commercial treatment planning system, RayStation, uses the minimax optimisation method. This approach was first presented by Goitein (1985)[60] and within RayStation it involves minimising the penalty of the worst-case scenario within a specified interval[59]. Hence, it does not use a probability density function but the user defines patient setup errors. The plan is optimised for multiple geometries and the worst value used in the objective function. One potential problem with this method is that low probability cases could be over optimised resulting in a loss of plan quality[54]. In addition, the approach could be overly conservative as fractionation is not accounted for and so the worst case is assumed for every fraction. Lowe *et al.* (2016)[61] developed a method to incorporate reducing setup uncertainties due to fractionation for a range of sites for proton therapy. It was shown that not incorporating the effect of fractionation reducing setup uncertainness can result in target dose compromise and increased dose to normal tissues.

It has been demonstrated in the context of proton therapy that stochastic programming and minimax optimisation can give similar results[62]. More recently, studies have shown that results can be different depending on uncertainties, geometry and planning objectives[63,64].

8.5 Clinical Examples of Robust Optimisation

8.5.1 Robust Optimisation using Protons

Robust optimisation was initially created for intensity modulated proton therapy (IMPT), as the sharp Bragg-peak dose fall-off and steep dose gradients cause these plans to be very sensitive to patient position uncertainties[65]. Several papers have reported that robust optimisation has helped to mitigate this problem and the most relevant papers for the project (those including lung plans) are discussed below.

Fredriksson *et al.* (2011)[59] used minimax optimisation to perform robust optimisation for IMPT on a lung case, paraspinal case and prostate case. The technique was compared to margins, single field uniform dose and material override techniques. It was found for each case that the minimax method provided superior lung sparing, spinal cord sparing and rectum sparing to the other methods while still providing good target coverage. The dose calculations were performed in RayStation using a pencil beam algorithm, but the minimax optimisation was carried out using Matlab (The MathWorks, Natick, MA).

Liu *et al.* (2012)[66] also used a worst-case robust optimisation method to plan a lung, skull base and a prostate. It was found that the plans were all less sensitive to range and setup uncertainties than conventional PTV plans and gave less dose to normal tissue for the same target coverage when uncertainties were present.

Li *et al.* (2015)[67] compared PTV-based and worst-case robustly optimised plans for 9 patients with lung cancer. Each patient had a weekly CT while on treatment and dose variation and equivalent uniform dose (EUD) were calculated on this. The dose variation was significantly lower for the robustly optimised plans. In addition, only 3 patients had an EUD change of greater than 5% using robust optimisation compared to 6 patients using PTV-margins.

Ge *et al.* (2019)[68] developed an in-house 4D robust optimisation system that included setup and range uncertainty for all respiratory phases. Ten patients with lung cancer were planned using this method and compared to the conventional PTV plans. The 4D robust plans were found to have superior target coverage and were more robust when uncertainties were present.

8.5.2 Robust Optimisation using Photons

More recently, robust optimisation has started to be used for photon treatment planning. There is limited evidence of robust optimisation being used for photon radiotherapy for a few sites with all papers presenting small studies.

A few papers have evaluated robust optimisation for breast planning with varying results. Mahmoudzadeh *et al.* (2015)[69] evaluated robust optimisation for 8 cancer patients receiving IMRT to the whole breast. A 4DCT was taken and probability mass functions created based on breathing cycles for the robust optimisation using a script in Matlab. The robustly optimised plans were found to provide equivalent or better heart sparing for all patients. Byrne and Hu (2016)[55], also evaluated robust optimisation for IMRT breast treatments but only created plans on a phantom. However, RayStation was used rather than an in-house script. The robustly optimised plans were found to be comparable to conventional planning at ensuring CTV coverage with setup variations. However, plan quality and OAR doses were not assessed in this study. In contrast, Nguyen *et al.* (2018)[70] compared optimisation using virtual bolus to robust optimisation in RayStation for 5 VMAT breast cancer patients and found that only the virtual bolus method was able to maintain target coverage. However, the OAR doses were found to be similar.

There are very small studies for robust optimisation in prostate planning but all show promising results. Chu *et al.* (2005)[71] developed a probabilistic model of robust optimisation for IMRT and used this for one prostate case. The method gave less dose to healthy tissue compared to conventional IMRT planning and maintained the target prescription dose under patient shifts. Baum *et al.* (2006)[72] included coverage probabilities into the optimiser for 10 prostate plans and showed that these plans were more robust for target coverage compared to margin-based plans. Bohoslavsky *et al.* (2013)[73] created a plugin for a planning system (Pinnacle, Philips Radiation oncology systems, Fitchburg, WI) to carry out robust optimisation. Three prostate cases were planned, achieving similar or better target coverage and rectal wall sparing compared to PTV-based plans.

Miura *et al.* (2017)[74] used robust optimisation in RayStation to create VMAT plans for targets within a phantom simulating stereotactic body radiation therapy (SBRT). It was found that the dose to 99% of the target (D99%) was not significantly different from PTV-based planning when applying a setup error to the plan. However, for a lesion at the patient periphery, it was found that the standard deviation of the D99% was significantly lower than

a PTV-based plan when applying setup errors. However, no assessment was made of the doses to OARs.

In a larger patient study, Fontanarosa *et al.* (2013)[75] compared robustly optimised plans to margin based plans for 20 IMRT head and neck cancer patients. Again, the robustly optimised plans provided lower OAR doses while maintaining the dose to the tumour. There is also a prospective randomised pilot trial currently underway to compare margins against robust optimisation in IMRT for head and neck squamous cell carcinoma (NCT03552965 (2018))[76] where the primary outcome is to measure xerostomia (dry mouth) at different time points. This should provide a larger dataset that is randomised, potentially yielding clinically relevant outcomes.

There is also evidence for the use of robust optimisation for lung planning and these papers are discussed in more detail in the following section.

8.5.3 Robust Optimisation for Photon Lung Plans

4D optimisation is designed to compensate for the blurring effect of tumour motion by optimising over all the breathing phases[57]. Papers have shown that using this technique can give high dose conformity and a reduction in dose to normal tissue[77,78]. The 4D optimisation method assumes no uncertainty on the tumour motion.

Chan *et al.* (2006)[79] improved upon the previous studies on 4D optimisation by developing a model of uncertainty in the motion PDF and including this in a robust optimisation algorithm. The PDF was created using the 4DCT and the Varian real-time position management (RPM) system (Varian Medical Systems, Palo Alto, USA) breathing trace for a particular patient. Uncertainties were created using the RPM trace from 4 different patients. A plan on a phantom was then robustly optimised using an in-house script using the PDF and uncertainties from patient data. The authors found that the robust method delivered 38% less dose to healthy tissue compared to a PTV-margin method. Although it showed the potential benefits of robust optimisation, this paper was a proof of concept rather than a full study.

Bortfeld *et al.* (2008)[57] extended the work by Chan *et al.* (2006)[79] to a clinical case rather than a phantom. Again, the breathing traces for 5 patients were recorded over their treatment course using the RPM system. The RPM amplitude was scaled for each patient to the anatomical amplitude from the 4DCT planning scan. A PDF was created for each patient

based on the amount of time the tumour spends in each phase. The PDF from 4 patients was used to give an uncertainty and the PDF from another patient used to test the robustness. Different combinations of the 5 patients were used and were compared to a margin method. It was found that the robust method delivered a comparable dose to the tumour but reduced the dose to the lung by 11% on average compared to the margin method. The margin method did deliver a more homogeneous dose to the tumour. However, the result is only based on data from 5 patients so might not be generalisable.

Vrancic *et al.* (2009)[80] also applied the method developed by Chan *et al.* (2006)[79] but delivered plans to a phantom to verify them. The data from 6 patients' RPM traces were used to obtain a PDF although these were a combination of patients with lung, mediastinum and liver cancer. Unlike the work by Bortfeld *et al.* (2008)[57], the plans were non-clinical but designed to deliver dose to a simple target. The plans were delivered to a 2D ion chamber array with the array programmed to move with the breathing cycle from 2 patients. The authors found that the robustly optimised treatment plan delivery gave a reduction of 12% in dose to areas outside the target compared to a margin-based plan. However, approximately 46% more MUs were required for the robust plan. A limitation of this study, Chan *et al.* (2006)[79] and Bortfeld *et al.* (2008)[57], is that they all assume the external RPM signal is correlated to tumour motion. It has been shown that the RPM surrogate can give a large difference between external and tumour motion in the ant-post direction[81].

Heath *et al.* (2009)[58] compared 2 4D robust optimisation techniques (probabilistic and a worst-case) to a mid-ventilation margin-based technique for 5 patients with lung cancer. The techniques were designed to be robust against different breathing patterns. They found that all methods produced similar target coverage but the two 4D robust approaches gave better OAR sparing. The authors also recommended use of a worst-case optimisation as it was more computationally efficient and was able to consider the dose variation in the OARs. The limitations of this study include the small dataset and the breathing variation at treatment being estimated rather than measured. The authors used amplitude and baseline variations from imaging at planning but estimated a standard deviation of 5 mm to account for breathing variations. A potential improvement suggested by the authors would be to adjust the plan based on daily 4DCBCT or fluoroscopy images. In addition, no measurements were made to validate the robustness of the different plans or to test the effect of interplay. This is when the target movement and multi-leaf collimator (MLC) movement are not synchronised, meaning parts of the tumour may receive less or no radiation if they are behind MLCs[82].

Nohadani *et al.* (2010)[83] implemented an optimisation method for lung IMRT plans using a spatiotemporal optimisation over all 4D phases with a Monte Carlo algorithm. Although indicated as a robust technique, this method was not a true robust optimisation as it still used PTV margins. The sensitivity of the plan was measured through modelling irregular breathing by extending a 4D phase so it overlapped the following phase. It was found that the 4D robust plan was not sensitive to irregular breathing for all phases but there were significant improvements for target coverage and OAR sparing compared to 3D gated treatments for tumours with large amplitudes of motion. However, this method was only tested for 2 patients, one with a small tumour and a large amplitude of motion and one with a large tumour and a small amplitude of motion. It was only tested through modelling rather than using a phantom.

An extension to the previous papers was provided by Chan and Mišić (2013)[39] who developed a 4D adaptive robust approach. Using the same PDFs as Bortfeld *et al.* (2008)[57], the patient's breathing motion PDF during treatment was combined with the original uncertainty to create a new uncertainty. This was repeated for each fraction in order to mitigate the uncertainties that occur each day and the uncertainties that might only be present at the start of the treatment course. It was found that the adaptive robust method improved tumour coverage compared to the static robust method and it also reduced OAR doses. However, the tumour dose homogeneity was slightly better for the static method and the maximum dose to the spinal cord was slightly lower but within clinical tolerance. The authors suggest that escalating doses to match the mean lung dose or V20 lung dose for the static or adaptive robust plans, could lead to significant improvements in tumour control. However, only 2 patient datasets were used for this study and no commercial software is yet available to incorporate an adaptive robustness approach, so the clinical viability is limited. The authors also do not indicate how the on-treatment PDF is measured. In addition, this approach would require extra work compared to other methods due to creating a new uncertainty every fraction.

More recently, the use of commercial treatment planning software for robust optimisation for lung planning is evident within the literature. Zhang *et al.* (2018)[84] planned 20 lung tumours at different locations within the lungs using robust optimisation and traditional PTV margins. For the plans using PTV margins, GTVs were outlined on each phase of a 4DCT and combined to create an ITV. This was expanded by 0.5 cm left-right, 0.5cm anterior-posterior and 1 cm superior-inferior to create a PTV. The robust optimisation plans were created in RayStation using minimax optimisation. The setup errors used were 0.5 cm left-

right and anterior-posterior and 1 cm superior-inferior based on RTOG 0236 and 0915 protocols[85,86]. IMRT and VMAT plans were created for both methods. The results were similar to the previous papers with the robust optimisation plans providing better target coverage, better conformity index, lower OAR doses but worse homogeneity index, all of which were statistically significant when compared to the margin-based plans. The mean dose and R95 (D95 (isodose that covers 95% of the ITV)/ prescription dose), variation was greater for the margin-based plans and the authors suggest this could be because the target volume was larger for these plans. In addition, the margin-based plans had higher monitor units, therefore the delivery time could be quicker for robustly optimised plans. A robustness test was carried out by perturbing dose distributions in all 3 directions with shifts from clinical experience and other studies[87,88]. It was found that for all perturbed doses, D99, D98 and D95 were all ≥95% of the prescription dose. No correlation was found between mean ITV dose and the tumour size, site or motion. Although this was a larger study, again no measurements were made to verify the delivery of the plans.

Liang *et al.* (2019)[89] compared VMAT PTV-based plans with robustly optimised plans in RayStation for lung SBRT treatments for a phantom and 9 patients using 4DCT scans. A PTV-based plan using a 5 mm margin was compared to a robustly optimised plan on an ITV using 5 mm setup uncertainties. A limitation of the paper is that the authors do not indicate how they decided on these setup errors. However, the robustness of the plans was tested more thoroughly than other studies. For the robustly optimised plans, the ITV D99 was evaluated for 14 error scenarios including diagonal directions. The authors also agreed with other studies with results showing both methods gave good tumour coverage, but the robust plan gave lower lung tissue doses for every phantom plan and patient plan. In contrast to Zhang *et al.* (2018)[84] it was found that the margin-based and ITV robust based plans had similar monitor units. This may be due to the different prescriptions and fractionations in the 2 papers. All error scenarios for both phantom and patient met the ITV D99 criteria. In addition to the other studies, the authors also report that high dose spillage and integral body dose were reduced with the robustly optimised plans. Again, the study had a small dataset and it did not account for actual tumour motion in the optimisation.

Liu *et al.* (2019)[90] created a lung cancer phantom simulation using 4DCT data from a patient and a spherical tumour. VMAT plans were created for 3 different sphere diameters using robust optimisation in RayStation. The uncertainties were estimated from patient's breathing amplitudes to ensure that there was 80% tumour probability position coverage. Breathing curves from 3 patients were used with the digital phantom to validate the plans. These were

obtained from fiducial markers imaged with x-ray fluoroscopy. It was found that the robust method significantly reduced dose uncertainty if the tumour amplitude was 10 mm or larger. The accumulated dose over 5 fractions to the tumour significantly increased for 2 patients (2% on average) that had large amplitudes, but the authors suggest that if the amplitude is less than 10 mm or the standard deviation of the amplitude is less than 1 mm that 4D-robust optimisation is not required as an average dose increase of 0.1% was found. However, this study only includes 3 patient breathing traces so more data is required to assess this conclusion.

Leung *et al.* (2020)[91] compared lung SBRT margin-based planning on the average intensity projection (AIP) and MidV, to robustly optimised planning on the AIP and phases for 13 patients with lung cancer. For margin-based planning, a 5 mm margin was added to the ITV for the AIP plans and a margin calculated using the van Herk formula[34] for the MidV GTV plans. The setup errors for the robust planning also came from the van Herk formula. The study found that the MidV robustly optimised plans produced lower GTV and lower OAR doses with significant results for chest $wall_{V30}$ (volume of chest wall receiving at least 30Gy) and normal $lung_{V20}$ (volume of normal lung receiving at least 20Gy). Each plan was calculated on every breathing phase with all plans providing GTV D_{50} (median dose of GTV) of at least the prescription dose. Plans were also renormalised to GTV D_{50} which reduced the difference in GTV coverage between all planning methods. For robustly optimised plans on the phases, there was only statistical difference in GTV coverage for GTV D_2 (minimum dose to hottest 2% of the GTV) compared to the margin-based MidV method. However, there are no measurements to assess the delivery of any of the plans assessed.

One full paper and a conference abstract were found that measured the delivery of robustly optimised lung plans rather than simulating errors, both using RayStation. In a conference abstract, Fusella *et al.* (2016)[92] investigated robust optimisation of lung SBRT for 3 patients and a moving phantom with plans robustly optimised over all phases. GafChromic film in a phantom was used to measure the robustly optimised plans and doses were perturbed in the planning system, simulating uncertainties to test the robustness of the plans. The simulated plans with errors of up to 3 mm, showed less than 2.5% difference in ITV, CTV and OAR dose-volume histograms. The film results showed good agreement to planned doses and it was found that the robust plans gave similar or slightly improved results compared to PTV plans. Unlike the other papers, there is no indication of any significant reduction in OAR doses. However, as this is not a full paper there is a lack of detail regarding the methods used and it has not been through the full peer review process.

In the full paper, Archibald-Heeren *et al.* (2017)[54] compared VMAT lung planning using PTV margins with and without the ITV overridden to tissue, average scans and robust optimisation using RayStation. All plans were created on a phantom (CIRS thoracic phantom) rather than patient scans and the 4DCT simulated by moving the tumour insert. For the margin methods the GTVs were outlined on each phase and combined to create an ITV with a 5 mm PTV margin added. Robust optimisation was performed over all phases, excluding intermediate breathing cycles and with offsets in the superior and inferior directions. The intermediate breathing cycle test was carried out to see if optimisation speed could be improved. The offset plan was to allow the evaluation of robust planning when multiple datasets are not available. Uncertainties of 5 mm were used which were obtained from Ruben *et al.* (2016)[93]. In addition, a margin-based plan was also created overriding the density of the ITV excluding the GTV. Measurements were made in the phantom with film and small volume chambers. The ion chamber results in the GTV and lung showed good agreement to the plans and gamma film results showed the delivered dose matched the planned dose well. The margin-based plans produced up to 25% dose escalation where the PTV contained air. When the density override was used, this was reduced but this also had the undesirable effect of an under dose to the GTV. The authors found that the robust methods reduced variation in the maximum dose across the breathing cycle and this was most pronounced for larger tumour motion. This is the opposite conclusion to Zhang *et al.* (2018)[84] who found no correlation. Although this paper provides the greatest number of measurements for verifying robustly optimised plans, the phantom and tumour movement were a very simple approximation compared to patient anatomy. In addition, no comment was made with regards to optimisation speed for the phase exclusion plan.

8.6 The Importance of Robust Optimisation Results

The majority of papers found have shown that robust optimisation provides lower doses to OARs while still maintaining the same target coverage and hence there may be potential to dose escalate. Toxicities such as radiation pneumonitis currently limit the doses that can be given to the tumour[94] and robust optimisation may mitigate this. Dose escalation has been shown to improve local control and overall survival for patients with lung cancer[95–97].

Alternatively, if the current doses were maintained, robust optimisation could reduce the dose to OARs and hence reduce side effects from treatment such as radiation pneumonitis in patients with lung cancer receiving SABR treatment. Although radiation pneumonitis that

is grade 3 or above is rare, it has been reported that there are life-threatening situations in up to 12% of cases[7,98], therefore it is important to reduce these toxicities.

8.7 On-Treatment Patient Imaging

Robustly optimised plans may give lower doses to the OARs in the planning system but this needs to correspond to the actual dose that is delivered so it is important to ensure the patient is in the correct position. 3D cone-beam CT (3DCBCT) is normally used for linac-based image guidance. However, this does not provide information about internal movement. In addition, the 3DCBCT is acquired over more than one breathing cycle which can cause the images to become blurred[99].

One solution is to use a 4DCBCT. This is a slower scan than a 3DCBCT in order to sample more of the breathing cycle. A breathing signal is extracted from the projections and the projections are then binned to form a respiratory correlated image[100]. 4DCBCT allows the tumour motion to be visualised and has been shown to reduce motion artefacts that are present in 3DCBCT scans and increase image guidance accuracy[101,102].

However, there are also drawbacks to the use of 4DCBCT. The acquisition time is longer than a 3DCBCT meaning the patient remains in the treatment position for longer, potentially increasing movement uncertainty and their breathing at imaging might not be representative of treatment[102]. The dose from a 4D-CBCT has also been shown to be higher than that from 3DCBCT[103]. In addition, it has been noted that there is no standardised method for matching 4DCBCT scans and there is variation between centres[99,104].

8.8 Project Aims

The project assesses technical aspects of lung radiotherapy planning that could be optimised for treatment. This includes assessing outlining using artificial intelligence in the form of DLCExpert and how this can be evaluated in a clinical setting. Performing lung tumour outlining using 3D and 4D CT scans is compared. The literature has shown that this can reduce PTV volumes but there is little assessment of the dosimetric impact especially for lung cancer patients not receiving SABR treatment. Plans are re-optimised for this project using both methods for a cohort of patients not receiving SABR treatment.

The project evaluates methods of robust optimisation using RayStation including measurements of these plans on a phantom using realistic breathing traces. The literature has

shown the potential benefits of robust optimisation over margins in small studies for lung photon planning. However, studies have not directly compared margin-based, 3D robust and 4D robust planning for SABR lung planning. This study assesses all 3 methods for SABR lung planning.

Although some studies assessed optimisation over breathing phases, these studies in general did not measure the delivery of the plans and did not use commercial software for robust optimisation. One of the studies that measured delivery[92] did not use patient specific traces. Archibald-Heeren *et al.* (2017)[54] did not use real 4DCT scans and planned to a phantom volume. Only Vrancic *et al.* (2009)[80] tested robust optimisation on actual breathing traces and this was only for 2 patients with motion obtained from an external marker rather than internal anatomy. The project involves programming a phantom with realistic breathing traces from 4DCT scans and assess the delivery of different robustness methods. In addition, a method is developed to extract patient breathing traces from patient 4DCBCT scans and the phantom programmed to simulate these which has not been attempted in previous studies. The dosimetry of different robustness methods is therefore assessed in a situation that is more clinically relevant by using actual tumour motion rather than an external surrogate.

8.9 Conclusions

The review showed evidence for the use of robust optimisation for photon lung planning but studies were small and limited. The majority of papers showed the potential of robust optimisation to provide adequate target coverage with reduced OAR doses compared to conventional margin methods. This means that robust optimisation has the potential to reduce toxicities or to dose escalate, potentially increasing overall survival. The project adds to the current literature by assessing robust optimisation on a clinically relevant lung dataset using RayStation. The project uses actual patient breathing traces to assess the delivery of the plans which has not been done using 4DCBCT.

The review has also shown that auto-contouring can be used to improve outlining in radiotherapy including lung, with DLC out performing manual contouring and atlas-based contouring. Although there are some studies comparing DLC to manual contouring, there is limited evidence of large-scale multi-centre studies. The project analyses results from a multi-centre study for prostate and head and neck with data for lung also analysed.

In addition, literature showed that outlining lung plans using a 4DCT resulted in smaller PTVs and reduced normal lung doses. The majority of papers were small studies and did not analyse other OARs or focused on SABR planning. The project adds to the current literature by assessing a larger cohort of patient PTV volumes for lung tumours with a variety of tumour stages.

9 Different Approaches to Measuring the Effectiveness of Deep Learning Contouring Implementation in Clinical Settings

This paper is an auto-contouring study that was initially carried out for head and neck and prostate with 3 other centres. It has been developed to include lung auto-contouring and the whole paper with head and neck and prostate analysis has been included for completeness. The analysis and methods used to evaluate auto-contouring for head and neck and prostate could also be applied to further lung data.

Walker Z.[1], Bartley G.[1], Kelly D.[2], Navarro C.[3], South C.[3], Temple S.[2], Chuter R.[4]

[1] Medical Physics, University Hospitals Coventry and Warwickshire NHS Trust, Coventry, UK; [2]Radiotherapy Physics, The Clatterbridge Cancer Centre NHS Foundation Trust, Wirral, UK; [3]Department of Medical Physics, Royal Surrey County Hospital NHS Foundation Trust, Guildford, UK; [4]The Christie Medical Physics and Engineering, The Christie NHS Foundation Trust, Manchester, UK.

Abstract

Purpose

To evaluate the use and implementation of deep learning contouring (DLC) for prostate and head and neck organs at risk (OARs) across 4 NHS centres in England using the commercial system Mirada DLCExpert.

Methods

103 CT scans from 2 centres were included for the prostate evaluation and 310 CT scans from 4 centres were included for the head and neck evaluation. Generic models in Mirada were used for the prostate evaluation and at 3 of the centres for the head and neck evaluation. The time taken to contour using the existing method at each centre was compared to the time taken to edit the contours using DLCExpert and statistical analysis performed. Dice similarity coefficient (DSC) and distance to agreement (DTA) were assessed for the OARs. 13 OARs for patients with lung cancer using a manual method and DLCExpert were also assessed for one centre and inter-observer variability was assessed for one centre. Centres were allowed to implement their own methodology for assessment of DLCExpert with paired and un-paired studies being performed.

Results

The mean time saved for prostate OAR contouring using DLCExpert compared to the existing clinical method across 2 centres was 1.5±1.5 minutes. At both centres the DTA and DSC showed the best agreement for the femoral heads and the worst agreement for the

rectum. The mean time saved for head and neck OAR contouring using DLCExpert compared to the existing clinical method across the 4 centres was 16.2±8.6 minutes. There was no time-saving for the centre that already used an atlas-based method, only for centres where a manual contouring method was used. The mandible, brainstem and right parotid scored highly for both DSC and DTA. For lungs, contouring using DLCExpert showed excellent agreement for the lungs and heart compared to clinical contours and the oesophagus showed least agreement to clinical contours.

Conclusions

Clinical implementation of non-centre specific models for prostate and head and neck OAR contouring using Mirada DLCExpert can provide time savings. A generic model can be implemented and tested in different ways with use of a paired or non-paired study to fit in with the clinical workload at the centre. The DSC and DTA values showed good agreement with clinical contours for the majority of structures. The potential for reducing inter-observer variability has been shown but further work is needed to confirm this.

9.1 Introduction

It is important to have accurate organ at risk (OAR) contours for radiotherapy planning to ensure healthy tissue is spared. Techniques such as volumetric modulated radiotherapy or intensity modulated radiotherapy allow highly conformal dose distributions with steep dose gradients to be created so it is imperative that the contours are accurate. The accuracy of OAR contouring has been shown to be correlated to toxicity[1,2]. Manual methods of contouring are very labour intensive and there is inter and intra-observer variation[3-5]. In addition, the contour quality and time spent contouring can depend on the experience of the user[1,6].

An alternative method is to use atlas-based auto-contouring which has been shown to reduce contouring time and improve consistency for sites such as head and neck, prostate, and lung[7-9]. However, atlas-based contouring is limited by the deformation between scans[10] and the limited range of patients within an atlas[11]. In addition, atlas-based auto-contouring has been shown to be inferior for small and thin OARs[12].

Recent advances in artificial intelligence have created further auto-contouring capabilities in the form of deep learning, using neural networks to train on large datasets of contoured

images[13]. Studies have shown that deep learning outperforms manual and atlas-based contouring[14-17].

However, there is very little evaluation of the same deep-learning contouring (DLC) system at multiple centres within the literature. Kiljunen *et al*. (2020)[15] carried out a study involving 6 centres to assess DLC for prostate OARs on CT scans but only 5 patients were analysed at each clinic. Oktay *et al*. (2020)[18] assessed DLC for 83 prostate and 26 head and neck CT scans from 3 centres but only 10 scans were used to assess the time saving of DLC. Also, individual images were assessed rather than evaluating clinical the implementation at each centre. Wong *et al*. (2020)[19] analysed DLC for 36 head and neck, 60 prostate and 21 central nervous system OARs at 2 centres. However, this was a conference abstract so there is not a detailed discussion of the results available.

This study aims to evaluate the use of DLC and the lessons learned from the introduction of a commercial DLC system (DLCExpert™, Mirada Medical Ltd., Oxford UK) for prostate and head and neck across four NHS centres in England.

A local evaluation for lung auto-contouring has also been included.

9.2 Methods

9.2.1 Deep Learning Contouring Software

Each centre was given the freedom to implement Mirada as was applicable to their clinic. All centres were using Mirada WBx 2.0 from September 2019 to June 2020 and Mirada WBx 2.2 from June 2020 to November 2020. The deep-learning contouring system within Mirada (DLCExpert™) implements convolutional neural networks (CNNs) in order to classify OARs on a CT scan. Each voxel is classified using a 14-layer multiclass CNN[14]. The prostate and lung models used were trained on CT scans contoured using internal guidelines and the head and neck model was trained on CT scans contoured using consensus guidelines[20].

9.2.2 Patient Selection

A total of 103 patient CT scans from 2 NHS centres (The Christie and Coventry) were included in the prostate study. Any images with significant artefacts e.g. from artificial hips were excluded. A total of 310 patient CT scans from 4 NHS centres (The Christie, Coventry, Clatterbridge, Surrey) were included in the head and neck study.

Coventry and Clatterbridge selected consecutive patients for the study; hence different patients were outlined for the original clinical method compared to the DLC method for the timing data. Clatterbridge timings were collected using an SQL query of the ARIA database (Varian Medical Systems, Palo Alto, USA) for all patients that had a head and neck planning task completed within 2 weeks of an import/OAR outlining task being completed. Timings from all other centres were recorded manually.

9.2.3 Contouring Time

OARs were outlined using the existing clinical method at each centre and the total time taken to outline selected OARs were recorded for each patient in the study. OARs were also contoured automatically using DLCExpert. The DLCExpert contours were edited to match local clinical contour guidance and the time taken recorded. The methods for each centre are summarised in Table 9.1 for prostate and Table 9.2 for head and neck.

9.2.4 Quantitative Evaluation

Since centres used paired and unpaired studies, timing data was assessed for statistical significance separately using paired and unpaired T-tests after the data was assessed for normality using the Shapiro-Wilk test. All statistical analysis was performed in SPSS (v25, IBM).

Contours created with the existing clinical method were quantitatively compared to those created with DLCExpert by assessing the Dice Similarity Coefficient (DSC) and distance to agreement (DTA). DSC is a measure of the intersection of 2 volumes (A and B) with a value of 0 meaning no overlap and a value of 1 meaning perfect overlap[21]. It is given by the following equation:

$$DSC_{A,B} = \frac{(2|A \cap B|)}{(|A| + |B|)}$$

The distance to agreement is the shortest distance from a point on one contour surface to the other contour surface. Mean DTA was used which is the mean of all the distances calculated[22]. The exact methods used were decided upon by each centre and included use of the software ADMIRE (v3.21.2, Elekta AB, Sweden) and in-house scripts within planning systems.

9.2.5 Inter-Observer Variability

Inter-Observer variability was assessed by The Christie for head and neck outlining. Manual and DLCExpert edited contours were outlined by 2 consultants and 2 registrars. All outliners contoured parotids, submandibular glands, eyes, larynx, oral cavity, mandible, pharyngeal constrictor muscles, brainstem, spinal cord, oesophagus, optic nerves and optic chiasm. DTA was calculated for different permutations of the different observers compared to each other for both manual and edited DLC contours.

9.2.6 Lung Study

The current thesis focuses on lung planning and DLC contouring can also be used for this site. A generic model (Thorax_CT_NL007_M0) was assessed on a subset of 13 patients with lung cancer at Coventry. A paired study was used where the DLC contour was compared to the clinical contour for each patient. The DSC and DTA were recorded.

Table 9.1: Methods of assessing auto-contouring using Mirada DLCExpert for prostate organs at risk.

	The Christie	**Coventry**
Number of patients	9 (same patients for existing method and DLC)	94 (42 manual, 42 DLC, 10 for DSC and DTA)
Study design	Paired	Unpaired
Number of manual contourers	2 (both outlined 9 each)	4
Staff group	Dosimetrists	Dosimetrists
Existing method	Manual	Manual
DLCExpert model	Generic Prostate_CT_NL006_GN	Generic Prostate_CT_NL006_GN (bladder and rectum) Prostate_CT_NL010_NN (femoral heads)
OARs	Bladder, femoral heads, rectum	Bladder, femoral heads, rectum
Targets	None	None
Editing software	Pinnacle v16 (Philips Radiation oncology systems, Fitchburg, WI)	RayStation v7 (RaySearch, Sweden)
Timing Method	Manual	Manual

Table 9.2: Methods of assessing auto-contouring using Mirada DLCExpert for head and neck organs at risk.

	The Christie	**Coventry**	**Clatterbridge**	**Surrey**
Number of Patients	10 (10 Manual, 10 DLC, 10 DSC and DTA)	50 (20 manual, 20 DLC, 10 for DSC and DTA)	224 (40 manual, 169 DLC, 15 for DSC and DTA)	26 (9 manual, 7 DLC 10 for DSC and scoring)
Study Design	Paired	Unpaired	Unpaired	Unpaired
Number of contourers	4 (all 4 outlined all 10 patients)	3	6	1
Staff group	Clinicians	Dosimetrists	Planning radiographers	Clinicians
Existing Method	Manual	Atlas	Manual	Manual
DLCExpert Model	Generic + Local	Generic	Generic	Generic
DLC OARs	Eyes, parotids, submandibular glands, brainstem, larynx, mandible, oral cavity, spinal cord	Brainstem mandible, parotids, spinal cord	Mandible, parotids, submandibular glands.	Brainstem, parotids, spinal cord
OARs from other source		Atlas for orbits, optic nerves, lens		Atlas for orbits, optic nerves, lens
Editing software	Pinnacle v16 (Philips Radiation oncology systems, Fitchburg, WI)	RayStation v7 (RaySearch, Sweden)	Eclipse v15.6 MR5 (Varian Medical Systems, Palo Alto, USA)	Eclipse v13.7 (Varian Medical Systems, Palo Alto, USA)
Timing Method	Manual	Manual	Aria (with >3 hours and <10 minutes removed)	Manual

9.3 Results

9.3.1 Prostate OAR Contouring

The total mean time saved for prostate OAR contouring using DLCExpert compared to the existing clinical method across the 2 centres was 1.5±1.5 minutes (Table 9.3). T-tests were performed as the Shapiro-Wilk test indicted the data from both centres was normally distributed. The paired T-test and unpaired T-tests indicate that the time differences between the manual and DLC contouring methods are not significant at the 5% level. The distribution of all results is shown in Figure 9.1

At both centres the DTA and DSC showed the best agreement for the femoral heads and the worst agreement for the rectum (Table 9.4 and Table 9.5).

Table 9.3: Average prostate organ at risk contouring times for 2 centres using manual contouring and Mirada DLCExpert. Standard errors used. P-value from paired T-test for The Christie and for unpaired T-test for Coventry.

	Average OAR contouring time (minutes)	
	The Christie	**Coventry**
Manual	15.0±0.7	12.5±0.5
DLCExpert	13.0±1.3	11.5±0.3
Average time difference (negative is time saving)	-2.0±1.4	-1.0±0.6
p-value	0.17	0.09

Table 9.4: Average dice similarity coefficient (DSC) for prostate organs at risk for 2 centres comparing manual contouring and Mirada DLCExpert. Standard errors used.

Structure	**DSC**	
	The Christie	**Coventry**
Rectum	0.58±0.05	0.71±0.02
Bladder	0.84±0.01	0.82±0.02
Femoral Head Left	0.90±0.08	0.82±0.01
Femoral Head Right	0.89±0.03	0.92±0.01

Table 9.5: Average distance to agreement (DTA) for prostate organs at risk for 2 centres comparing manual contouring and Mirada DLCExpert. Standard errors used.

Structure	DTA (mm)	
	The Christie	**Coventry**
Rectum	4.8±0.4	5.4±0.8
Bladder	2.5±0.3	2.0±0.3
Femoral Head Left	2.2±0.7	1.4±0.2
Femoral Head Right	2.3±0.6	1.2±0.1

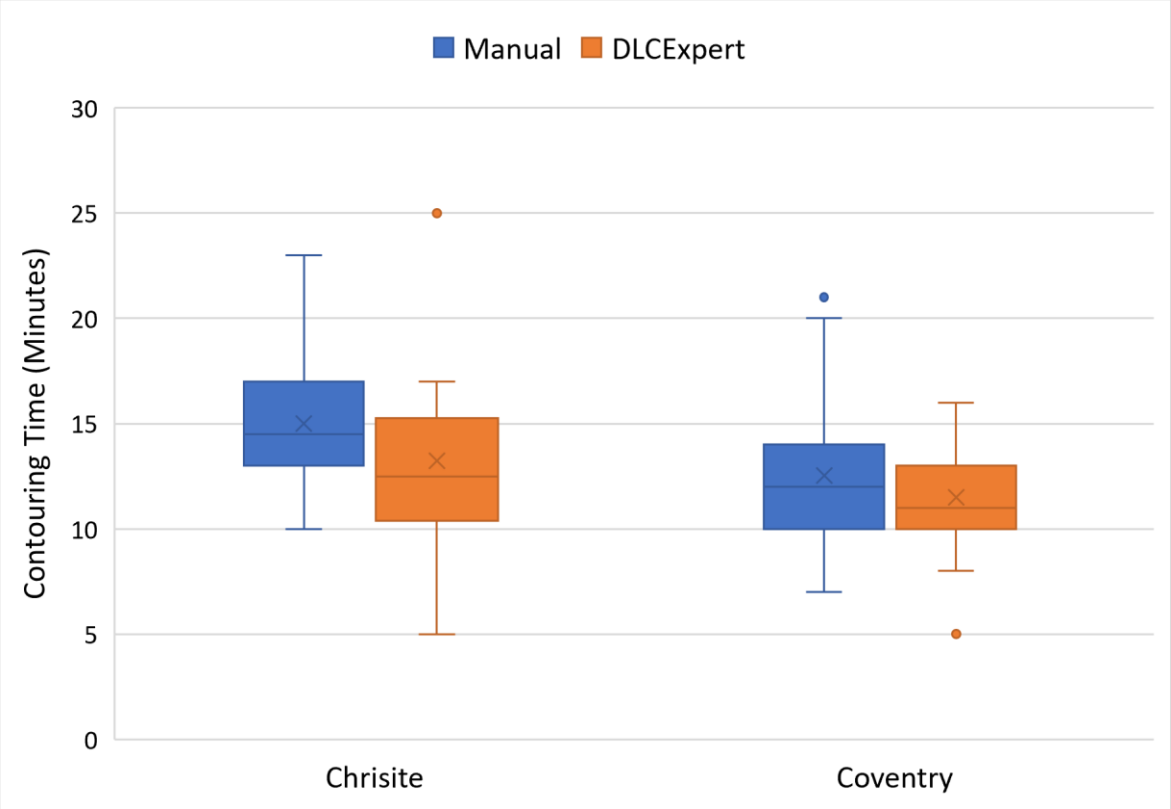

Figure 9.1: Box and whisker plot of contouring times for prostate organs at risk from 2 centres using manual and DLC contouring. The boxes indicate the interquartile range (IQR), the line indicates the median and the cross indicates the mean. The whiskers indicate the highest and lowest values within 1.5 times the IQR and data outside this range indicated by circles.

9.3.2 Head and Neck OAR Contouring

The total mean time saved for head and neck OAR contouring using DLCExpert compared to the existing clinical method across the 4 centres was 16.2±8.6 minutes (Table 9.6). If the existing clinical method is manual, (excluding Coventry) the average time saving was 22.5±8.4 minutes. A paired T-test was performed for The Christie data as the Shapiro-Wilk test indicted the data was normally distributed. The other data was assessed using a Wilcoxon signed rank test. The p-values indicate that the difference between the existing and DLC contouring methods are significant at the 5% level for The Christie and Coventry. The distribution of all results is shown in Figure 9.2 and Figure 9.3.

The mandible, brainstem and right parotid scored highly for both DSC and DTA across all centres where the structures were analysed (Table 9.7 and Table 9.8).

Table 9.6: Average head and neck organ at risk contouring times for 4 centres using an existing clinical method and Mirada DLCExpert. Standard errors used.

	Average OAR contouring time (minutes)			
	The Christie	**Coventry**	**Clatterbridge**	**Surrey**
Existing Method	18.3±1.5	11.9±1.2	74.7±7.6	10.4±1.0
DLCExpert	10.0±0.8	18.00±0.6	62.5±3.1	8.4±0.2
Average time difference (negative is time saving)	-8.3±1.7	+6.1±1.3	-12.2±8.2	-2.0±1.0
p-value	<0.01	0.01	0.54	0.279

Table 9.7: Average dice similarity coefficient (DSC) for head and neck organs at risk for 4 centres comparing existing clinical contouring and Mirada DLCExpert. Standard errors used. – indicates the structure was not analysed by that centre

	DSC			
	The Christie	**Coventry**	**Clatterbridge**	**Surrey**
Brainstem	0.77±0.02	0.80±0.01	-	0.80±0.01
Mandible	0.84±0.02	0.90±0.01	0.85±0.01	-
Parotid Left	0.68±0.04	0.82±0.02	0.75±0.02	0.81±0.01
Parotid Right	0.75±0.03	0.84±0.01	0.72±0.02	0.81±0.01
Spinal Cord	0.69±0.04	0.68±0.04	-	0.78±0.02
Submandibular Left	0.52±0.07	-	0.71±0.02	-
Submandibular Right	0.63±0.07	-	0.66±0.02	-
Larynx	0.62±0.04	-		
Oral Cavity	0.74±0.03	-		

Table 9.8: Average distance to agreement (DTA) for head and neck organs at risk 3 centres comparing the existing clinical contouring and Mirada DLCExpert. Standard errors used. – indicates the structure was not analysed by that centre.

	DTA (mm)		
	The Christie	**Coventry**	**Surrey**
Brainstem	2.8±0.3	1.7±0.1	1.8±0.2
Mandible	2.1±0.5	0.6±0.1	-
Parotid Left	4.3±0.7	2.4±0.5	2.3±0.5
Parotid Right	2.9±0.3	2.4±0.4	2.6±0.3
Spinal Cord	6.6±3.3	1.0±0.1	3.1±0.6
Submandibular Left	3.9±0.7	-	-
Submandibular Right	3.1±0.7	-	-
Larynx	5.1±1.3	-	-
Oral cavity	5.5±0.6	-	-

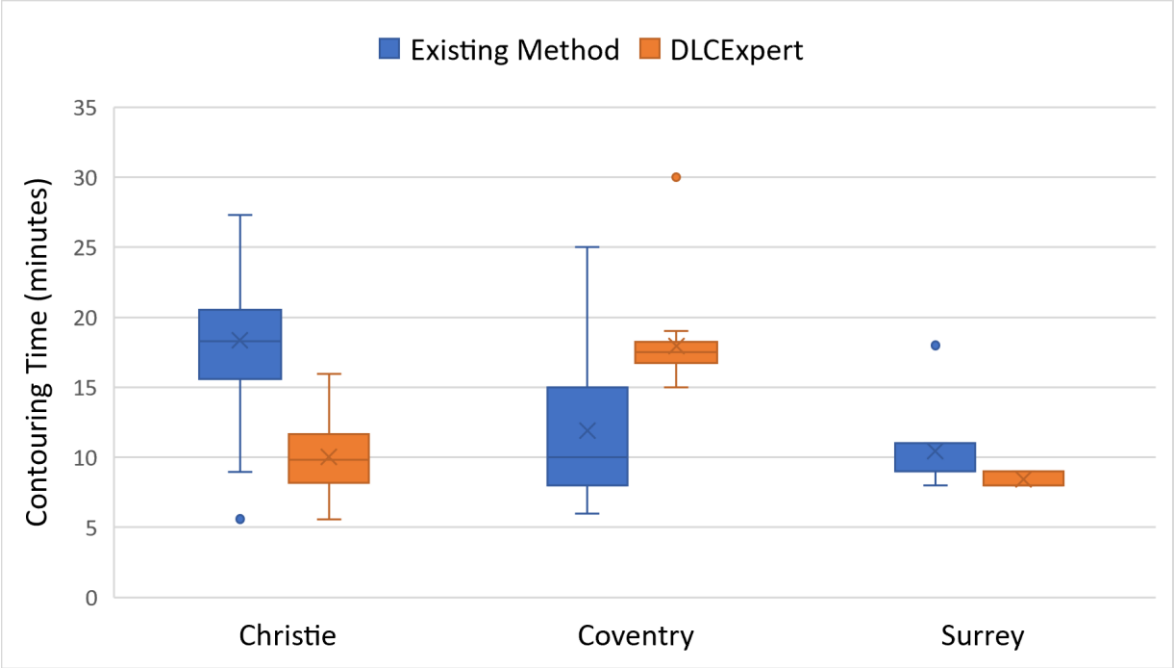

Figure 9.2: Box and whisker plot of contouring times for head and neck organs at risk from 3 centres using an existing clinical method (manual contouring for The Christie and Surrey and Atlas-based contouring for Coventry) and DLC contouring. The boxes indicate the interquartile range (IQR), the line indicates the median and the cross indicates the mean. The whiskers indicate the highest and lowest values within 1.5 times the IQR and data outside this range indicated by circles.

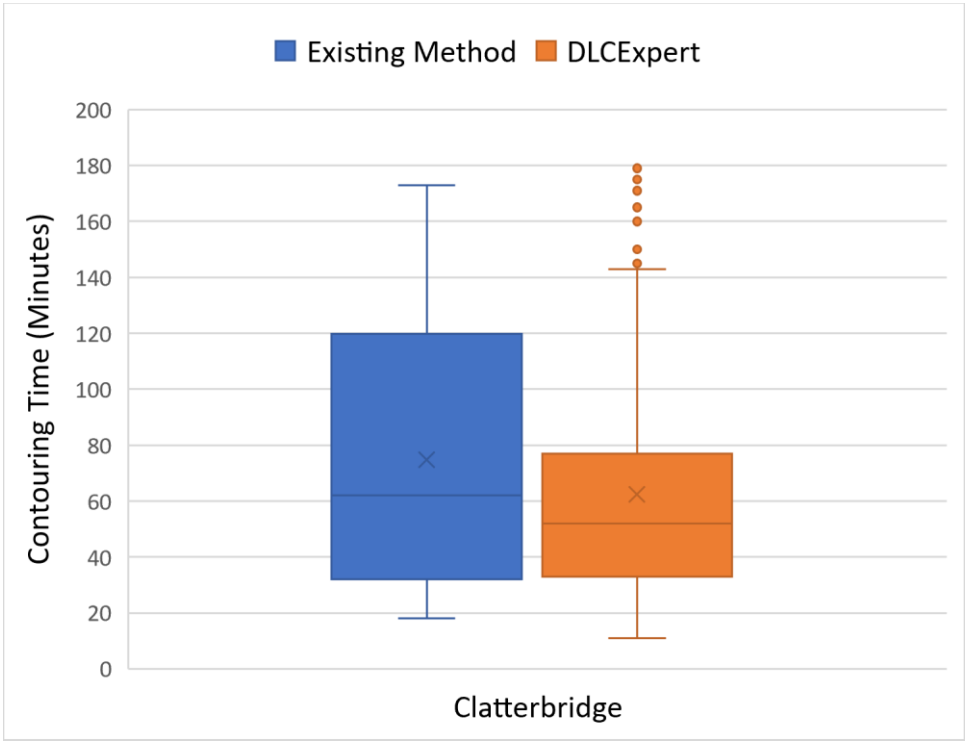

Figure 9.3: Box and whisker plot of contouring times for head and neck organs at risk from a centre using an existing clinical method (manual contouring) and DLC contouring. Timings were collected using the record and verify system Aria. The boxes indicate the interquartile range (IQR), the line indicates the median and the cross indicates the mean. The whiskers indicate the highest and lowest values within 1.5 times the IQR and data outside this range indicated by circles.

9.3.3 Inter-Observer Variability

The results from The Christie inter-observer variability study showed that the DTA between the observers for the majority of DLC-edited OARs for head were less than manual contours (Figure 9.4).

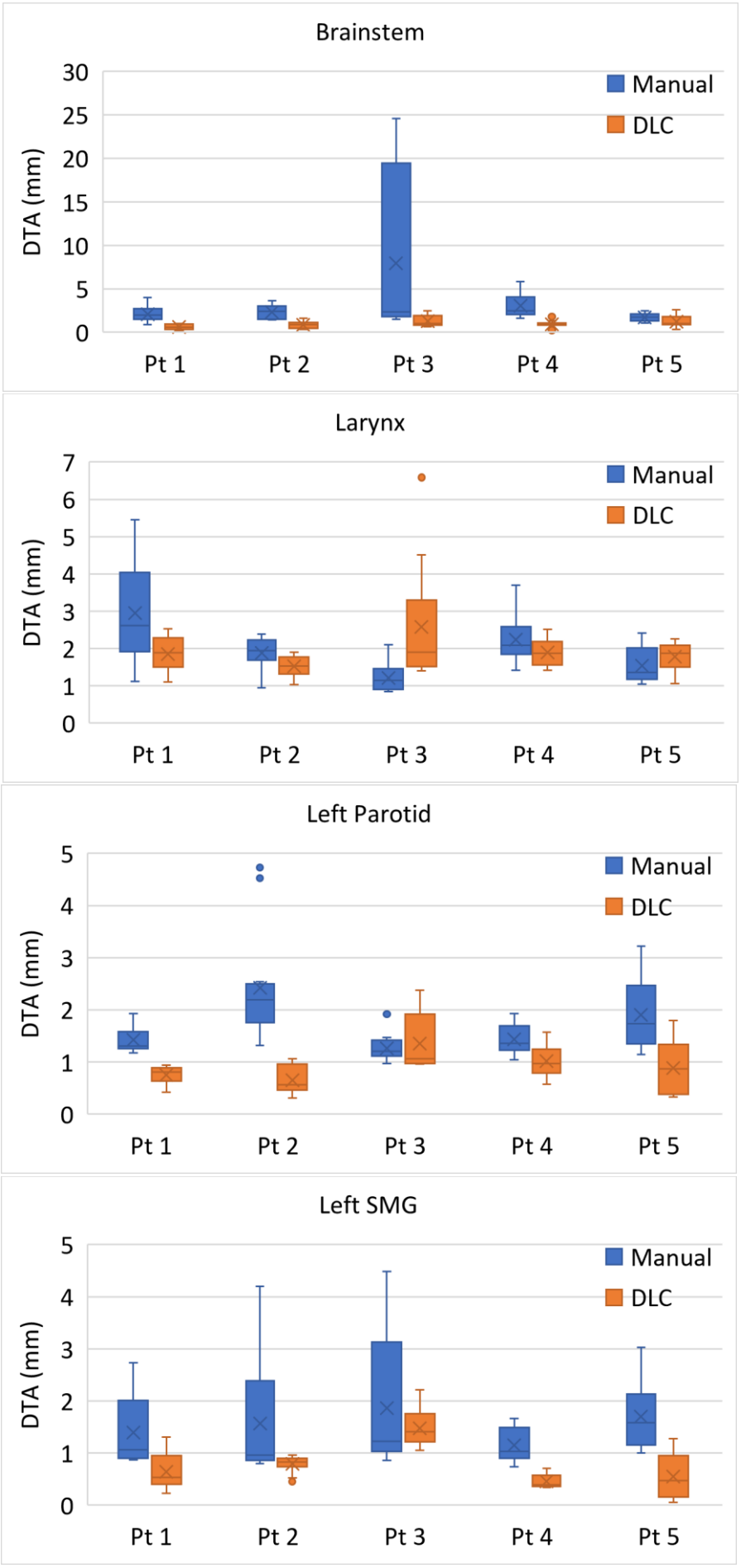

Figure 9.4: Distance to agreement (DTA) for manual and MiradaDLC edited head and neck OARs for different permutations of 4 observers compared to each other.

9.3.4 Lung OAR Contouring

The results show excellent agreement for both lungs. The oesophagus contouring produced contours that showed least agreement to clinical contours with a large DTA and low DSC (Table 9.9).

Table 9.9: Average distance to agreement (DTA) and dice similarity coefficient (DSC) for lung organs at risk for 13 patients at Coventry.

Structure	DTA (mm)	DSC
Lung Right	2.0±0.6	0.97±0.003
Lung Left	1.1±0.1	0.97±0.004
Cord	1.1±0.12	0.78±0.03
Heart	5.2±0.8	0.86±0.02
Oesophagus	6.3±3.2	0.64±0.06

9.4 Discussion

The timing data for prostate contouring showed a time saving using Mirada DLCExpert for both centres analysed, although this was not statistically significant. Kiljunen *et al*. (2020)[15] found a larger time saving of 12 minutes (46%) compared to manual contouring for their multi-centre study of 30 prostate patient CT images. However, this also included the prostate, seminal-vesicles and penile bulb in addition to the OARs analysed in this study which may be why the time saving is larger. Zabel *et al*. (2021)[23] found a time saving of 8.5 minutes (44%) using DLC software on 15 prostate CT scans for bladder and rectum outlining but the manual contouring included contouring by a radiation therapist and editing by a radiation oncologist. The times collected in the current study only include initial manual contouring and therefore manual contouring will be faster.

The time savings for using Mirada DLCExpert for head and neck contouring were for centres that used manual contouring as their existing clinical method. Oktay *et al*. (2020)[18] found a time saving of 93% using DLC software compared to manual contouring for head and neck CT scans. A maximum time saving of 45% was found in this current study. However, Oktay

et al. (2020)[18] measured an average manual contouring time of 87 minutes for experts which was longer than the average time taken in any of the centres analysed in this current study.

The centre where the time saving using Mirada DLCExpert was statistically significant had a combined model using their own data and the generic model. This suggests that DLC models developed with local data may provide a larger time-saving benefit. In addition, The Christie tested more structures than the other centres which may contribute to the larger time saving. Coventry was the only centre to observe a time increase when using DLCExpert which could be because the centre has a well-established atlas-based contouring system and the timing study was only carried out for a limited number of structures.

The DSCs obtained show the generic model performed well for the bladder and femoral heads. The DSC for rectum and bladder were slightly lower than other studies where generic models were used but the results for the femoral heads were better than or comparable to other studies (Table 9.10).

Table 9.10: Mean Dice Similarity Coefficient (DSC) for prostate OARs from the study compared to literature.

Structure	**Mean DSC**				
	The Christie	**Coventry**	**Kiljunen *et al*. (2020)**	**Oktay *et al*. (2020) Mean (SD)**	**Zabel *et al*. (2020)**
Rectum	0.58±0.05	0.71±0.02	0.84	0.87 (0.03)	0.86
Bladder	0.84±0.01	0.82±0.02	0.93	0.96 (0.02)	0.97
Femoral Head Left	0.90±0.08	0.82±0.01	0.68	0.98 (0.01)	-
Femoral Head Right	0.89±0.03	0.92±0.01	0.69	0.98 (0.01)	-

The majority of DSCs obtained for head and neck OARs were comparable to other studies, for example, Oktay *et al*. (2020)[18] (mean (SD): mandible 0.938 (0.025), left parotid 0.843 (0.046), brainstem 0.849 (0.068)) and Ibragimov *et al*. (2017)[24] (mandible 0.895±0.036, left

parotid 0.766±0.031, left SMG 0.697±0.133). The DSCs for spinal cord were lower than other studies (e.g. Oktay *et al.* (2020)[18] (Mean (SD): 0.806(0.077)) and Ibragimov *et al.* (2017)[24] (0.87±0.032). However, it should be noted that the model by Ibragimov *et al.* (2017)[24] was tested on data from the same centre so was not a generic model.

The DSCs for lung showed the generic model performed extremely well for both lungs and heart. The DSCs for lungs, heart and spinal cord were comparable to Lustberg *et al.* (2018)[17] and Vu *et al.* (2020)[25] who found DSCs for lungs close to 1, heart approximately 0.9 [17], 0.85 [25] and spinal cord 0.83 [17], 0.96 [25]. They also found that their models underperformed for the oesophagus with a DSC of approximately 0.7 [17] and 0.63 [25] which is consistent with the data in this study. However, they both used a model trained on their own clinical data rather than a generic model.

Each centre was given the freedom to choose their own method of recording contouring times and this resulted in centres using paired studies and non-paired studies with different patient numbers. A sample size calculation was performed for both prostate and head and neck timing using a standard statistical method for an unpaired and paired data set[26]. A significance level of 0.05, an 80% power and a standardised difference of 0.3 were chosen. Using the standard deviation from the data in this study, a difference between the 2 datasets of approximately 0.6 minutes and 0.7 minutes would be detectable for prostate and head and neck respectively for the paired study. A difference between the 2 datasets of approximately 0.3 minutes and 0.5 minutes would be detectable for prostate and head and neck respectively for the unpaired study. The calculation gave 51 patients required in each group for an unpaired study. If the study was paired then only 26 patients would be required in total. The benefit of an unpaired study however, is that no additional clinical work needs to be undertaken as measurements do not need to be repeated.

The results from The Christie suggests that inter-observer variability is improved through the use of DLC contouring which agrees with other studies[15]. However, this is a small study and further assessment is needed across a larger multi-centre dataset which has currently not been carried out within the literature.

A limitation of the study is that different DSC/DTA software was used by each centre so the values cannot be directly compared. However, they do give an indication of which contours were closer to clinical ones than others. It has been shown that a DSC larger than 0.65 should give a time saving[27] and although no individual contour times were calculated, the majority of contours analysed here had a DSC greater than 0.65. However, it has recently been shown

for a lung study[28] that surface DSC and added path length provide a better indicator of time-saving using auto-segmentation. It would be useful to assess these metrics for each structure.

Vandewinckele *et al*., (2020)[29] have produced recommendations for implementation and quality assurance of artificial intelligence applications in radiotherapy. In addition to the overlap and distance metrics used here, they also recommend to compare the overall volume and the dosimetric impact of the delineation uncertainty. It may be that the dosimetric impact of a DLC contour that is minimally different to a clinical contour is not clinically significant. van Rooj *et al*., (2019)[30] showed that differences in DLC contours patients with head and neck cancer did not produce clinically significant differences in radiotherapy plans.

9.5 Conclusions

The study shows clinical implementation of non-centre specific models for prostate and head and neck OAR contouring using Mirada DLCExpert can provide time savings. The study demonstrates that a generic model can be implemented and tested in different ways with use of a paired or non-paired study in order to fit in with the clinical workload at the centre. The DSC and DTA values showed good agreement with clinical contours for the majority of structures. The potential for reducing inter-observer variability has been shown but further work is needed to confirm this.

References

1. Walker, G. V.; Awan, M.; Tao, R.; Koay, E. J.; Boehling, N. S.; Grant, J. D.; Sittig, D. F.; Gunn, G. B.; Garden, A. S.; Phan, J.; Morrison, W. H.; Rosenthal, D. I.; Mohamed, A. S. R.; Fuller, C. D., (2014) 'Prospective Randomized Double-Blind Study of Atlas-Based Organ-at-Risk Autosegmentation-Assisted Radiation Planning in Head and Neck Cancer' ,. *Radiotherapy and Oncology*, *112* (3), pp. 321–325 doi: 10.1016/j.radonc.2014.08.028.
2. Mukesh, M.; Benson, R.; Jena, R.; Hoole, A.; Roques, T.; Scrase, C.; Martin, C.; Whitfield, G. A.; Gemmill, J.; Jefferies, S., (2012) 'Interobserver Variation in Clinical Target Volume and Organs at Risk Segmentation in Post-Parotidectomy Radiotherapy: Can Segmentation Protocols Help?' ,. *British Journal of Radiology*, *85* (1016), pp. 16–20 doi: 10.1259/bjr/66693547.
3. Steenbakkers, R. J. H. M.; Duppen, J. C.; Fitton, I.; Deurloo, K. E. I.; Zijp, L.; Uitterhoeve, A. L. J.; Rodrigus, P. T. R.; Kramer, G. W. P.; Bussink, J.; De Jaeger, K.; Belderbos, J. S. A.; Hart, A. A. M.; Nowak, P. J. C. M.; Van Herk, M.; Rasch, C. R. N., (2005) 'Observer Variation in Target Volume Delineation of Lung Cancer Related to Radiation Oncologist-Computer Interaction: A "Big Brother" Evaluation' ,. *Radiotherapy and Oncology*, *77* (2), pp. 182–190 doi: 10.1016/j.radonc.2005.09.017.

4. Bhardwaj, A.; Kehwar, T.; Chakarvarti, S.; Jayant Sastri, G.; Oinam, A.; Pradeep, G.; Kumar, V.; Indranil, M.; Sharma, S., (2021) 'Variations in Inter-Observer Contouring and Its Impact on Dosimetric and Radiobiological Parameters for Intensity-Modulated Radiotherapy Planning in Treatment of Localised Prostate Cancer' ,. *Journal of Radiotherapy in Practice*, *7*(2), pp.77-88 doi: 10.1017/S1460396908006316.

5. Brouwer, C. L.; Steenbakkers, R. J. H. M.; van den Heuvel, E.; Duppen, J. C.; Navran, A.; Bijl, H. P.; Chouvalova, O.; Burlage, F. R.; Meertens, H.; Langendijk, J. A.; van 't Veld, A. A., (2012) '3D Variation in Delineation of Head and Neck Organs at Risk' ,. *Radiation Oncology*, *7* (1) doi: 10.1186/1748-717X-7-32.

6. Schick, K.; Sisson, T.; Frantzis, J.; Khoo, E.; Middleton, M., (2011) 'An Assessment of OAR Delineation by the Radiation Therapist' ,. *Radiography*, *17* (3), pp. 183–187 doi: 10.1016/j.radi.2011.01.003.

7. La Macchia, M.; Fellin, F.; Amichetti, M.; Cianchetti, M.; Gianolini, S.; Paola, V.; Lomax, A. J.; Widesott, L., (2012) 'Systematic Evaluation of Three Different Commercial Software Solutions for Automatic Segmentation for Adaptive Therapy in Head-and-Neck, Prostate and Pleural Cancer' ,. *Radiation Oncology*, *7* (1), pp. 1 doi: 10.1186/1748-717X-7-160.

8. Simmat, I.; Georg, P.; Georg, D.; Birkfellner, W.; Goldner, G.; Stock, M., (2012) 'Assessment of Accuracy and Efficiency of Atlas-Based Autosegmentation for Prostate Radiotherapy in a Variety of Clinical Conditions' ,. *Strahlentherapie und Onkologie*, *188* (9), pp. 807–813 doi: 10.1007/s00066-012-0117-0.

9. Kim J, Han J, Ailawadi S, Baker J, Hsia A, Xu Z, R. S., (2016) 'SU-F-J-113: Multi-Atlas Based Automatic Organ Segmentation for Lung Radiotherapy Planning' ,. *Medical Physics*, *45* (6), pp. 3433–3433.

10. Zhong, H.; Kim, J.; Chetty, I. J., (2010) 'Analysis of Deformable Image Registration Accuracy Using Computational Modeling' ,. *Medical Physics*, *37* (3), pp. 970–979 doi: 10.1118/1.3302141.

11. Larrue, A.; Gujral, D.; Nutting, C.; Gooding, M., (2015) 'The Impact of the Number of Atlases on the Performance of Automatic Multi-Atlas Contouring' ,. *Physica Medica*, *31* (2015), pp. e30 doi: 10.1016/j.ejmp.2015.10.020.

12. Teguh, D. N.; Levendag, P. C.; Voet, P. W. J.; Al-Mamgani, A.; Han, X.; Wolf, T. K.; Hibbard, L. S.; Nowak, P.; Akhiat, H.; Dirkx, M. L. P.; Heijmen, B. J. M.; Hoogeman, M. S., (2011) 'Clinical Validation of Atlas-Based Auto-Segmentation of Multiple Target Volumes and Normal Tissue (Swallowing/Mastication) Structures in the Head and Neck' ,. *International Journal of Radiation Oncology Biology Physics*, *81* (4), pp. 950–957 doi: 10.1016/j.ijrobp.2010.07.009.

13. Meyer, P.; Noblet, V.; Mazzara, C.; Lallement, A., (2018) 'Survey on Deep Learning for Radiotherapy' ,. *Computers in Biology and Medicine*, *98*, pp. 126–146 doi: 10.1016/j.compbiomed.2018.05.018.

14. Dijk, L. V. Van; Bosch, L. Van Den; Aljabar, P.; Peressutti, D.; Both, S.; Steenbakkers, R. J. H. M.; Langendijk, J. A.; Gooding, M. J.; Brouwer, C. L., (2020) 'Improving Automatic Delineation for Head and Neck Organs at Risk by Deep Learning Contouring' ,. *Radiotherapy and Oncology*, *142*, pp. 115–123 doi: 10.1016/j.radonc.2019.09.022.

15. Kiljunen, T.; Akram, S.; Niemelä, J.; Löyttyniemi, E.; Seppälä, J.; Lehtiö, K.; Nikkinen, J.; Gershkevitsh, E.; Borkvel, A.; Adamson, M.; Master, Z.; Lee, M.;

Chua, K.; Joensuu, T.; Kononen, J., (2020) 'A Deep Learning-Based Automated CT Segmentation of Prostate Cancer Anatomy for Radiation Therapy' ,. *Diagnostics*, *10*(11), pp.959 doi: 10.3390/diagnostics10110959.

16. Nikolov, S.; Blackwell, S.; Zverovitch, A.; Mendes, R.; Livne, M.; De Fauw, J.; Patel, Y.; Meyer, C.; Askham, H.; Romera-Paredes, B.; Kelly, C.; Karthikesalingam, A.; Chu, C.; Carnell, D.; Boon, C.; D'Souza, D.; Moinuddin, S. A.; Garie, B.; McQuinlan, Y.; Ireland, S.; Hampton, K.; Fuller, K.; Montgomery, H.; Rees, G.; Suleyman, M.; Back, T.; Hughes, C.; Ledsam, J. R.; Ronneberger, O., (2018) 'Deep Learning to Achieve Clinically Applicable Segmentation of Head and Neck Anatomy for Radiotherapy' ,. *Journal of Medical Internet Research*, *23*(7), pp. e26151 doi: 10.2196/26151.

17. Lustberg, T.; Soest, J. Van; Gooding, M.; Peressutti, D.; Aljabar, P.; Stoep, J. Van Der; Elmpt, W. Van; Dekker, A., (2018) 'Clinical Evaluation of Atlas and Deep Learning Based Automatic Contouring for Lung Cancer' ,. *Radiotherapy and Oncology*, *126* (2), pp. 312–317 doi: 10.1016/j.radonc.2017.11.012.

18. Oktay, O.; Nanavati, J.; Schwaighofer, A.; Carter, D.; Bristow, M.; Tanno, R.; Jena, R.; Barnett, G.; Noble, D.; Rimmer, Y.; Glocker, B.; O'Hara, K.; Bishop, C.; Alvarez-Valle, J.; Nori, A., (2020) 'Evaluation of Deep Learning to Augment Image-Guided Radiotherapy for Head and Neck and Prostate Cancers' ,. *JAMA Network Open*, pp. 1–11 doi: 10.1001/jamanetworkopen.2020.27426.

19. Wong, J.; Huang, V.; Wells, D. M.; Giambattista, J. A.; Giambattista, J.; Kolbeck, C.; Otto, K.; Alexander, A. S., (2020) 'Implementation of Deep Learning-Based Auto-Segmentation for Radiotherapy Planning Structures: A Multi-Center Workflow Study' ,. *International Journal of Radiation Oncology Biology Physics*, *108* (3), pp. S101 doi: 10.1016/j.ijrobp.2020.07.2278.

20. Brouwer, C.L.; Steenbakkers, R.J.; Bourhis, J.; Budach, W.; Grau, C.; Grégoire, V.; Van Herk, M.; Lee, A.; Maingon, P.; Nutting, C.; O'Sullivan, B., (2015) 'CT-based delineation of organs at risk in the head and neck region: DAHANCA, EORTC, GORTEC, HKNPCSG, NCIC CTG, NCRI, NRG Oncology and TROG consensus guidelines' ,. *Radiotherapy and Oncology*, *117* (1), pp.83-90. doi: 10.1016/j.radonc.2015.07.041.

21. Dice, L.R., (1945) 'Measures of the amount of ecologic association between species',. *Ecology*, *26* (3), pp. 297–302 doi: 10.2307/1932409.

22. Chalana, V.; Kim, Y., (1997) 'A methodology for evaluation of boundary detection algorithms on medical images',. *IEEE Trans. Med. Imaging*, *16* (5), pp. 642–652 doi: 10.1109/42.640755.

23. Zabel, W. J.; Conway, J. L.; Gladwish, A.; Skliarenko, J.; Didiodato, G.; Goorts-matthews, L.; Mrt, T.; Michalak, A.; Mrt, T.; Reistetter, S.; Mrt, T.; King, J.; Nakonechny, K.; Malkoske, K.; Tran, M. N.; Mcvicar, N., (2021) 'Clinical Evaluation of Deep Learning and Atlas-Based Auto-Contouring of Bladder and Rectum for Prostate Radiation Therapy' ,. *Practical Radiation Oncology*, *11* (1), pp. e80–e89 doi: 10.1016/j.prro.2020.05.013.

24. Ibragimov, B.; Xing, L., (2017) 'Segmentation of Organs-at-Risks in Head and Neck CT Images Using Convolutional Neural Networks:' ,. *Medical Physics*, *44* (2), pp. 547–557 doi: 10.1002/mp.12045.

25. Vu, C. C.; Siddiqui, Z. A.; Zamdborg, L.; Thompson, A. B.; Quinn, T. J.; Castillo,

E.; Guerrero, T. M., (2020) 'Deep Convolutional Neural Networks for Automatic Segmentation of Thoracic Organs-at-Risk in Radiation Oncology – Use of Non-Domain Transfer Learning' ,. *Journal of Applied Clinical Medical Physics*, *21* (6), pp. 108–113 doi: 10.1002/acm2.12871.

26. Sim, J.; Wright, C., (2002) *Research in Healthcare, Concepts Designs and Methods*; Nelson Thornes.

27. Langmack, K. A.; Perry, C.; Sinstead, C.; Mills, J.; Saunders, D., (2014) 'The Utility of Atlas-Assisted Segmentation in the Male Pelvis Is Dependent on the Interobserver Agreement of the Structures Segmented' ,. *British Journal of Radiology*, *87* (1043) doi: 10.1259/bjr.20140299.

28. Vaassen, F.; Hazelaar, C.; Vaniqui, A.; Gooding, M.; van der Heyden, B.; Canters, R.; van Elmpt, W., (2020) 'Evaluation of Measures for Assessing Time-Saving of Automatic Organ-at-Risk Segmentation in Radiotherapy' ,. *Physics and Imaging in Radiation Oncology*, *13* (November 2019), pp. 1–6 doi: 10.1016/j.phro.2019.12.001.

29. Vandewinckele, L.; Claessens, M.; Dinkla, A.; Brouwer, C.; Crijns, W.; Verellen, D.; van Elmpt, W., (2020) 'Overview of Artificial Intelligence-Based Applications in Radiotherapy: Recommendations for Implementation and Quality Assurance' ,. *Radiotherapy and Oncology*, *153*, pp. 55–66 doi: 10.1016/j.radonc.2020.09.008.

30. Rooij, W. Van; Dahele, M.; Brandao, H. R.; Delaney, A. R.; Slotman, B. J.; Verbakel, W. F., (2019) 'Deep Learning-Based Delineation of Head and Neck Organs at Risk : Geometric and Dosimetric Evaluation' ,. *Radiation Oncology Biology*, *104* (3), pp. 677–684 doi: 10.1016/j.ijrobp.2019.02.040.

10 Evaluation of 3D and 4D Tumour Volumes for Lung Treatment Planning

Walker Z.[1], Shrimali R.[1], Hamilton J.[1], Best J.[1], Rogers J.[1]
[1] Medical Physics, University Hospitals Coventry and Warwickshire NHS Trust, Coventry, UK

Abstract

Purpose

To assess the difference in target volumes and dosimetric impact of using a 4DCT compared to a 3DCT for lung radiotherapy tumour outlining.

Methods

Gross tumour volumes were outlined for 29 patients with lung cancer using a 3DCT (GTV_{3D}) and a 4DCT (GTV_{4D}). PTVs were created using 1.5 cm superior/inferior, 1 cm anterior/posterior/left/right margins for the GTV_{3D} and 5 mm isotropic margins for the GTV_{4D}. All patients were planned in RayStation using 6MV volumetric modulated arc therapy (VMAT) with one or two arcs, with the dose prescribed to the PTV from the 4DCT (PTV_{4D}). 20 patients were retrospectively re-planned with the dose prescribed to the PTV from the 3DCT (PTV_{3D}), ensuring that the original clinical goals for tumour volume coverage and organs at risk (OARs) were still met. The volumes of GTVs and PTVs using both methods and were compared. The doses to the OARs were compared using a Wilcoxon signed rank test.

Results

The GTV_{4D} volumes were larger than the GTV_{3D} volumes in 93% of patients analysed. The PTV_{4D} volumes were smaller than the PTV_{3D} volumes in 86% of patients. There was a statistically significant difference in both GTV and PTV volumes when using the 4DCT to outline compared to the 3DCT ($p<0.001$). The OAR doses were statistically significantly lower for the lungs $V_{5,}$ ($p=0.002$), lungs V_{10} ($p=0.002$), average heart ($p=0.04$) and 1cc cord ($p=0.007$).

Conclusions

The use of 4DCT for lung tumour outlining significantly reduces the PTV volume and the doses to OARs. This could reduce radiation induced toxicity or alternatively allow for dose escalation.

10.1 Introduction

Treating tumours with radiotherapy can be challenging for sites where the tumour is moving. A 4DCT can be used for radiotherapy treatment planning to capture the full range of respiratory motion of a tumour and the organs at risk (OARs), thus allowing planning target volume (PTV) margins to be reduced[1,2]. It is of particular importance for patients with lung cancer where tumour motion can be large. Studies show that amplitudes in the superior-inferior direction are largest, with average amplitudes of 6.9 mm and 12 mm quoted in literature[3,4] and up to 53 mm being observed[3].

Several studies have investigated the differences in outlines created for lung tumours using a 3DCT or 4DCT[5-8] as well as 3D and 4D PET/CT[9]. These have shown that outlining using a 4D dataset can reduce target volumes compared to using a 3D dataset.

Few studies have compared the dosimetric impact of the differences in 3D and 4D CT outlines through re-optimising plans. Wang *et al*., (2009)[10] and Hof *et al.*, (2009)[11] evaluated doses for patients receiving lung stereotactic ablative radiotherapy (SABR). Both studies found that using 4D PTVs decreased lung doses but doses to other OARs were not assessed. Bai *et al*., (2014)[12] assessed doses for non-SABR lung cancer patient CT outlines and again found that dose to lung was lower using 4D PTVs in addition to the spinal cord and heart doses. However, this was a small-scale study of 10 patients who all had stage T1 tumours. A larger study of different stage tumours re-optimising lung plans using 3D or 4D PTVs has not been performed.

The sparing of normal tissue through using 4D outlining may allow for dose escalation[12] and therefore greater tumour control. Studies have shown that dose escalation in non-small-cell lung cancer can give improvements in tumour control[13,14] and this could improve overall survival.

This study investigates the differences between outlining lung tumours using a 3D or 4D CT and how optimising the plan using 3D or 4D outlined tumour volumes affects the doses to OARs. The dataset is from clinical patients with a variety of tumour stages.

10.2 Methods

10.2.1 Patient Selection

Twenty-nine patients with lung tumours were included in this study that had a 4DCT for radiotherapy planning. As this was a prospective study and the outlining was part of the planning process, as many patients were recruited as possible but these were not consecutive as those where a 3D outline was not saved were excluded. In addition, those with a clinical target volume (CTV) expansion outside standard protocol were excluded. The patients analysed were treated by 3 different clinicians. The tumour characteristics are given in Table 10.1.

Table 10.1: Tumour characteristics for lung tumours included in the study. n is the number of tumours. One was a colorectal metastasis and did not have a tumour stage.

Tumour stage	**n**	**Nodal involvement**	**n**	**Metastatic**	**n**	**Location**	**n**
1	4	N0	4	M0	18	Rt upper	9
2	2	N1	6	M1	10	Lt upper	7
3	10	N2	13			Lt lower	1
4	12	N3	5			Rt lower	3
						Mediastinum	1
						Unspecified	7

10.2.2 Image Acquisition

All patients were scanned at University Hospital Coventry on a GE discovery CT590 (GE Medical Systems) and had a contrast-enhanced helical 3DCT from the larynx to the mid-abdomen, covering the entire lung volumes for treatment planning. Patients had a localised axial 4DCT for tumour outlining with scan limits specified by a clinician. Patients were scanned in free-breathing and were uncoached with the breathing trace obtained using the Varian real-time position management RPM system (Varian Medical Systems, Palo Alto, CA) with 2 marker reflective block placed on the surface of the patient. The 4DCT was reconstructed into 10 bins using the Advantage4D software (GE Medical Systems). The

images were acquired at the planning appointment, with the patient in the same position, and the resulting images were fused for planning.

10.2.3 Tumour Delineation

Patients were outlined using the anatomy module in RayStation (version 7, RaySearch, Sweden). The local outlining protocol mandates that the radiation oncologist starts by outlining the GTV on the 3DCT image, before using the fused 4DCT to add in the motion envelope in order to create an internal target volume (ITV). Therefore, the GTV outlined on the 3DCT (GTV_{3D}) and the ITV were saved at the time of outlining by the oncologist. An isotropic 0.5 cm CTV margin and an anisotropic PTV margin of 1 cm left/right/anterior/posterior and 1.5 cm superior/inferior were added to the GTV_{3D} to create PTV_{3D}. This outlining method was previously used at the centre prior to the introduction of 4DCT. Immediately after outlining the GTV_{3D}, clinicians use the 4DCT to contour a moving GTV (GTV_{4D}). This was copied to the 3DCT and a 0.5 cm isotropic CTV and a 0.5 cm isotropic PTV margin were added to create a PTV_{4D} as per the current local protocol.

The average PTV volumes using the 2 methods were calculated and compared using a Wilcoxon signed rank test as the data was found to be not normally distributed. The volumes of $4D_{GTV}$ and $4D_{PTV}$ outside the $3D_{PTV}$ were calculated to assess any geometric misses as in Callahan *et al.* (2014)[9].

10.2.4 Treatment Planning

The 3DCT was used for planning and dosimetric calculations with OARs outlined on this scan and the scan subsequently used as reference image for online verification using cone-beam CT. All patients were planned in RayStation using 6MV VMAT with one or two arcs, with the dose prescribed to the PTV_{4D}. Twenty of the patients were re-planned with the dose prescribed to the PTV_{3D}, ensuring that the original clinical goals for tumour volume coverage and OARs were still met. Conformity indices were calculated for the prescription dose and half of the prescription dose using both methods to ensure that the conformity in both plans was similar. The OAR doses from the PTV_{3D} plans were compared to the clinical PTV_{4D} plans. The percentage volume of PTV_{4D} covered by 95% of the prescription dose from the 3D plan (D95) was assessed as in Callahan *et al.* (2014)[14]. The doses to the OARs from the 2 methods were compared using a Wilcoxon signed rank test. All statistical analysis was performed in SPSS (V25, IBM).

10.3 Results

10.3.1 GTV and PTV Volumes

The GTV_{4D} volumes were larger than the GTV_{3D} volumes for 27 of 29 patients (93%) (Figure 10.1). For the entire cohort on average the GTV_{4D} was larger compared to GTV_{3D} by 26(±5)% (range -1% to +98%).

The PTV_{4D} volumes were smaller than the PTV_{3D} volumes for 25 patients of 29 (86%) (Figure 10.2). For the entire cohort, on average the PTV_{4D} was smaller compared to the PTV_{3D} by 24(±3)% (range -52% to +16%).

There was a statistically significant difference in both GTV and PTV volumes when using the 4DCT to outline compared to the 3DCT (Table 10.2). The distribution of the results is shown in Figure 10.3.

Table 10.2: Mean volume of 3D and 4D GTVs and PTVs for 29 lung tumours and the difference in means. The p-value significance was computed from a Wilcoxon signed rank test comparing the volumes of the 3D and 4D structures.

Structure	Mean Volume (cm^3)	Difference in means 4D-3D (cm^3)	p-value
3DGTV	170.8±33.0	+21.0±47.3	<0.001
4DGTV	191.8±34.0		
3DPTV	610.1±69.8	-143.6±93.8	<0.001
4DPTV	466.5±62.7		

Five patients had a volume of 4DGTV extending outside the 3DPTV. The average percentage volume of 4DGTV missed was 0.12(±0.06)% (range 0.02% to 0.3%).

Twenty-five patients had a volume of 4DPTV extending outside the 3DPTV. The average percentage volume of 4DPTV missed was 3.22 (±0.59)% (range 0% to 27.65%).

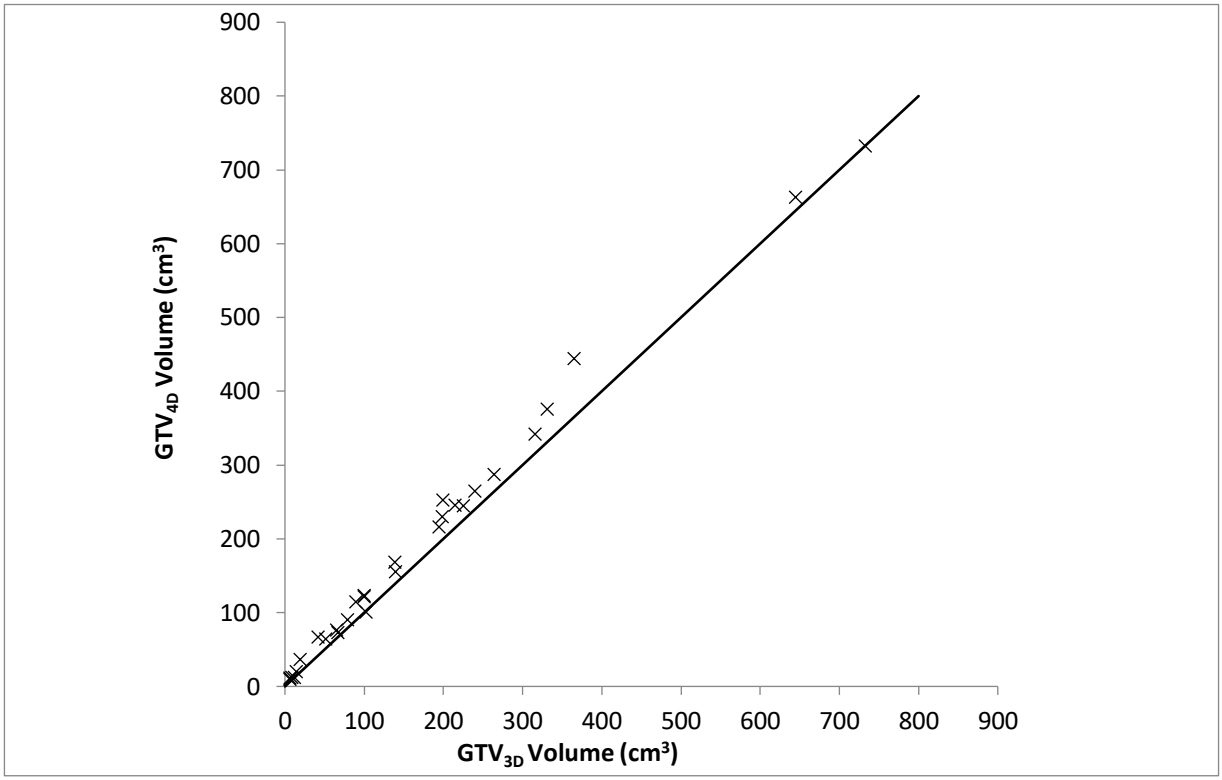

Figure 10.1: GTV_{4D} vs GTV_{3D} for 29 lung tumours. The black line is a one-to-one relationship between the GTV_{4D} and the GTV_{3D}.

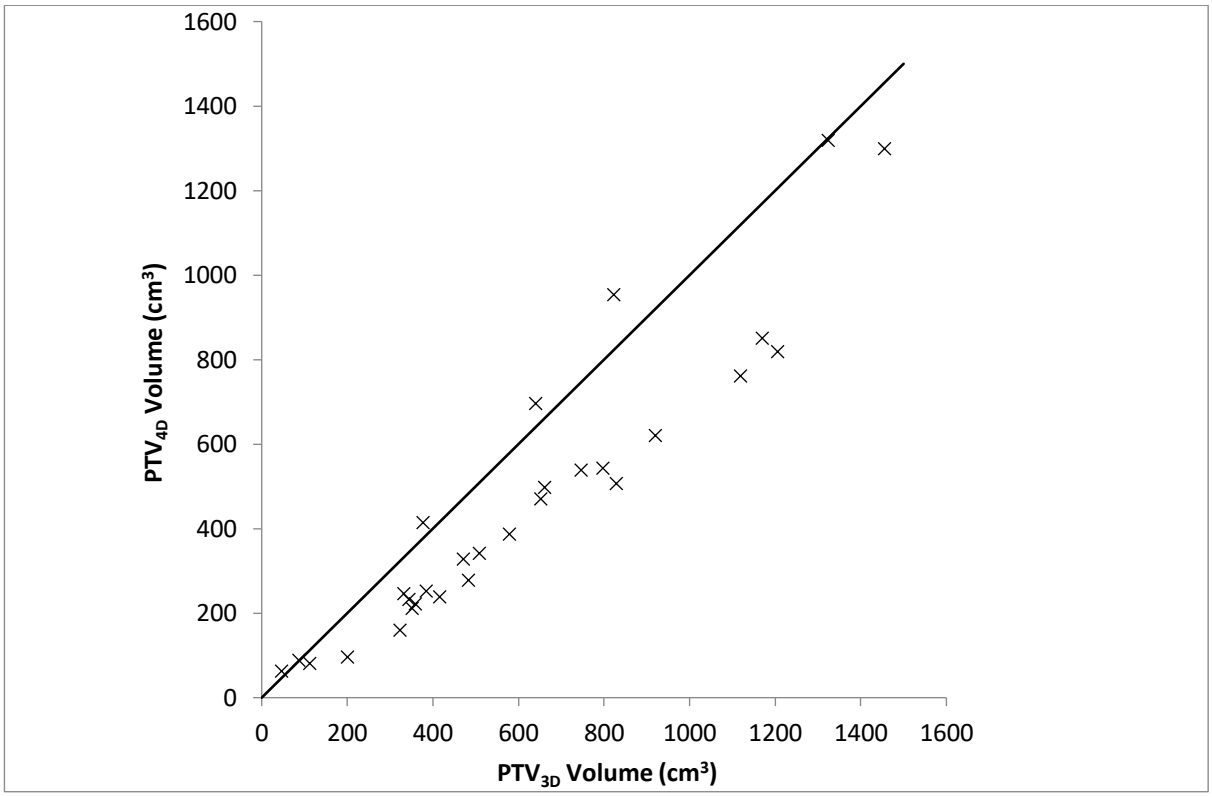

Figure 10.2: PTV_{4D} vs PTV_{3D} for 29 lung tumours. The black line is a one-to-one relationship between the PTV_{4D} and the PTV_{3D}.

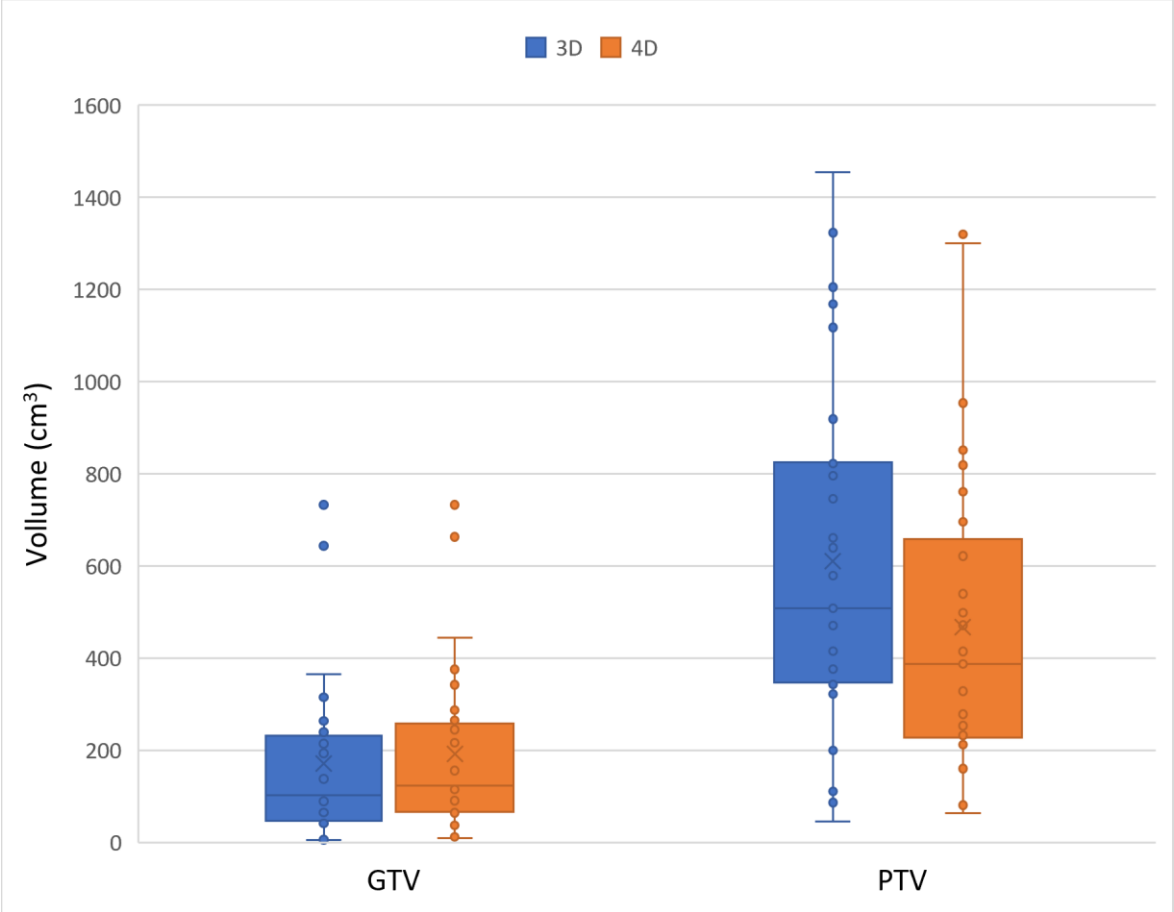

Figure 10.3: Box and whisker plot of 3D and 4D GTV and PTV volumes for 29 lung tumours. The boxes indicate the interquartile range (IQR), the line indicates the median and the cross indicates the mean. The whiskers indicate the highest and lowest values within 1.5 times the IQR and circles indicate all data points.

10.3.2 Treatment Plans

Eighteen plans had areas of the PTV_{4D} that would not have been covered by the D95 of the 3D plan. The average percentage volume of PTV_{4D} not covered by the D95 from the 3D plan was 3.5±2.3%.

The OAR doses were statistically significantly lower for the lungs V_5, lungs V_{10}, average heart and 1cc cord using the 4D outlines compared to the 3D outlines (Table 10.3).

Table 10.3: Average organ at risk (OAR) doses for plans using a PTV_{3D} outline and a PTV_{4D} outline. Doses for lungs are for lungs excluding ITV or GTV_{3D}. P-values are from a Wilcoxon signed rank test.

OAR	3D Outline	4D Outline	p-value
Lungs V_5 (%)	47.2±2.9	42.8±3.1	0.002
Lungs V_{10} (%)	31.1±2.5	28.8±2.6	0.002
Lungs V_{20} (%)	20.9±2.0	20.8±2.7	0.052
Heart average (Gy)	10.0±1.8	8.5±1.6	0.004
Cord 1cc (Gy)	25.4±2.3	23.3±2.1	0.007

10.4 Discussion

The results show that the GTV_{4D} was larger than the GTV_{3D} for 93% of patients analysed and this was statistically significant. The average volume increase of 26% when the GTV is outlined using the 4DCT is comparable to other studies, for example Ahmed *et al.* (2017)[8] who observed an increase of 25%. This suggests that a 4DCT is required to capture the full range of respiratory motion of lung tumours.

The PTV_{4D} was smaller compared to the PTV_{3D} by 24% on average which was also comparable to other studies such as Hof *et al*., (2009)[11] who found a 31% reduction and Bai *et al*. (2014)[12] who found a 15.5% reduction. The study here also indicates that the PTV_{3D} margins that were previously used at the centre were not always adequate to cover the tumour motion with 5 patients having GTV_{4D} outside PTV_{3D}. However, these volumes were very small in comparison to the tumour volume and would not be clinically significant as the volumes are likely to be less than inter-observer variability when outlining. It has been shown that the mean dice score from contouring of CTV from a large set of trial data outlined by 21 clinicians was 0.8[15]. This variation would be larger than the maximum percentage volume difference seen here of 0.3%. In the work here, different clinicians have outlined different patients. Further work could be carried out to assess inter-observer variation of tumour delineation within the current dataset.

The difference in OAR doses for the 4D plan compared to the 3D plan were statistically significant for the heart, cord and lungs V_{10} and V_5. The absolute reduction in average dose was similar to Bai *et al*. (2014)[12] as shown in Table 10.4, although they also found the lung V_{20} to be statistically significant. All plans in the study still met the clinical goals for lung planning even though the 4D doses were statistically significantly lower. However, reducing

doses to OARs can reduce toxicity. Ghita *et al.* (2019)[16] found significant correlation between V_{10} and mean lung dose with late response in a lung study irradiating mice. It has also been shown that V_5, V_{10}, V_{20}, mean lung dose of the ipsilateral lung and V_5, V_{10}, V_{20}, V_{30} and mean lung dose of the bilateral lung of the ipsilateral lung are associated with Grade ≥2 radiation-induced lung injury[17]. Liao *et al.* (2010)[18] found strongest correlations with pneumonitis for V_5 to V_{30} in the ipsilateral lung. However, it has been suggested that mean lung dose or average dose in proportion to the whole lung volume may be better indicators of radiation pneumonitis in stereotactic radiotherapy[19]. Further work will be required to assess this for the patients in this study.

Table 10.4: Dose difference for OARs using 4D tumour outlining compared to 3D tumour outlining in this study and literature. The differences are the 3D parameter values minus the 4D parameter values.

	Absolute difference in parameter (3D-4D)	
Parameter	**Current Study**	**Bai *et al*. (2014)**
Lungs V_5 (%)	4.4	3.12
Lungs V_{10} (%)	2.3	4.75
Lungs V_{20} (%)	0.1	3.0
Heart average (Gy)	1.5	0.78
Cord 1cc (Gy)	2.1	1.95

Although the absolute differences in doses are small, the reduction in heart dose is still important clinically. The Radiation Therapy Oncology Group trial 06172[20] evaluating different doses for non-small cell lung cancer, reported that heart dose was associated with a worse overall survival at a median follow-up of 2 years. A reduction in the OAR doses could allow for dose escalation and dose escalation has been shown to improve local control and overall survival for patients with lung cancer[21,22].

In the current study the 3D and 4D GTVs for each patient were both outlined in one session by the same clinician at the same sitting with the same background information (radiology, pathology and clinical information) for each patient. This will have helped to reduce some of the bias that may affect planning studies using retrospectively outlined structures. There could be a potential bias from creating the 4D contours using the knowledge of the 3D contours but all contours were reviewed across all phases before they were accepted.

Another limitation is that the 3D and 4D plans were not always planned by the same members of staff. In order to reduce any dependence of plan quality on the observer producing the plan, the same planning parameters were used in the 3D plan as the clinical 4D plan as a starting point. The number of iterations for optimisation were not available for the clinical plans so this could not be matched. However, the conformity index for the GTV was compared and there was found to be an average of 0.001 difference between the 3D and 4D plans.

10.5 Conclusions

The previous 3D PTV margins used did not always incorporate the full range of motion, although the volumes not covered were very small. The use of 4DCT for lung tumour outlining significantly reduces the PTV volume and the doses to organs at risk. This could reduce radiation induced toxicity or alternatively allow for dose escalation.

10.6 References

1. Rietzel, E.; Liu, A. K.; Doppke, K. P.; Wolfgang, J. A.; Chen, A. B.; Chen, G. T. Y.; Choi, N. C., (2006) 'Design of 4D Treatment Planning Target Volumes' ,. *International Journal of Radiation Oncology Biology Physics*, *66* (1), pp. 287–295 doi: 10.1016/j.ijrobp.2006.05.024.
2. Khan, F.; Bell, G.; Antony, J.; Palmer, M.; Balter, P.; Bucci, K.; Chapman, M. J., (2009) 'The Use of 4DCT to Reduce Lung Dose: A Dosimetric Analysis' ,. *Medical Dosimetry*, *34* (4), pp. 273–278.
3. Sarudis, S.; Karlsson Hauer, A.; Nyman, J.; Bäck, A., (2017) 'Systematic Evaluation of Lung Tumor Motion Using Four-Dimensional Computed Tomography' ,. *Acta Oncologica*, *56* (4), pp. 525–530 doi: 10.1080/0284186X.2016.1274049.
4. Seppenwoolde, Y.; Shirato, H.; Kitamura, K.; Shimizu, S.; Van Herk, M.; Lebesque, J. V.; Miyasaka, K., (2002) 'Precise and Real-Time Measurement of 3D Tumor Motion in Lung Due to Breathing and Heartbeat, Measured during Radiotherapy' ,. *International Journal of Radiation Oncology Biology Physics*, *53* (4), pp. 822–834 doi: 10.1016/S0360-3016(02)02803-1.
5. Bradley, J. D.; Nofal, A. N.; El Naqa, I. M.; Lu, W.; Liu, J.; Hubenschmidt, J.; Low, D. A.; Drzymala, R. E.; Khullar, D., (2006) 'Comparison of Helical, Maximum Intensity Projection (MIP), and Averaged Intensity (AI) 4D CT Imaging for Stereotactic Body Radiation Therapy (SBRT) Planning in Lung Cancer' ,. *Radiotherapy and Oncology*, *81* (3), pp. 264–268 doi: 10.1016/j.radonc.2006.10.009.
6. Li, F. X.; Li, J. Bin; Zhang, Y. J.; Liu, T. H.; Tian, S. Y.; Xu, M.; Shang, D. P.; Ma, C. S., (2011) 'Comparison of the Planning Target Volume Based on Three-

Dimensional CT and Four-Dimensional CT Images of Non-Small-Cell Lung Cancer' ,. *Radiotherapy and Oncology*, *99* (2), pp. 176–180 doi: 10.1016/j.radonc.2011.03.015.

7. Li, F.; Li, J.; Zhang, Y.; Xu, M.; Dongping, S.; Tingyong, F.; Liu, T.; Shao, Q., (2013) 'Geometrical Differences in Gross Target Volumes between 3dct and 4dct Imaging in Radiotherapy for Non-Small-Cell Lung Cancer' ,. *Journal of Radiation Research*, *54* (5), pp. 950–956 doi: 10.1093/jrr/rrt017.

8. Ahmed, N.; Venkataraman, S.; Johnson, K.; Sutherland, K.; Loewen, S. K., (2017) 'Does Motion Assessment with 4-Dimensional Computed Tomographic Imaging for Non-Small Cell Lung Cancer Radiotherapy Improve Target Volume Coverage?' ,. *Clinical Medicine Insights: Oncology*, *11* doi: 10.1177/1179554917698461.

9. Callahan, J.; Kron, T.; Siva, S.; Simoens, N.; Edgar, A.; Everitt, S.; Schneider, M. E.; Hicks, R. J., (2014) 'Geographic Miss of Lung Tumours Due to Respiratory Motion: A Comparison of 3D vs 4D PET/CT Defined Target Volumes' ,. *Radiation Oncology*, *9* (1), pp. 1–8 doi: 10.1186/s13014-014-0291-6.

10. Wang, L.; Hayes, S.; Paskalev, K.; Jin, L.; Buyyounouski, M. K.; Ma, C. C. M.; Feigenberg, S., (2009) 'Dosimetric Comparison of Stereotactic Body Radiotherapy Using 4D CT and Multiphase CT Images for Treatment Planning of Lung Cancer: Evaluation of the Impact on Daily Dose Coverage' ,. *Radiotherapy and Oncology*, *91* (3), pp. 314–324 doi: 10.1016/j.radonc.2008.11.018.

11. Hof, H.; Rhein, B.; Haering, P.; Kopp-Schneider, A.; Debus, J.; Herfarth, K., (2009) '4D-CT-Based Target Volume Definition in Stereotactic Radiotherapy of Lung Tumours: Comparison with a Conventional Technique Using Individual Margins' ,. *Radiotherapy and Oncology*, *93* (3), pp. 419–423 doi: 10.1016/j.radonc.2009.08.040.

12. Bai, T.; Zhu, J.; Yin, Y.; Lu, J.; Shu, H.; Wang, L.; Yang, B., (2014) 'How Does Four-Dimensional Computed Tomography Spare Normal Tissues in Non-Small Cell Lung Cancer Radiotherapy by Defining Internal Target Volume?' ,. *Thoracic Cancer*, *5* (6), pp. 537–542 doi: 10.1111/1759-7714.12126.

13. Wang, L.; Correa, C. R.; Zhao, L.; Hayman, J.; Kalemkerian, G. P.; Lyons, S.; Cease, K.; Brenner, D.; Kong, F. M., (2009) 'The Effect of Radiation Dose and Chemotherapy on Overall Survival in 237 Patients With Stage III Non-Small-Cell Lung Cancer' ,. *International Journal of Radiation Oncology Biology Physics*, *73* (5), pp. 1383–1390 doi: 10.1016/j.ijrobp.2008.06.1935.

14. Machtay, M.; Bae, K.; Movsas, B.; Paulus, R.; Gore, E. M.; Komaki, R.; Albain, K.; Sause, W. T.; Curran, W. J., (2012) 'Higher Biologically Effective Dose of Radiotherapy Is Associated with Improved Outcomes for Locally Advanced Non-Small Cell Lung Carcinoma Treated with Chemoradiation: An Analysis of the Radiation Therapy Oncology Group' ,. *International Journal of Radiation Oncology Biology Physics*, *82* (1), pp. 425–434 doi: 10.1016/j.ijrobp.2010.09.004.

15. Tsang, Y.; Hoskin, P.; Spezi, E.; Landau, D.; Lester, J.; Miles, E.; Conibear, J., (2019) 'Assessment of Contour Variability in Target Volumes and Organs at Risk in Lung Cancer Radiotherapy' ,. *Technical Innovations and Patient Support in Radiation Oncology*, *10*, pp. 8–12 doi: 10.1016/j.tipsro.2019.05.001.

16. Ghita, M.; Dunne, V. L.; McMahon, S. J.; Osman, S. O.; Small, D. M.; Weldon, S.; Taggart, C. C.; McGarry, C. K.; Hounsell, A. R.; Graves, E. E.; Prise, K. M.; Hanna, G. G.; Butterworth, K. T., (2019) 'Preclinical Evaluation of Dose-Volume Effects and Lung Toxicity Occurring In and Out-of-Field' ,. *International Journal of*

Radiation Oncology Biology Physics, *103* (5), pp. 1231–1240 doi: 10.1016/j.ijrobp.2018.12.010.

17. Chen, J.; Hong, J.; Zou, X.; Lv, W.; Guo, F.; Hong, H.; Zhang, W., (2015) 'Association between Absolute Volumes of Lung Spared from Low-Dose Irradiation and Radiation-Induced Lung Injury after Intensity-Modulated Radiotherapy in Lung Cancer: A Retrospective Analysis' ,. *Journal of Radiation Research*, *56* (6), pp. 883–888 doi: 10.1093/jrr/rrv057.

18. Liao, Z. X.; Komaki, R. R.; Thames, H. D.; Liu, H. H.; Tucker, S. L.; Mohan, R.; Martel, M. K.; Wei, X.; Yang, K.; Kim, E. S.; Blumenschein, G.; Hong, W. K.; Cox, J. D., (2010) 'Influence of Technologic Advances on Outcomes in Patients With Unresectable, Locally Advanced Non-Small-Cell Lung Cancer Receiving Concomitant Chemoradiotherapy' ,. *International Journal of Radiation Oncology Biology Physics*, *76* (3), pp. 775–781 doi: 10.1016/j.ijrobp.2009.02.032.

19. Harder, E. M.; Park, H. S. M.; Chen, Z.; Decker, R. H., (2015) 'Pulmonary Dose Volume Predictors of Radiation Pneumonitis After Stereotactic Body Radiation Therapy' ,. *International Journal of Radiation Oncology*Biology*Physics*, *93* (3), pp. E427 doi: 10.1016/j.ijrobp.2015.07.1635.

20. Bradley, J. D.; Paulus, R.; Komaki, R.; Masters, G.; Blumenschein, G.; Schild, S.; Bogart, J.; Hu, C.; Forster, K.; Magliocco, A.; Kavadi, V.; Garces, Y. I.; Narayan, S.; Iyengar, P.; Robinson, C.; Wynn, R. B.; Koprowski, C.; Meng, J.; Beitler, J.; Gaur, R.; Curran, W.; Choy, H., (2015) 'Standard-Dose versus High-Dose Conformal Radiotherapy with Concurrent and Consolidation Carboplatin plus Paclitaxel with or without Cetuximab for Patients with Stage IIIA or IIIB Non-Small-Cell Lung Cancer (RTOG 0617): A Randomised, Two-by-Two Factorial Phase 3 Study' ,. *The Lancet Oncology*, *16* (2), pp. 187–199 doi: 10.1016/S1470-2045(14)71207-0.

21. Belderbos, J. S. A.; Heemsbergen, W. D.; De Jaeger, K.; Baas, P.; Lebesque, J. V., (2006) 'Final Results of a Phase I/II Dose Escalation Trial in Non-Small-Cell Lung Cancer Using Three-Dimensional Conformal Radiotherapy' ,. *International Journal of Radiation Oncology Biology Physics*, *66* (1), pp. 126–134 doi: 10.1016/j.ijrobp.2006.04.034.

22. Brower, J. V.; Amini, A.; Chen, S.; Hullett, C. R.; Kimple, R. J.; Wojcieszynski, A. P.; Bassetti, M.; Witek, M. E.; Yu, M.; Harari, P. M.; Baschnagel, A. M., (2016) 'Improved Survival with Dose-Escalated Radiotherapy in Stage III Non-Small-Cell Lung Cancer: Analysis of the National Cancer Database' ,. *Annals of Oncology*, *27* (10), pp. 1887–1894 doi: 10.1093/annonc/mdw276.

11 Extraction of Breathing Traces from 4D Cone-Beam CT

Walker Z.[1], Chuter R.[2], Rogers J.[1]
[1] Medical Physics, University Hospitals Coventry and Warwickshire NHS Trust, Coventry, UK; [2]The Christie Medical Physics and Engineering, The Christie NHS Foundation Trust, Manchester, UK;

Abstract

Purpose

To develop and test a method of breathing trace extraction from binned 4D cone-beam CT (4DCBCT) data. This would be of benefit as this data is normally clinically available rather than individual projection data and the tumour motion is used rather than a surrogate.

Methods

The Amsterdam shroud script from the open-source Reconstruction Toolkit (RTK) was used to create an Amsterdam shroud from binned moving images. A Python script was created to obtain the amplitude change at each breathing phase in the craniocaudal direction by taking a profile through each phase in the Amsterdam shroud image and shifting to match the adjacent phase. For 4DCBCT images, the breathing period for each phase was obtained by extracting frame rate and phase from the scan.sort file. The scan.sort file is a text file generated in Elekta XVi for each 4DCBCT reconstructed scan and contains frames and their allocated phase. The method was tested for a generated dataset of a square box moving by a fixed number of pixels, a 4DCT and 4DCBCT of an in-house phantom moving at 1.5 cm amplitude and a 4DCT and 4DCBCT of 2 lung cancer patient tumours. The method was also compared to computing the centroid of a moving outline.

Results

The script agreed with the generated data to within 2%, with the largest error seen at 1 mm movement. The script overestimated the amplitude of the phantom movement across the breathing cycle and by 4% at the peak for the phantom 4DCT. This was better than the centroid method which gave a peak amplitude of 8% less than expected. For the 4DCBCT, the script underestimated the amplitude of the phantom movement across the breathing cycle and by 17% at the peak. The centroid method performed better on the 4DCBCT giving a peak amplitude 7% larger than expected.

Conclusions

A method using the Amsterdam shroud on binned images was shown to work for theoretical data. On 4DCT images, the method outperformed a tumour centroid method. However, for 4DCBCT, the results were not adequate, with the amplitude being underestimated by the method. Further development and testing are required to see if this method could be adapted for 4DCBCT.

11.1 Introduction

Respiratory motion can cause tumours in the thorax and abdomen to move[1,2] which can cause issues for radiotherapy treatment where a precise dose is planned and delivered to a tumour volume. To evaluate tumour movement for radiotherapy treatment planning, a 4DCT can be used. On treatment, the tumour movement can be assessed using 4D cone-beam CT (4DCBCT) using a kV imager mounted to the linear accelerator gantry.

To produce a 4D dataset, a breathing trace needs to be correlated with the images obtained. The breathing trace can be obtained using an external surrogate such as a marker block on the patient surface[3] or an abdominal belt[4]. The problem with use of a surrogate it that is external and it may not correlate with the internal motion[5,6]. Fiducial markers can be used which are implanted but this invasive and fiducial migration is also a concern[7].

Methods have also been developed to extract a breathing trace from the images obtained. One method uses pixel variations between image projections within a region of interest to obtain a breathing trace at each angle[10,11]. Another method uses an Amsterdam shroud technique. This applies a cranio-caudal filter to images and projects each image on the cranio-caudal axis. The images are then combined to create a 2D image known as an Amsterdam shroud. The temporal derivate (i.e. subtracting each column from the adjacent column) of the shroud is taken and projected onto the cranio-caudal axis. Each 1D column aligned to the adjacent column giving displacements which indicate the breathing signal[8,9]. This is the method used by Elekta for 4D reconstruction in their CBCT (XVi) system. Other methods for breathing trace extraction have also been developed. Vergalasova *et al.* (2011)[13] used a Fourier method by monitoring changes in Fourier transform phase to obtain a

breathing signal. Yan *et al*., (2013)[12] used local principal component analysis (LPCA) which uses feature extraction and distinguishing gantry movements from breathing movements.

All methods found in the literature for 4DCBCT breathing trace extraction require individual projections and these are not always readily available. One study used binned data for breathing trace extraction from 4DCT only, using a volume of interest method[13]. The study presented here develops and tests a method of breathing trace extraction from 4DCBCT using binned data with an Amsterdam shroud technique to see if this would be a feasible approach. This would be of benefit as binned data is normally available in clinics and breathing trace extraction from these images would be useful for programming of phantoms with realistic breathing traces for measurements to assess planning techniques or delivery. The traces extracted will also be from the tumour motion rather than a surrogate.

11.2 Methods

11.2.1 Breathing Trace Extraction

Phase-binned images were exported from XVi and a Python script created to import the images and allow the user to select the coronal slice and area of focus for movement analysis (Figure *11.1*).

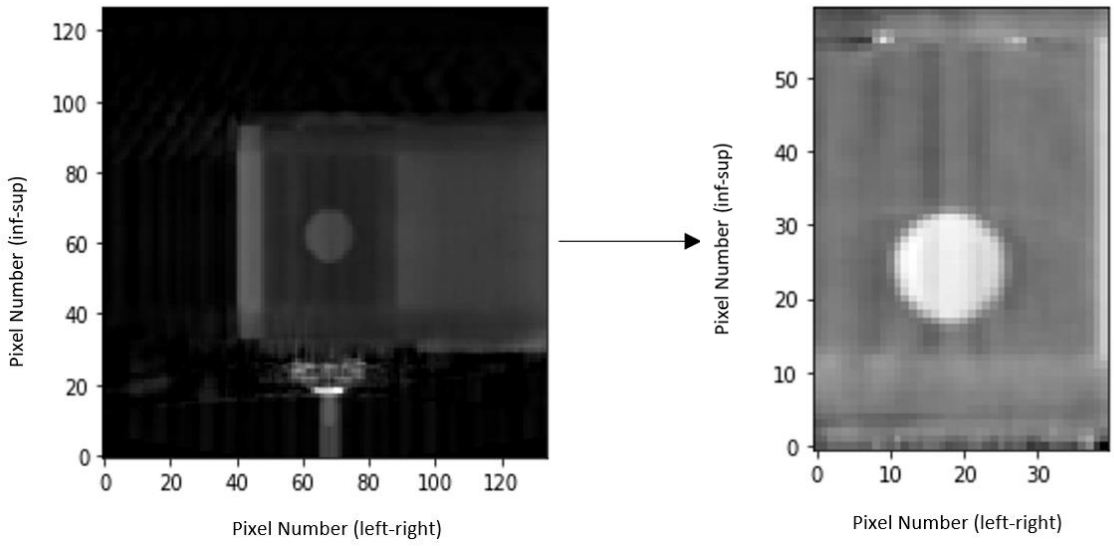

Figure 11.1: Left-Coronal slice of the 50% phase XVi of moving phantom. Right-Area of this slice cropped for use in Amsterdam shroud code.

The selected area was analysed using the Reconstruction Toolkit (RTK) Amsterdam shroud script (RTK 2.2.0)[14]. RTK is open-source software that is used for CBCT reconstruction and

has scripts for image manipulation. The Amsterdam shroud script projects each 2D image onto a 1D axis after applying filtering and was run on each phase for the selected area to give an Amsterdam shroud image (Figure 11.2).

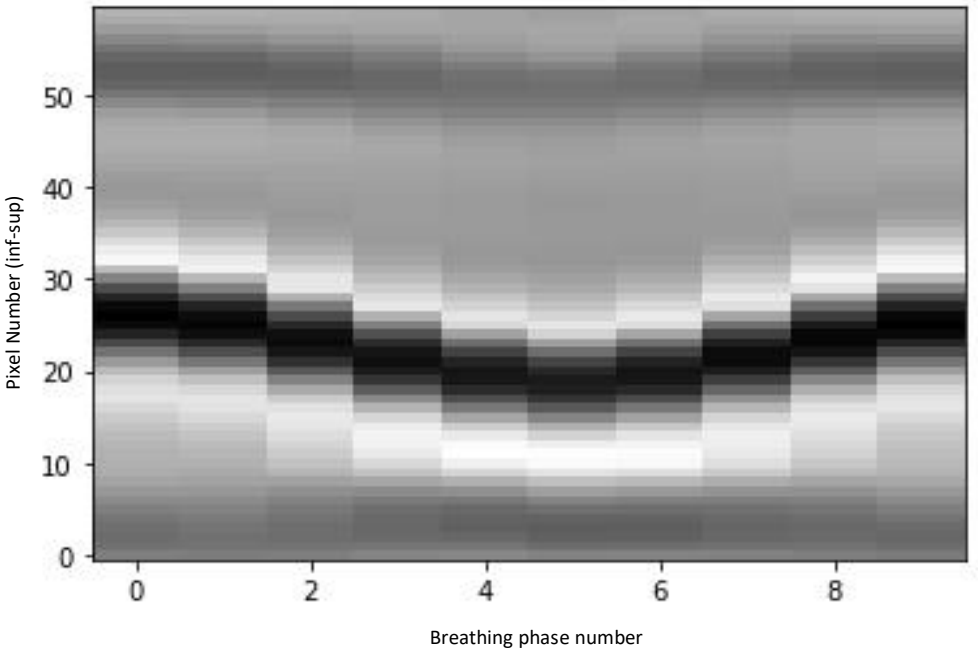

Figure 11.2: Example of an Amsterdam shroud for each breathing phase of a moving phantom using the Python script and RTK software.

The amplitude was calculated from the Amsterdam shroud in the cranio-caudal direction for each of the ten phases by computing a profile for each phase and matching it to the adjacent phase in Python (Figure 11.3). The displacement needed to match one phase to the next in pixels was multiplied by the length per pixel to obtain a displacement in millimetres. Each coronal slice throughout the visible tumour volume was assessed and the slice with the maximum total amplitude selected.

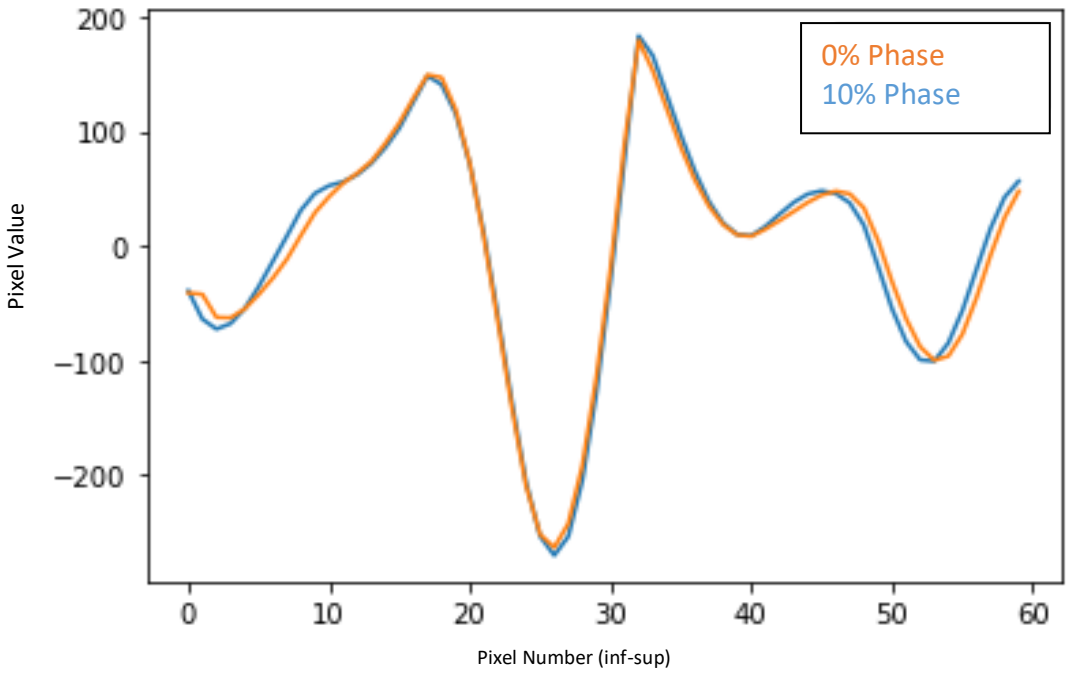

Figure 11.3: Example of the profile taken in the inferior to superior direction from the Amsterdam shroud for 0% phase and 10% phase using the script in Python. The result shows the match after the 10% profile has been shifted.

11.2.2 Tests with synthetic data

The process for obtaining a breathing amplitude was tested for synthetic datasets of a white square moving in the sup-inf direction with a black background. The square was tested with movements of 10, 5, 4, 3, 2 and 1 pixels sup-inf to replicate the range of movements seen in 4DXVi scans.

11.2.3 Phantom Test

The process was tested for an in-house phantom moving with a fixed amplitude of 1.5 cm and period of 4 s. It was scanned using 4DCT with the Varian Real-Time Position Management (RPM) system (Varian Medical Systems, Palo Alto, USA) using a marker block with 2 reflectors as a surrogate for tumour motion and a 4DCBCT was acquired using 4DXVi (version 5.0.4, Elekta, Crawley, UK). For the 4DCT, the amplitude from each bin was compared to a sine wave with the amplitude and frequency of the phantom. The average breathing period was obtained from the RPM breathing trace file by calculating the time between the peaks of the trace.

For the 4DXVi, the breathing period for each phase was obtained by extracting the frame rate and phase from the scan.sort XVi file. The calculated amplitude of each phase from the

Python analysis was applied to the corresponding phase from the scan.sort XVi file to give a breathing cycle. The breathing cycle generated was compared to a sine wave with the amplitude and frequency of the phantom. The sine wave was also binned into 10 points and compared to the generated breathing cycle as the binned sine wave would represent the best cycle that could be achievable using the binned data. The sine waves were fitted to the generated data by selecting the offset that would minimise the residuals of the sine wave and the generated data.

11.2.4 Comparison to Centroid of Tumour

The gross tumour volume (GTV) for the in-house phantom was outlined on each breathing phase and the centroid of each outline calculated using a script developed in RayStation to obtain the maximum displacement of the outline in each cardinal direction. This was carried out for the 4DCT and the 4DXVi. The maximum displacement in the superior-inferior direction was then compared to the Amsterdam shroud method.

The method was tested for 2 patients with lung cancer who had previously received stereotactic ablative radiotherapy (SABR) and had previously had a 4DXVi. The GTV had been outlined on each breathing phase by a clinician and the centroid calculated using the method explained above. The maximum displacement in the superior-inferior direction was compared to the Amsterdam shroud method. The amplitudes were also compared with the trace obtained at the planning 4DCT scan using an external surrogate.

11.3 Results

11.3.1 Tests with synthetic data

The script agreed with generated data to within 2% with the largest error seen at 1 mm movement (Table 11.1).

Table 11.1: Comparison of pixel movement for generated sets of data using the Amsterdam shroud script and the expected results.

Movement (pixels)		
Expected	**Script**	**Difference to expected (%)**
1	1.02	2.00
2	1.99	-0.50
3	3.02	0.67
4	3.99	-0.25
5	4.92	-1.60
10	9.93	-0.70

11.3.2 Phantom Test

For the 4DCT, the script overestimated the amplitude of the phantom movement across the breathing cycle and by 4% at the peak (Figure 11.4).

For the 4DXVi, the script underestimated the amplitude of the phantom movement across the breathing cycle and by 17% at the peak (Figure 11.5). Using the scan.sort XVi file to calculate the time between the 0% phases gave a frequency of 4s which matched the phantom period.

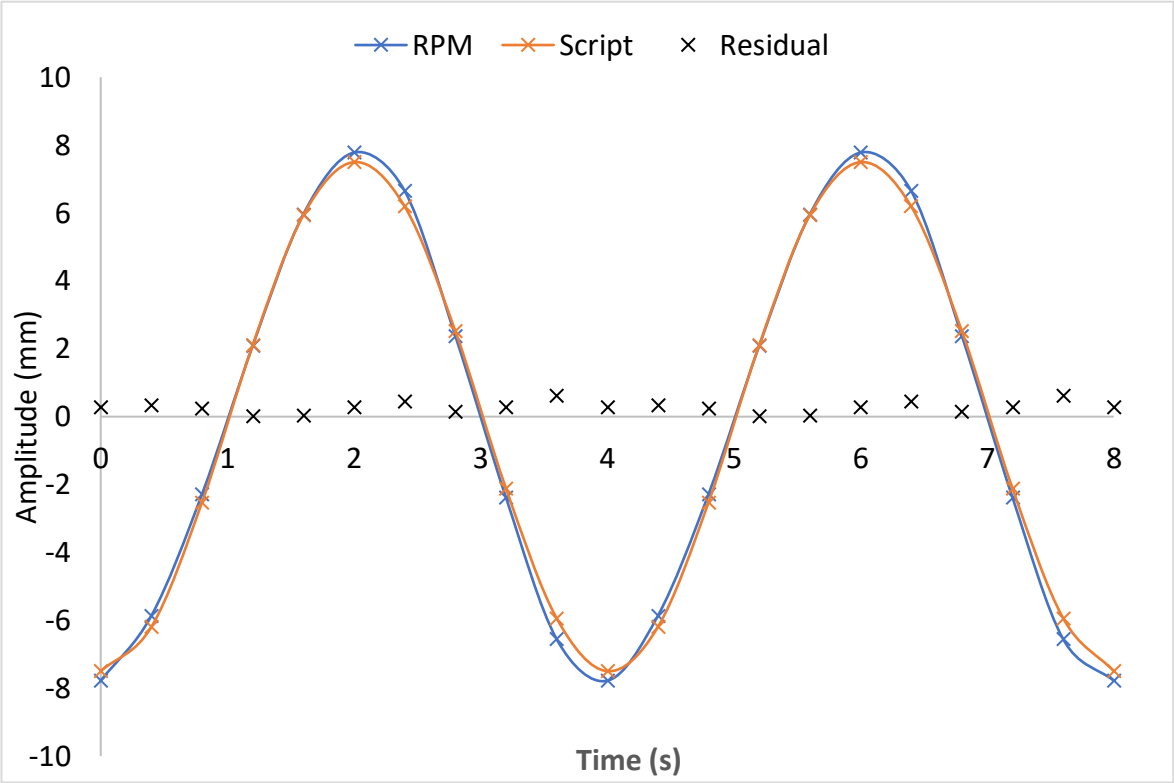

Figure 11.4: Generated breathing cycle from a 4DCT using the Amsterdam Shroud script compared to a sine wave from a moving phantom.

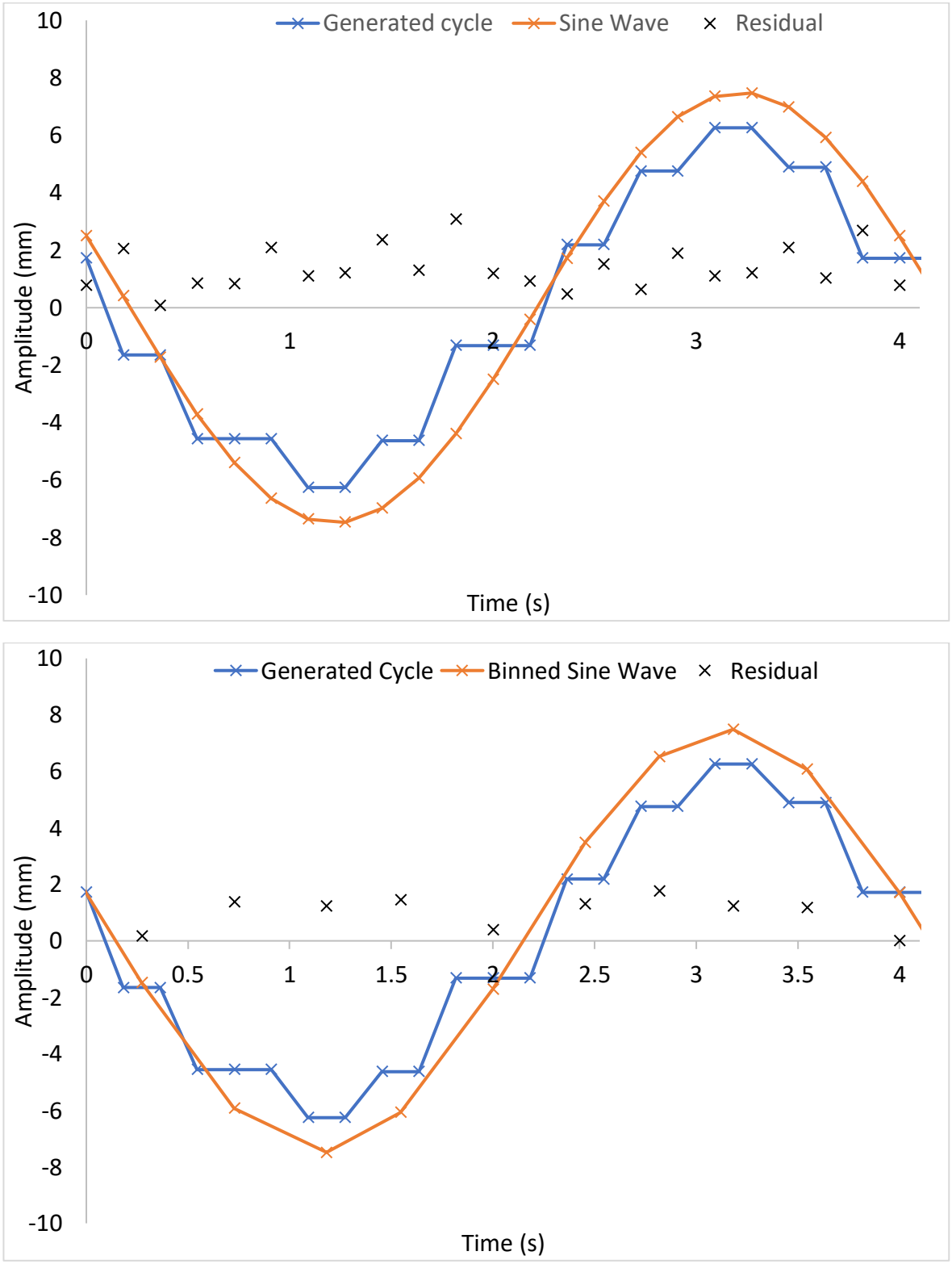

Figure 11.5: Generated breathing cycle from a 4DCBCT using the Amsterdam Shroud script compared to a sine wave from a moving phantom (top) and a binned sine wave (bottom).

11.3.3 Comparison to Centroid of Tumour

The script managed to extract a trace for all scans tested. Implementing the Amsterdam shroud script on the 4DCT of the phantom gave a peak amplitude of 4% larger than expected. This was more accurate than the centroid method which gave a peak amplitude of 8% less than expected. However, the centroid method performed better on the 4DXVi giving a peak amplitude 7% larger than expected compared to 17% lower than expected using the script method (Table 11.2). The amplitudes obtained from the patient XVi scans were larger than from the CT scans.

Table 11.2: Tumour amplitudes from a centroid method and script method for 2 patients and a moving phantom using 4DCT and 4DXVi images, including specified amplitudes for the phantom. The average amplitude from the Real-Time Position Management system (RPM) at the time of 4DCT is also given where available.

	Peak Amplitude (mm)			
Scan	**Centroid Method**	**Script Method**	**Specified**	**RPM Average**
Phantom CT	13.8	15.5	15.0	-
Patient A CT	11.3	8.7	-	10.0
Patient B CT	3.5	4.1	-	5.8
Phantom XVi	16.1	12.5	15.0	-
Patient A XVi	-	17.0	-	-
Patient B XVi	-	5.9	-	-

11.4 Discussion

The Amsterdam shroud technique used showed good agreement with a theoretical dataset amplitude of within 2% showing that in principle the method could extract a signal from a moving object. There was no consistent overestimation or underestimation or trend between amplitude and error. However, this was only tested for 5 theoretical situations where there was maximum contrast between the pixel value of a moving object and the background pixel value.

The Amsterdam shroud technique showed better agreement to a known amplitude from a phantom for 4DCT than 4DXVi. The agreement was better than using a centroid method for 4DCT but worse than using a centroid method for 4DXVi. The difference in amplitude using the Amsterdam shroud technique for the 4DXVi suggests that the method is not good enough to be used with binned 4DXVi data. This could be due to the lower contrast to noise ratio (CNR) of the 4DXVi scans compared to the 4DCT scans. Calculating this for the tumour insert of the phantom compared to the lung gives a CNR of 8 for the 4DXVI and 16 for the 4DCT. Other studies do not report comparisons with a known amplitude as their aim was to extract a signal to obtain a breathing trace to reconstruct the data. Instead, the data was

assessed to see if a periodic signal was obtained and the quality of the reconstruction assessed[8,15].

Another reason for the large difference in amplitude for the 4DXVi in this study may be due to the binned data and low contrast causing a blurred edge of the tumour insert in the Amsterdam shroud. Rit *et al.* (2012)[16] used an Amsterdam shroud method to extract a breathing trace from 33 lung cancer patient CBCTs using the diaphragm. They found that when there was lack of horizontality of the diaphragm, the Amsterdam shroud was blurred and this prevented breathing trace extraction. The algorithm used failed in 28% of patients.

A potential problem with the method used in this study is that the tumour motion was assessed rather than diaphragm motion. The aim was to produce a breathing trace that would correspond to tumour motion hence why the tumour volume was selected as the region of interest on the scans. Studies have shown that the diaphragm is a good surrogate for tumour motion in the sup-inf direction[17,18,19] and the Amsterdam shroud technique was originally designed to extract a signal from the diaphragm rather than a tumour[8]. Further work could be conducted to select the diaphragm rather than the tumour as a region of interest and compare this to current result. However, due the tumour position, the diaphragm is not always visible in the patient scan.

A potential benefit of the Amsterdam shroud method adopted in this study is the use of binned data as individual projections are not always readily available. Also, the signal from individual projections may not represent the true signal as different parts of the tumour or diaphragm might be tracked at different gantry angles[9]. Wolthaus *et al*., (2006)[13] used binned data for 4DCT breathing trace extraction using a volume of interest for the tumour and for the diaphragm. The trace from the tumour showed good agreement with the trace from the diaphragm but no assessment to a known amplitude was made. Further work is needed to assess if the method used in the current study can be used for 4DCT.

Due to the poor result for XVi, it is possible that another method may be more suited to breathing trace extraction using binned data such as pixel intensity or a Fourier transform method. Martin *et al*. (2014)[15] assessed these methods and the Amsterdam shroud method for 4DCBCTs of mice and found that all methods were comparable but that the Amsterdam shroud method had lower errors in projection sorting. However, this was not for binned data so further assessment is needed for this.

11.5 Conclusions

A method using the Amsterdam shroud on binned data has been presented and this was shown to work for theoretical data. The method performed better than a centroid method outlining a moving volume of known displacement. However, for a 4DXVi of known displacement, the results were not adequate, with the amplitude being underestimated by the method. Further development and testing are required to see if this method could be adapted for 4DXVi.

11.6 References

1. Abbas, H.; Chang, B.; Chen, Z., (2014) 'Motion Management in Gastrointestinal Cancers' ,. *Journal of Gastrointestinal Oncology*, *5* (3), pp. 223–235 doi: 10.3978/j.issn.2078-6891.2014.028.
2. Sarudis, S.; Karlsson Hauer, A.; Nyman, J.; Bäck, A., (2017) 'Systematic Evaluation of Lung Tumor Motion Using Four-Dimensional Computed Tomography' ,. *Acta Oncologica*, *56* (4), pp. 525–530 doi: 10.1080/0284186X.2016.1274049.
3. Vedam, S. S.; Keall, P. J.; Kini, V. R.; Mostafavi, H.; Shukla, H. P.; Mohan, R., (2003) 'Acquiring a Four-Dimensional Computed Tomography Dataset Using an External Respiratory Signal' ,. *Physics in Medicine and Biology*, *48* (1), pp. 45–62 doi: 10.1088/0031-9155/48/1/304.
4. Kleshneva, T.; Muzik, J.; Alber, M., (2006) 'An Algorithm for Automatic Determination of the Respiratory Phases in Four-Dimensional Computed Tomography' ,. *Physics in Medicine and Biology*, *51* (16) doi: 10.1088/0031-9155/51/16/N01.
5. Hoisak, J. D. P.; Sixel, K. E.; Tirona, R.; Cheung, P. C. F.; Pignol, J. P., (2004) 'Correlation of Lung Tumor Motion with External Surrogate Indicators of Respiration' ,. *International Journal of Radiation Oncology Biology Physics*, *60* (4), pp. 1298–1306 doi: 10.1016/j.ijrobp.2004.07.681.
6. Koch, N.; Liu, H. H.; Starkschall, G.; Jacobson, M.; Forster, K.; Liao, Z.; Komaki, R.; Stevens, C. W., (2004) 'Evaluation of Internal Lung Motion for Respiratory-Gated Radiotherapy Using MRI: Part I - Correlating Internal Lung Motion with Skin Fiducial Motion' ,. *International Journal of Radiation Oncology Biology Physics*, *60* (5), pp. 1459–1472 doi: 10.1016/j.ijrobp.2004.05.055.
7. Bhagat, N.; Fidelman, N.; Durack, J. C.; Collins, J.; Gordon, R. L.; Laberge, J. M.; Kerlan, R. K., (2010) 'Complications Associated with the Percutaneous Insertion of Fiducial Markers in the Thorax' ,. *CardioVascular and Interventional Radiology*, *33* (6), pp. 1186–1191 doi: 10.1007/s00270-010-9949-0.
8. Zijp, L.; Sonke, J.-J.; van Herk, M., (2004) 'Extraction of the Respiratory Signal from Sequential Thorax Cone-Beam X-Ray Images' ,. *International Conference on the Use of Computers in Radiation Therapy*, pp. 507–509.
9. Sonke, J. J.; Zijp, L.; Remeijer, P.; Van Herk, M., (2005) 'Respiratory Correlated Cone Beam CT' ,. *Medical Physics*, *32* (4), pp. 1176–1186 doi: 10.1118/1.1869074.
10. Kavanagh, A.; Evans, P. M.; Hansen, V. N.; Webb, S., (2009) 'Obtaining Breathing

Patterns from Any Sequential Thoracic X-Ray Image Set' ,. *Physics in Medicine and Biology*, *54* (16), pp. 4879–4888 doi: 10.1088/0031-9155/54/16/003.

11. Hu, J.; Haworth, S. T.; Molthen, R. C.; Dawson, C. A., (2004) 'Dynamic Small Animal Lung Imaging via a Postacquisition Respiratory Gating Technique Using Micro-Cone Beam Computed Tomography' ,. *Academic Radiology*, *11* (9), pp. 961–970 doi: 10.1016/j.acra.2004.05.019.

12. Yan, H.; Wang, X.; Yin, W.; Pan, T.; Ahmad, M.; Mou, X.; Cerviño, L.; Jia, X.; Jiang, S. B., (2013) 'Extracting Respiratory Signals from Thoracic Cone Beam CT Projections.' ,. *Physics in medicine and biology*, *58* (5), pp. 1447–1464 doi: 10.1088/0031-9155/58/5/1447.

13. Wolthaus, J. W. H.; Schneider, C.; Sonke, J. J.; van Herk, M.; Belderbos, J. S. A.; Rossi, M. M. G.; Lebesque, J. V.; Damen, E. M. F., (2006) 'Mid-Ventilation CT Scan Construction from Four-Dimensional Respiration-Correlated CT Scans for Radiotherapy Planning of Lung Cancer Patients' ,. *International Journal of Radiation Oncology Biology Physics*, *65* (5), pp. 1560–1571 doi: 10.1016/j.ijrobp.2006.04.031.

14. Rit, S.; Vila Olivia, M.; Brousmiche, S.; Labarbe, R.; Sarrut, D.; Sharp, G. C., (2014). 'The Reconstruction Toolkit (RTK), an open-source cone-beam CT reconstruction toolkit based on the Insight Toolkit (ITK) ',. *Journal of Physics: Conference Series*, 489, 012079

15. Martin, R.; Rubinstein, A.; Ahmad, M.; Court, L.; Pan, T., (2015) 'Evaluation of Intrinsic Respiratory Signal Determination Methods for 4D CBCT Adapted for Mice' ,. *Medical Physics*, *42* (1), pp. 154–164 doi: 10.1118/1.4903264.

16. Rit, S.; Van Herk, M.; Zijp, L.; Sonke, J. J., (2012) 'Quantification of the Variability of Diaphragm Motion and Implications for Treatment Margin Construction' ,. *International Journal of Radiation Oncology Biology Physics*, *82* (3), pp. e399–e407 doi: 10.1016/j.ijrobp.2011.06.1986.

17. Cervîo, L. I.; Chao, A. K. Y.; Sandhu, A.; Jiang, S. B., (2009) 'The Diaphragm as an Anatomic Surrogate for Lung Tumor Motion' ,. *Physics in Medicine and Biology*, *54* (11), pp. 3529–3541 doi: 10.1088/0031-9155/54/11/017.

18. Lu, W.; Parikh, P. J.; El Naqa, I. M.; Nystrom, M. M.; Hubenschmidt, J. P.; Wahab, S. H.; Mutic, S.; Singh, A. K.; Christensen, G. E.; Bradley, J. D.; Low, D. A., (2005) 'Quantitation of the Reconstruction Quality of a Four-Dimensional Computed Tomography Process for Lung Cancer Patients' ,. *Medical Physics*, *32* (4), pp. 890–901 doi: 10.1118/1.1870152.

19. Rietzel, E.; Pan, T.; Chen, G. T. Y., (2005) 'Four-Dimensional Computed Tomography: Image Formation and Clinical Protocol' ,. *Medical Physics*, *32* (4), pp. 874–889 doi: 10.1118/1.1869852.

12 Robust Optimisation for Lung SABR Planning

Walker Z.[1], Baugh G.[1], Chuter R.[2], Rogers J.[1]
[1] Medical Physics, University Hospitals Coventry and Warwickshire NHS Trust, Coventry, UK; [2]The Christie Medical Physics and Engineering, The Christie NHS Foundation Trust, Manchester, UK

Abstract

Purpose

Robust optimisation offers a solution to the inaccuracies using planning target volumes (PTVs) for lung planning, by including a full range of gross tumour volume (GTV) positions. The aim of this research is to evaluate the difference between methods of robust optimisation for stereotactic ablative radiotherapy (SABR) lung planning using 4DCT.

Methods

Fourteen lung cancer patients who had previously received volumetric modulated arc therapy (VMAT) SABR were planned in RayStation using a margin-based PTV method, robust optimisation on a 3D scan and robust optimisation over 10 4D phases. Two 4D robust plans were created. One (4D robust (D99)) was optimised to ensure the GTV D99 received that of the original plan and the other (4D robust (PTV)) optimised to ensure that the GTV received the original prescription dose. Clinical goals were compared and robustness assessed for the 3D robust method by perturbing the dose. An in-house moving phantom was programmed with 2 patient breathing traces obtained from 4DCT and on-treatment 4D cone-beam CT scans. Plans were delivered to the phantom to assess the dosimetry.

Results

The GTV D99 was comparable for both the margin-based and 3D robust plans under perturbation. Lung V_{20Gy} and $V_{12.5Gy}$ for 3D robust planning were statistically significantly lower than those from the margin-based plans. GTV D99 and GTV D50 were higher on average across all phases for the 4D robust (D99) plans compared to the margin-based plans. GTV D99, D50 and D2 were lower on average across all phases for the 4D robust (PTV) plans compared to the margin-based plans. The variance of the margin-based plans was higher than that from the 4D robust (D99) plans for D99, D50 and D2 and this was statistically significant. The variance of the margin-based plans was lower than that from the 4D robust (PTV) plans for D50 and D2 and this was statistically significant. The average organ at risk (OAR) doses were higher for the 4D robust (GTV D99) plans when deformed onto the 3DCT than the margin-based plans except for the chest wall dose. The lungs, oesophagus and skin doses were higher and this was statistically significant. The average

OAR doses for the 4D robust (PTV) plans when deformed onto the 3DCT were similar to margin-based plans except for the dose to 0.5cc of lung which was lower and this was statistically significant. Chamber measurements were within 2.5% of the expected treatment planning system doses for all but 2 of the robust plan deliveries.

Conclusions

Robust optimisation on a 3D CT scan could be implemented clinically with comparable plans being achieved with reduced lung doses. Robust optimisation over breathing phases can produce less variable GTV coverage across breathing phases.

12.1 Introduction

Approximately 20% of non-small cell lung cancers (NSCLC) are early stage (I or II) at diagnosis[1]. Although the tumours may be operable, many of these patients have other co-morbidities, therefore surgery would be too risky and hence stereotactic ablative radiotherapy (SABR) can be used as an alternative.

Due to the large amount of movement in the lung, immobilisation to limit movement or 4D imaging are recommended for lung SABR treatments[2]. A 4DCT scan can be used to obtain an internal target volume (ITV). This is an outline of the gross tumour volume (GTV) taking into account the tumour motion. Planning target volume (PTV) margins are traditionally used to account for other uncertainties in radiotherapy treatment delivery. There are inherent inaccuracies from using these in lung radiotherapy planning as dose optimisation will occur over large amounts of air or lung tissue with a lower density to that of the tumour volume. It has been shown that a high fluence delivery is needed to deliver dose to this tissue due to the lack of electronic equilibrium[3].

One solution to these inaccuracies is to use robust optimisation within the planning system which optimises the dose for variation of patient and tumour position in addition to traditional clinical goals. Robust optimisation is widely used in proton therapy with some examples of use for lung cancer in the literature[4-6]. However, it has only recently become commercially available for photon planning with a few small studies assessing its use for lung cancer treatment[7-9] and only one evaluating its use in lung SABR[10].

This study uses the commercial treatment planning system, RayStation (version 7 and 9, RaySearch Laboratories, Stockholm, Sweden) which applies a minimax robust optimisation method that involves minimising the penalty of the worst-case scenario[4]. The aim of the study is to evaluate the use of RayStation for robust optimisation of SABR lung plans using

3D and 4D robust optimisation methods and to compare these to the currently used PTV-margin based method.

12.2 Methods

12.2.1 Scanning

Fourteen consecutive patients with lung cancer previously treated with SABR were included in this retrospective planning study. The tumour locations and prescriptions are shown in Table 12.1. All patients were scanned on a GE discovery CT590 (GE Medical Systems) and had a helical 3DCT for treatment planning from the larynx to the mid-abdomen to encompass the organs at risk (OARs) and a localised axial 4DCT for tumour outlining with scan limits specified by a clinician as per local protocol. The 4DCT was binned into 10 phases and reconstructed to produce an average intensity projection (Ave-IP) and a maximum intensity projection (MIP) using the software Advantage4D (GE Medical Systems).

Table 12.1:Number of patients (n) with locations and prescriptions assessed in the study.

Location	**n**
Left upper lobe	4
Right upper lobe	6
Right lower lobe	3
Right middle lobe	1

Prescription	**n**
54Gy/3#	6
55Gy/5#	7
55Gy/8#	1

12.2.2 Outlining

All patient CT scans were outlined using the anatomy module in RayStation. For the clinical plans, OARs were outlined by dosimetrists on the 3DCT and ITVs outlined by clinicians using the MIP and checked on the phases by the clinician. For the retrospective study, clinicians outlined GTVs on the 0% and 50% phases corresponding to inhale and exhale respectively. The outlines were propagated to all phases using deformable registration in RayStation and checked and edited by the clinician. Deformable registration was carried out between adjacent phases. For example, the 0% phase was registered to the 10% phase and the 50% phase registered to 60% phase. OARs were deformed from the 3DCT to all phases and also checked and edited.

12.2.3 Planning Methods

A summary of all planning methods assessed are shown in Figure 12.1.

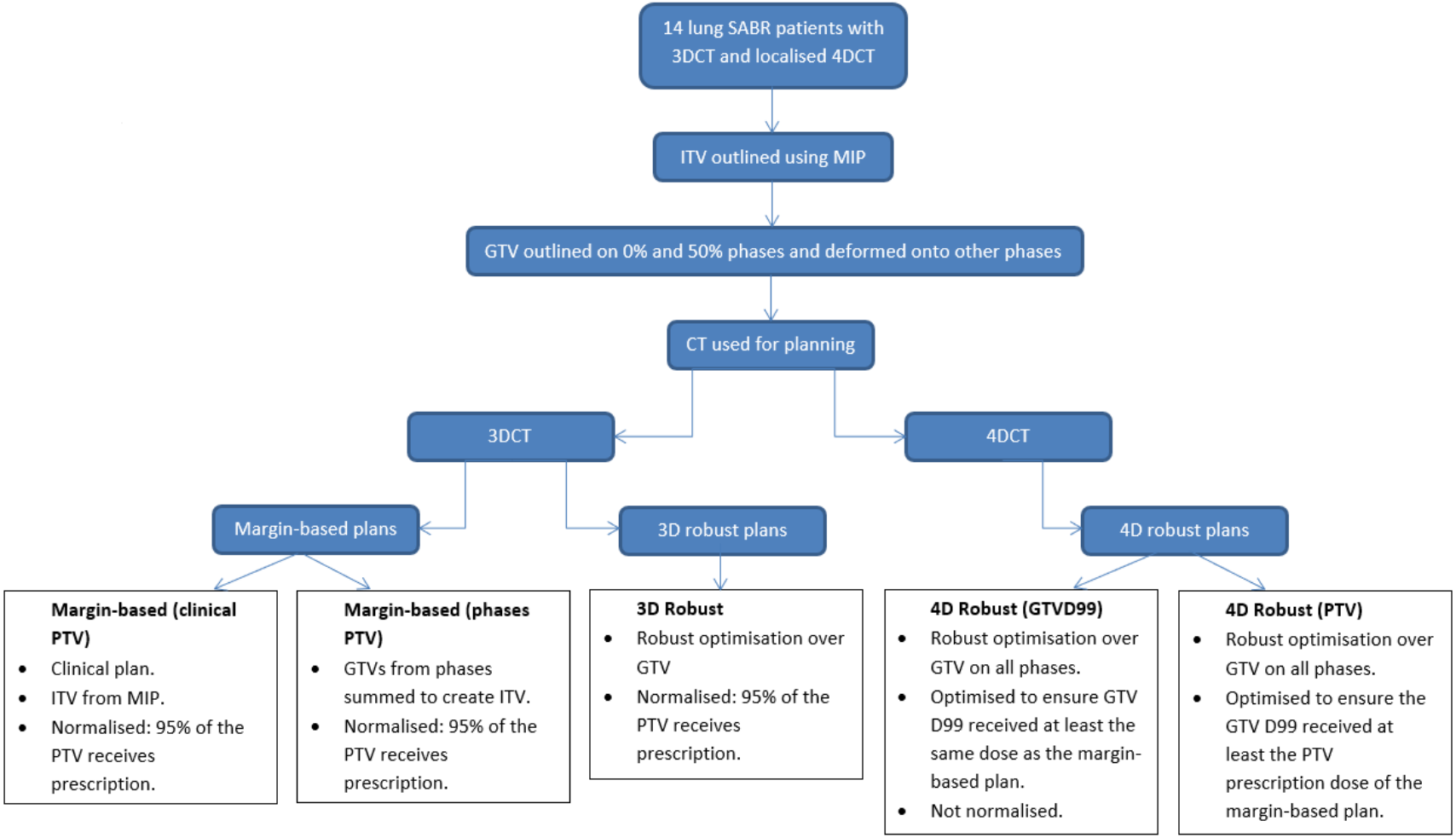

Figure 12.1: Scans and planning methods used.

12.2.4 Margin-based Planning

All patients had clinical radiotherapy plans created for lung SABR with prescription doses given in Table 12.1. Plans were created in RayStation using partial arc flattening filter free VMAT delivery with 6MV x-rays and had 5 mm isotropic PTV margins applied to the ITV. Plans were optimised to ensure 95% of the PTV received the prescription isodose and the OAR doses met the optimal constraints from the UK SABR Consortium guidelines[2]. Where achievement of optimal constraints was not possible, mandatory constraints were accepted. If mandatory constraints could not be achieved then this was discussed with the clinician who would decide whether to proceed with the plan. Plans were initially optimised with the air in the PTV overridden to the density of water to optimise the segments and then a further monitor unit only optimisation carried out with no density override. These plans will be referred to as margin-based (clinical PTV).

12.2.5 3D Robust Planning

Patients were retrospectively planned in RayStation using robust optimisation on the 3DCT. No PTV margin was applied to the ITV and 5 mm isotropic errors in patient position were applied for the robust optimisation giving 7 scenarios for robust optimisation. There are 6 scenarios for each patient setup uncertainty in addition to the nominal scenario of no patient setup uncertainty. The same partial VMAT arc angles and isocentre were applied as in the margin-based plans. The optimisation parameters were amended to optimise over the robust ITV rather than the PTV and the plan optimised to ensure the ITV achieved the same dose to 99% of the volume (D99) as the PTV-based plan. The dose-fall off was amended to account for the robust ITV settings and all other optimisation parameters that were in the original optimisation were included. The plans were renormalised to ITV D99 to compare to the original margin-based plans.

12.2.6 4D Robust Planning

Patients were retrospectively planned using robust optimisation over the 0%, 20% and 50% phases with the 20% phase selected as the nominal scan. No PTV margin was applied to the ITV and 5 mm isotropic errors in patient position were applied for the robust optimisation. This gave 21 scenarios for robust optimisation (7 scenarios for each phase selected). The same GTV optimisation parameters as the 3D robust planning were used except for transition structures were not included. Transition structures are rinds around the PTV which are used to control the dose to normal tissue. These were not used for the 4D robust plans as a

transition structure would have to be created on each phase and optimised over each phase, therefore increasing the calculation time significantly. The dose-fall off was amended to account for the robust GTV on each phase. These plans will be referred to as 4D robust (GTV D99). Plans were also created using the same 4D robust settings but with the dose to the GTV optimised to receive the original prescription dose. These plans will be referred to as 4D robust (PTV). The 4D robust plans were not renormalised to a particular phase as this could affect the coverage on other phases.

3DCT and 4DCT scans were taken of an in-house thorax phantom with a tumour insert moving 1.5 cm in the sup-inf direction. The scan was reconstructed into 10 phases and the tumour insert over the phases was outlined. The lung and cord were outlined on the 3D scan. A margin-based 3D plan and 4D robust plan (GTV D99) were created as detailed above. The 4D robust plan was optimised over all phases (70 scenarios) and also over the 0%, 20% and 50% phases. An optimisation over all of the phases was also performed for one of the patients whose tumour was moving with an average amplitude of the dataset. This was to test the difference between optimising over all phases or over 3 phases.

12.2.7 Re-optimising of Margin-based Plans

The GTVs from all the phases were copied to the 3DCT and summed and a 5 mm margin added to create a phases PTV. A new 3D margin-based plan was created using the same parameters as the clinical plan but re-optimised to ensure 95% of the phases PTV received the prescription dose. This was to allow for a fair comparison to the 4D robust optimisation. These will be referred to as margin-based (phases PTV) plans.

12.2.8 Analysis

The OAR doses from 3D robust planning methods were compared to the margin-based (clinical PTV) plans and a Wilcoxon signed rank test performed. This was used as the data was found to be not normally distributed. All 3D robust plans and clinical margin-based were perturbed in 1 mm increments by up to 5 mm in the x, y and z directions in RayStation to assess the robustness of the plans.

The dose from the margin-based (clinical PTV), margin-based (phases PTV), 4D robust (D99) and 4D robust (PTV) plans were recalculated on each breathing phase and the GTV doses compared. The doses for the 4D robust plans on each phase were then deformed to the 3D CT and summed in order to compare OAR doses to the margin-based (phases PTV) plans.

12.2.9 Phantom Imaging and Planning

A script was developed in RayStation to calculate the centroid of each GTV to obtain the maximum displacement of the outline for each patient in each cardinal direction. The patient with the maximum GTV displacement (patient A) and the patient with an average GTV displacement (patient B) were selected to be measured. Breathing traces for these patients in the superior-inferior directions had previously been obtained from their 4D cone-beam CT (CBCT) images using an Amsterdam shroud script created by the author[11].

The breathing traces were formatted to be imported into software controlling a CIRS dynamic thorax phantom movement (CIRS Motion Control 2.1.2, 2013) and were set to be the superior-inferior motion of the phantom. An image of the phantom is shown in Figure *12.2*. Due to the low resolution of the 4D cone-beam CT (4DCBCT), the motion in the left-right and ant-post directions were obtained by calculating the maximum displacement of the GTV centre on the CT scan from the centroid script. This was manually entered into the CIRS software.

A 4DCT scan of the CIRS dynamic thorax phantom was obtained using the departmental clinical SABR lung protocol with the phantom movement programmed with CBCT breathing traces from the script for patient A and patient B. The phantom was also scanned with the breathing traces for patient A and B obtained from the Real-time Position Management (RPM) system (Varian Medical Systems, Palo Alto, USA) at the time of the 4DCT planning scan. Each scan was performed with a pinpoint chamber within the 2 cm spherical tumour insert as this was nearest the tumour size of patients A and B. The scans were reconstructed into 10 breathing phases, a maximum intensity projection (MIP) and an average intensity projection (Ave-IP). The images were imported into RayStation and the pinpoint chamber volume outlined. A quality assurance (QA) plan was created to calculate doses from a margin-based (clinical PTV) plan, 3D robustly optimised plan and a 4D robust (GTVD99) plan for both patients on the phantom scan for the corresponding movement. The isocentre was shifted on the phantom to ensure the chamber was in the high dose region.

12.2.10 Pinpoint Dose Measurements

All beams were delivered using an Elekta Versa HD linear accelerator (Elekta, Crawley, UK). The CIRS phantom was positioned on the couch with the phantom movement set as in the QA plan. A 4DCBCT was performed for each setup and the scan matched to the average intensity projection scan of the phantom. Couch shifts were applied to ensure the phantom was in the correct position. The PTW pinpoint chamber type 31014 was used with a sensitive volume of 0.015cm^3 (radius of sensitive volume 1mm and length of sensitive volume 5mm).

The plans were delivered twice each and the pinpoint dose calculated, corrected for output and compared to the average chamber dose in the planning system.

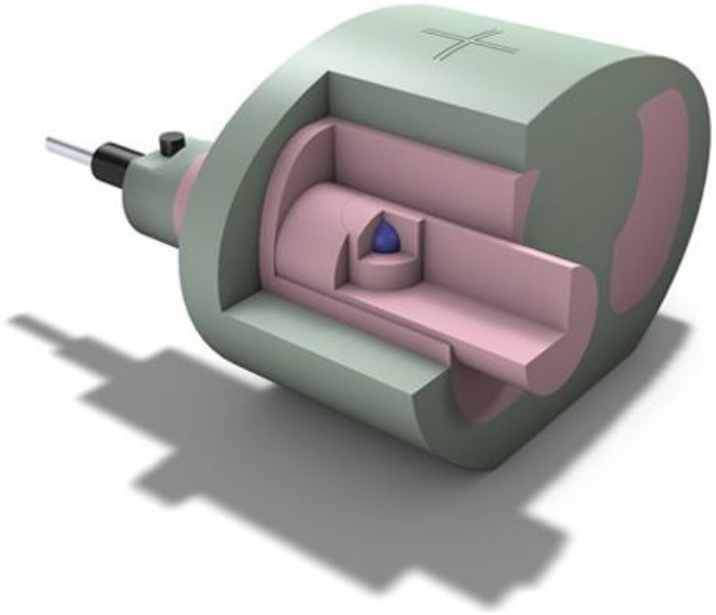

Figure 12.2: Image of the CIRS moving lung phantom used for pinpoint measurements. The cylindrical rod of lung equivalent material moves and the pinpoint chamber was placed in the centre of the tumour (blue sphere). Image reproduced from https://www.cirsinc.com/products/radiation-therapy/dynamic-thorax-motion-phantom/

12.3 Results

12.3.1 3D Robust Planning

The GTV D99 was comparable for both the margin-based and robust plans when the patient was shifted in the right-left and ant-post directions (Figure 12.3). The GTV D99 was higher for the robust plans shifted in the superior and inferior directions, although this was not statistically significant (Table 12.2).

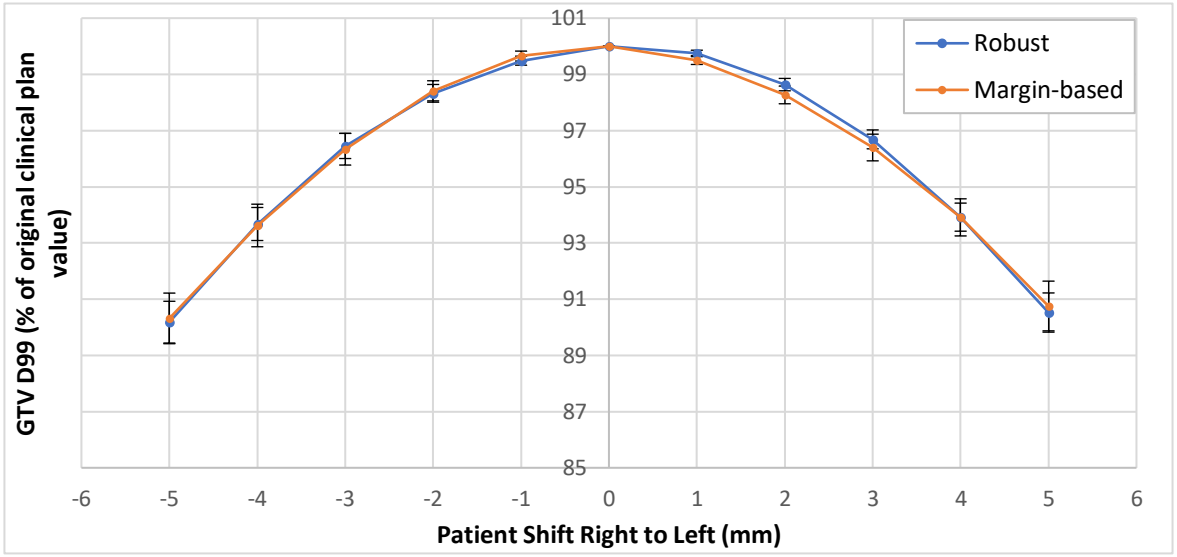

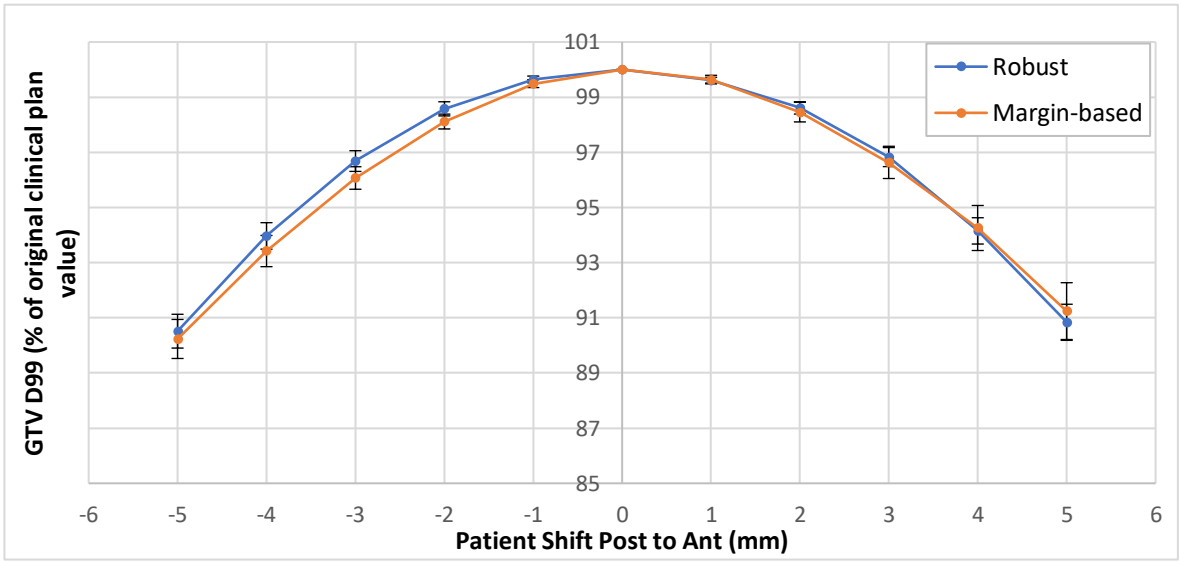

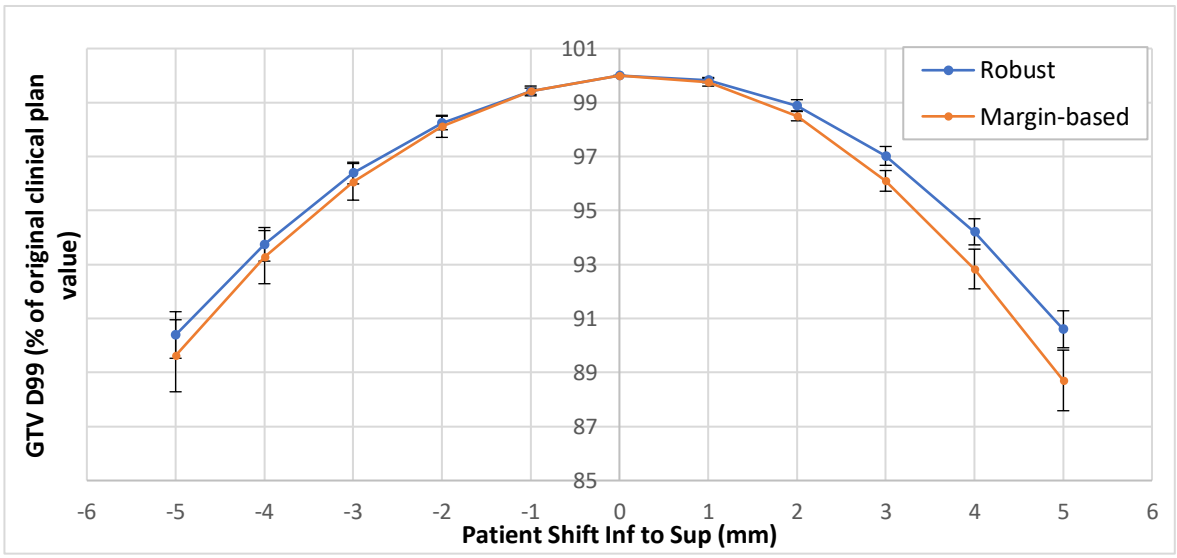

Figure 12.3: Plots of GTV D99 for margin-based (clinical PTV) and 3D robustly optimised plans for different patient shifts. Shift directions: top: right to left, middle: post to ant, bottom inf to sup.

Table 12.2: P-values for different patient shift scenarios from a Wilcoxon signed rank test for GTV D99 comparing the margin-based (clinical PTV) and the 3D robust planning methods.

	p-value		
Shift (mm)	**Right to left**	**Post to Ant**	**Inf to Sup**
-5	0.925	0.387	0.975
-4	0.778	0.286	0.975
-3	0.778	0.331	0.975
-2	0.638	0.331	0.975
-1	0.510	0.249	0.975
1	0.245	0.730	0.414
2	0.397	0.778	0.158
3	0.778	0.826	0.124
4	0.975	0.683	0.124
5	0.638	0.433	0.140

The 3D robust planning method produced plans where dose constraints were met or where they were not met, they were also not met in the original clinical plan. Most doses to the OARs were comparable between the 3D robust plans and the margin-based plans (Figure 12.4 and Figure 12.5). The volume of normal lung receiving at least 20Gy (V_{20Gy}) and the volume of normal lung receiving at least 12.5Gy ($V_{12.5Gy}$) for 3D robust planning were statistically significantly lower at the 5% level than those from the clinical margin-based plans (Table 12.3). The monitor units for the 3D robust plans were lower on average than the margin-based plans but the difference was not statistically significant at the 5% level (Table 12.4).

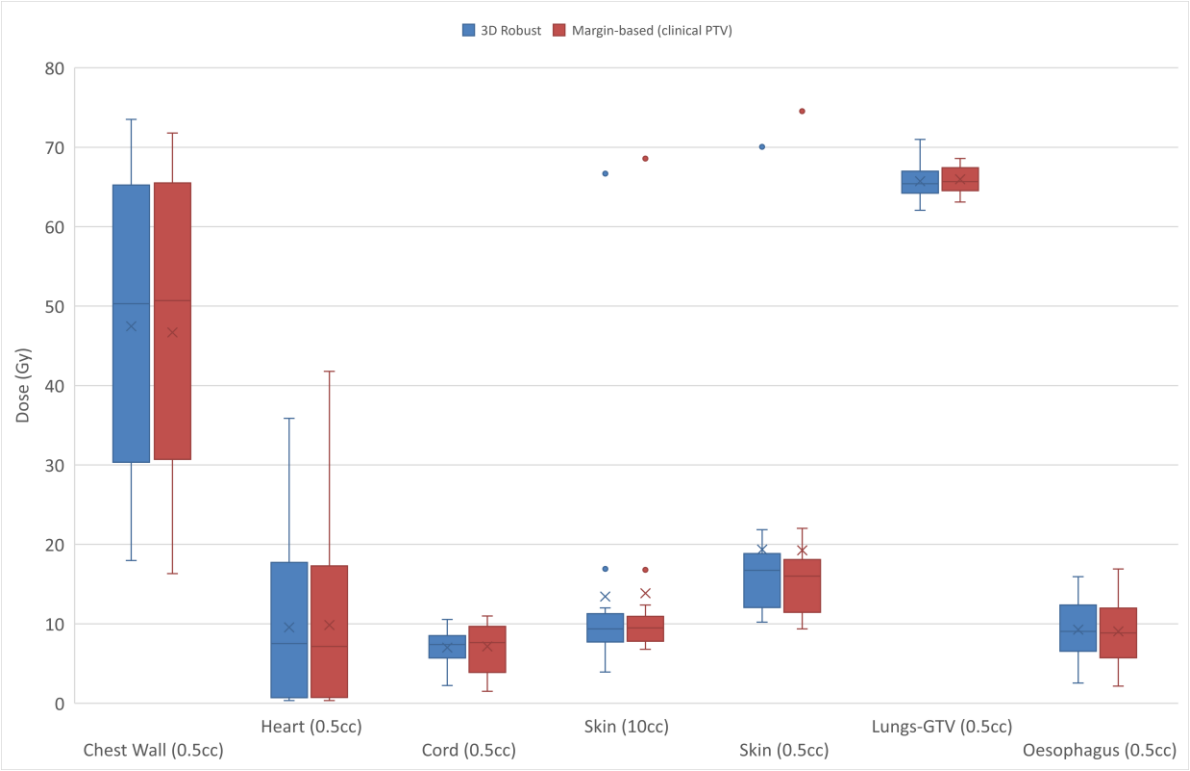

Figure 12.4: Box and whisker plot of doses to volumes of organs at risk using margin-based planning and 3D robust optimisation for SABR lung patients. The boxes indicate the interquartile range (IQR), the line indicates the median and the cross indicates the mean. The whiskers indicate the highest and lowest values within 1.5 times the IQR and data outside this range indicated by circles.

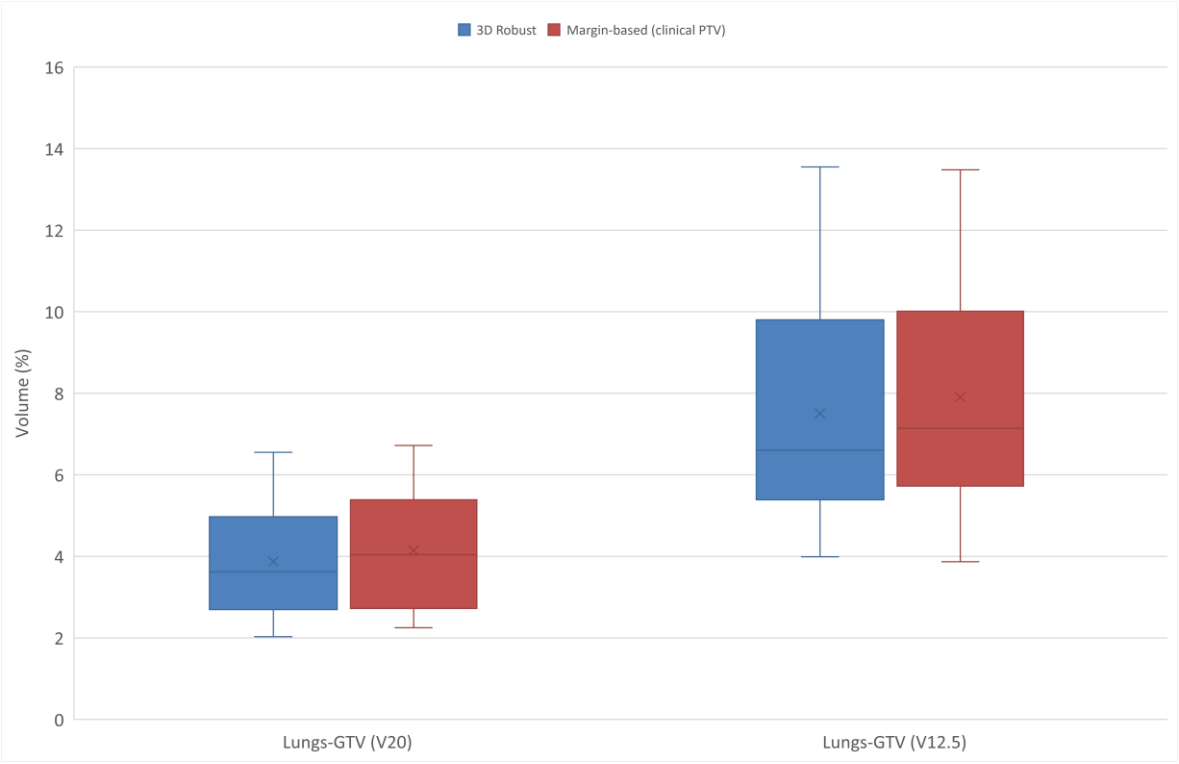

Figure 12.5: Box and whisker plot of volume of lungs-GTV risk receiving 20Gy and 12.5Gy using margin-based planning and 3D robust optimisation for SABR lung cancer patients. The boxes indicate the interquartile range (IQR), the line indicates the median and the cross indicates the mean. The whiskers indicate the highest and lowest values within 1.5 times the IQR and data outside this range indicated by circles.

Table 12.3: Doses to organs at risk for 3D robust plans and margin-based (clinical PTV) plans. P-values are from a Wilcoxon signed rank test.

	Dose (Gy)		
OAR	**3D Robust**	**Margin**	**p-value**
Chest Wall (0.5cc)	47.4±5.0	46.7±5.1	0.116
Heart (0.5cc)	9.6±2.8	9.9±3.1	0.937
Cord (0.5cc)	7.0±3.1	7.2±0.8	0.778
Skin (10cc)	13.4±4.2	13.9±4.3	0.875
Skin (0.5cc)	19.3±4.0	19.3±4.4	0.875
Lungs-GTV (0.5cc)	65.7±0.6	66.0±0.5	0.470
Oesophagus (0.5cc)	9.3±1.0	9.0±1.1	0.706
OAR	**Volume (%)**		**p-value**
Lungs-GTV (V20)	3.9±0.4	4.1±1.1	0.026
Lungs-GTV (V12.5)	7.5±0.8	7.9±0.8	0.012

Table 12.4: Monitor units for 3D robust and margin-based (clinical PTV) plans. P-values are from a Wilcoxon signed rank test.

Method	**MU**	**p-value**
3D Robust	2995.6±255.8	0.245
Margin	3152.4±252.3	

12.3.2 4D Robust Planning

GTV D99 and GTV D50 were higher on average across all phases for the 4D robust (D99) plans compared to both margin-based plans. GTV D2 was lower on average across all phases for the 4D robust (D99) plans compared to both margin-based plans (Figure 12.6 and Table 12.5). GTV D99, D50 and D2 were lower on average across all phases for the 4D robust (PTV) plans compared to both margin-based plans (Figure 12.6 and Table 12.6).

The variance of the margin-based (phases PTV) plans was higher than that from the 4D robust (D99) plans for D99, D50 and D2 and this was statistically significant at the 5% level using Levene's test (Table 12.5). This test was used as it tests for homogeneity of variances. The variance of the margin-based (phases PTV) plans was lower than that from the 4D robust (PTV) plans for D50 and D2 and this was statistically significant at the 5% level using Levene's test (Table 12.6).

The monitor units for the 4D robust plans were lower on average than the margin-based plans with the difference being statistically significant for the 4D robust (PTV) plans (Table 12.7).

When the 4D robust (PTV) plans were deformed onto the 3DCT then summed, the dose to 95% of the PTV was lower than the original clinical prescription for 5 of the patients (Table 12.8). This was carried out to compare this method to the clinical margin-based plans.

Figure 12.6: Box and whisker plot of top: GTVD99, middle: GTV D50 and bottom GTVD2, using 4D robust planning and margin-based planning methods for SABR lung cancer patients. The boxes indicate the interquartile range (IQR), the line indicates the median and the cross indicates the mean. The whiskers indicate the highest and lowest values within 1.5 times the IQR and data outside this range indicated by circles.

Table 12.5: Mean values for D99, D50 and D2 and variance for 4D robust (GTV D99) plans and margin-based (phases PTV) plans. Errors on the mean are quoted. P-values are given for Levene's test of variances.

	D99			D50			D2		
	Mean (%)	**Variance**	**p-value**	**Mean (%)**	**Variance**	**p-value**	**Mean (%)**	**Variance**	**p-value**
4D Robust (GTV D99)	120.2±0.3	9.9	0.004	128.6±0.2	5.8	<0.001	132.8±0.3	10.3	<0.001
Margin-Based (Phases PTV)	116.2±0.3	16.8		127.8±0.4	22.4		134.3±1.5	32.7	

Table 12.6: Mean values for D99, D50 and D2 and variance for 4D robust (PTV) plans and margin-based (phases PTV) plans. Errors on the mean are quoted. P-values are given for Levene's test of variances.

	D99			D50			D2		
	Mean (%)	**Variance**	**p-value**	**Mean (%)**	**Variance**	**p-value**	**Mean (%)**	**Variance**	**p-value**
4D Robust (PTV)	107.2±0.3	13.4	0.113	116.6±0.5	35.2	0.002	121.3±0.6	58.2	0.001
Margin-Based (Phases PTV)	116.2±0.3	16.8		127.8±0.4	22.4		134.3±1.5	32.7	

Table 12.7: Monitor units (MU) for 4D robust planning methods and margin-based planning methods for SABR lung cancer patients with p-values from a Wilcoxon rank test.

Method	**MU**	**p-value**
4D Robust (GTV D99)	2894.2±244.4	0.249
Margin (phases PTV)	3065±285.3	
4D Robust (PTV)	2526.0±221.4	0.006
Margin (phases PTV)	3065±285.3	

Table 12.8: Values of PTV D95 for each patient after deforming the 4D Robust (PTV) plans onto each phase and summing on the 3DCT.

Patient	PTV D95 (%)
1	99.5
2	86.6
3	94.4
4	98.5
5	111.3
6	109.1
7	97.2
8	106.3
9	101.1
10	110.8
11	104.4
12	100.0
13	114.6
14	109.9

The average OARs doses were higher for the 4D robust (GTV D99) plans when deformed onto the 3DCT than the margin-based (phases PTV) plans except for the chest wall dose (Figure 12.7 and Figure 12.8). The lungs, oesophagus and skin doses were higher and this was statistically significant at the 5% level (Table 12.9).

The average OARs doses for the 4D robust (PTV) plans when deformed onto the 3DCT were similar to margin-based (phases PTV) plans (Figure 12.7 and Figure 12.8) except for the dose to 0.5cc of lung which was lower and this was statistically significant at the 5% level (Table 12.10).

Table 12.9: Organ at risk doses for 4D robust plans (prescribed to GTV D99) compared to margin-based plans using a PTV obtained from the phases. P-values are from a Wilcoxon signed-rank test.

OAR	Dose (Gy)		p-value
	4D Robust (GTV D99)	Margin (phases PTV)	
Chest Wall (0.5cc)	42.6±4.3	42.9±4.8	0.249
Heart (0.5cc)	10.0±2.9	8.6±2.6	0.056
Cord (0.5cc)	7.8±1.0	7.3±0.9	0.594
Skin (10cc)	15.0±4.4	14.0±4.2	0.035
Skin (0.5cc)	19.1±4.5	18.6±4.3	0.245
Lungs-GTV (0.5cc)	67.4±0.5	66.5±0.6	0.140
Oesophagus (0.5cc)	9.6±1.1	8.4±1.0	0.022

OAR	Volume (%)		p-value
Lungs-GTV (V20)	4.5±0.6	3.8±0.6	0.005
Lungs-GTV (V12.5)	8.6±1.0	7.3±0.9	0.003

Table 12.10: Organ at risk doses for 4D robust plans (prescribed to clinical PTV prescription dose) compared to margin-based plans using a PTV obtained from the phases. P-values are from a Wilcoxon signed-rank test.

OAR	Dose (Gy)		p-value
	4D Robust (PTV)	Margin (phases PTV)	
Chest Wall (0.5cc)	41.2±4.5	42.9±4.8	0.463
Heart (0.5cc)	9.6±2.8	8.6±2.6	0.124
Cord (0.5cc)	7.3±0.8	7.3±0.9	0.650
Skin (10cc)	13.9±4.3	14.0±4.2	0.660
Skin (0.5cc)	19.1±4.4	18.6±4.3	0.594
Lungs-GTV (0.5cc)	60.2±1.1	66.5±0.6	0.001
Oesophagus (0.5cc)	8.9±1.0	8.4±1.0	0.510

OAR	Volume (%)		p-value
Lungs-GTV (V20)	4.1±0.4	3.8±0.6	0.433
Lungs-GTV (V12.5)	8.2±0.9	7.3±0.9	0.167

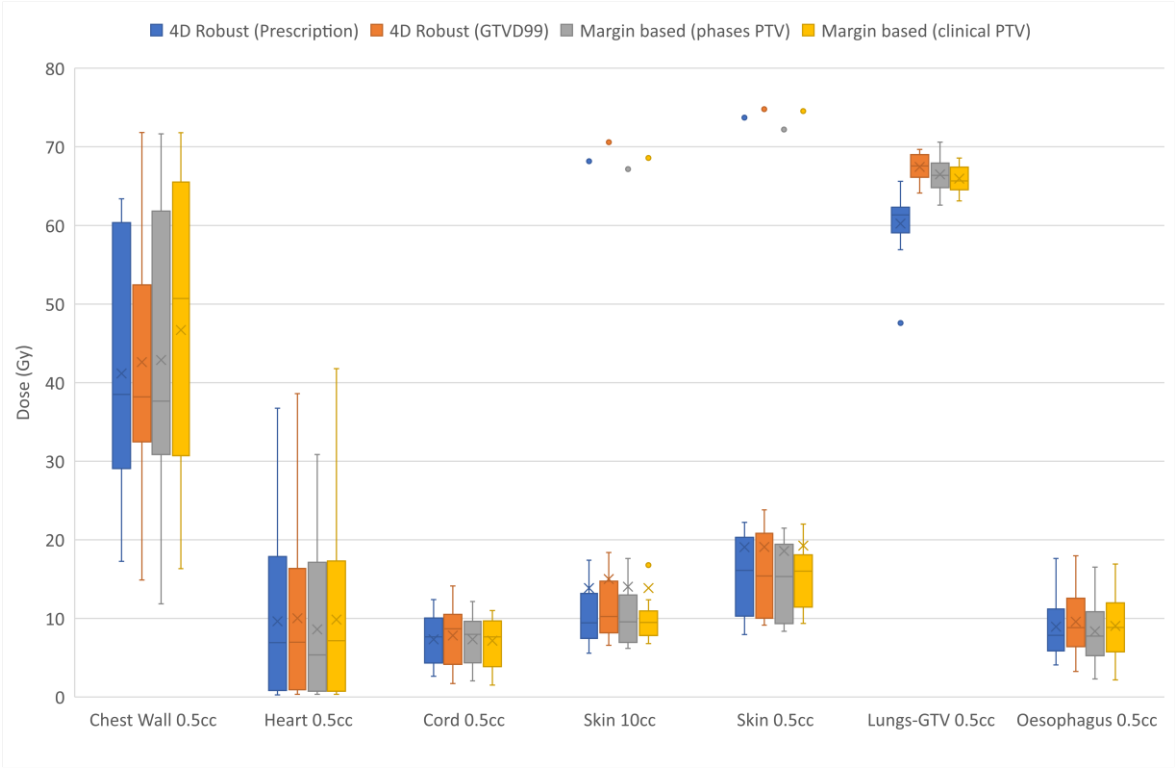

Figure 12.7: Box and whisker plot of doses to volumes of organs at risk using margin-based planning and 3D robust optimisation for SABR lung cancer patients. The boxes indicate the interquartile range (IQR), the line indicates the median and the cross indicates the mean. The whiskers indicate the highest and lowest values within 1.5 times the IQR and data outside this range indicated by circles.

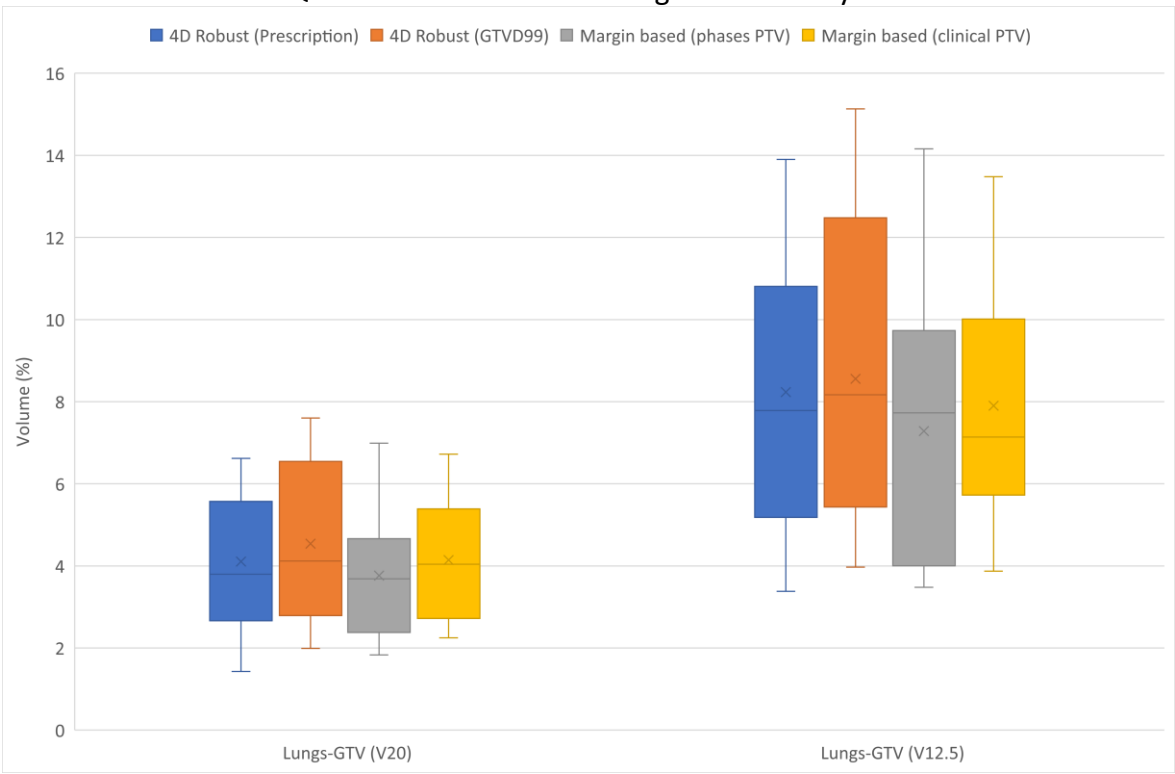

Figure 12.8: Box and whisker plot of volumes of lungs-GTV receiving 20Gy and 12.5Gy using margin-based planning methods and 4D robust optimisation for SABR lung cancer patients. The boxes indicate the interquartile range (IQR), the line indicates the median and the cross indicates the mean. The whiskers indicate the highest and lowest values within 1.5 times the IQR and data outside this range indicated by circles.

Optimising over all of the phases or just the 0, 20 and 50% phases made minimal difference to the clinical plan and the phantom plan. Figure 12.9 and Figure 12.10 show results for all phases deformed and summed onto the 3DCT.

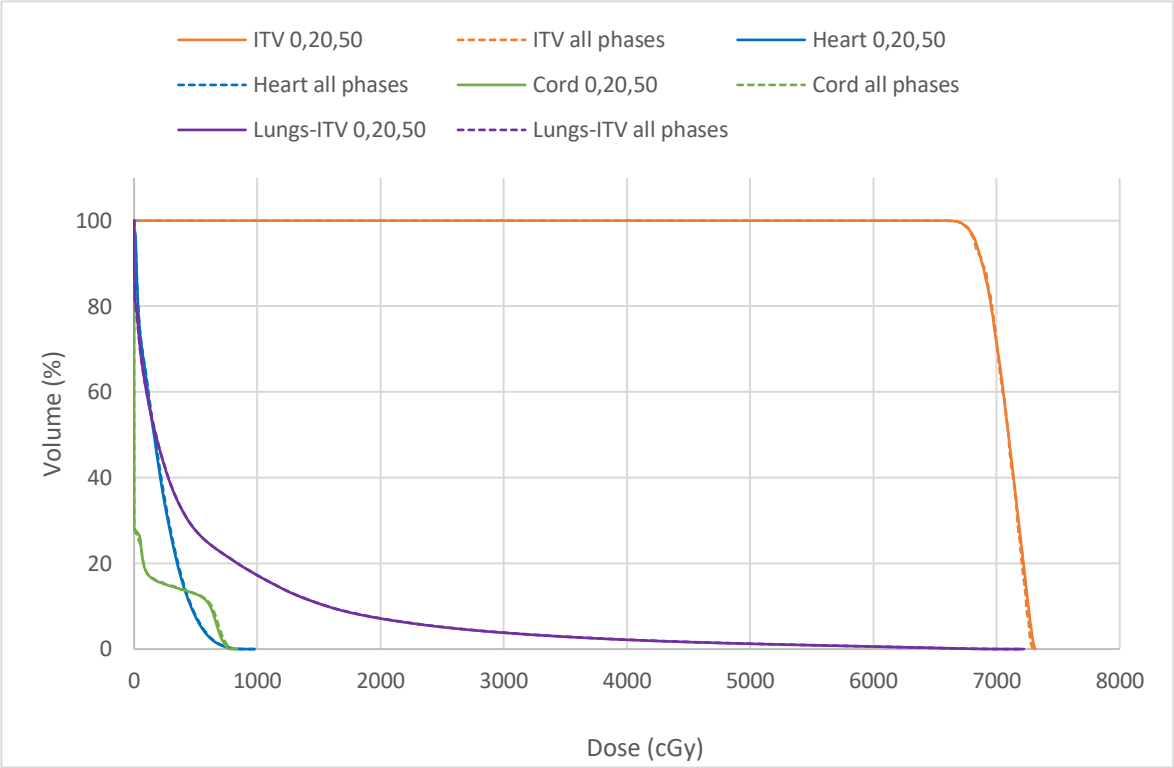

Figure 12.9: Dose-volume histogram for a 4D robust (GTV D99) plan for a SABR lung cancer patient optimised over all phases and optimised over the 0, 20 and 50% phases. Results are for all phases deformed and summed onto the 3DCT.

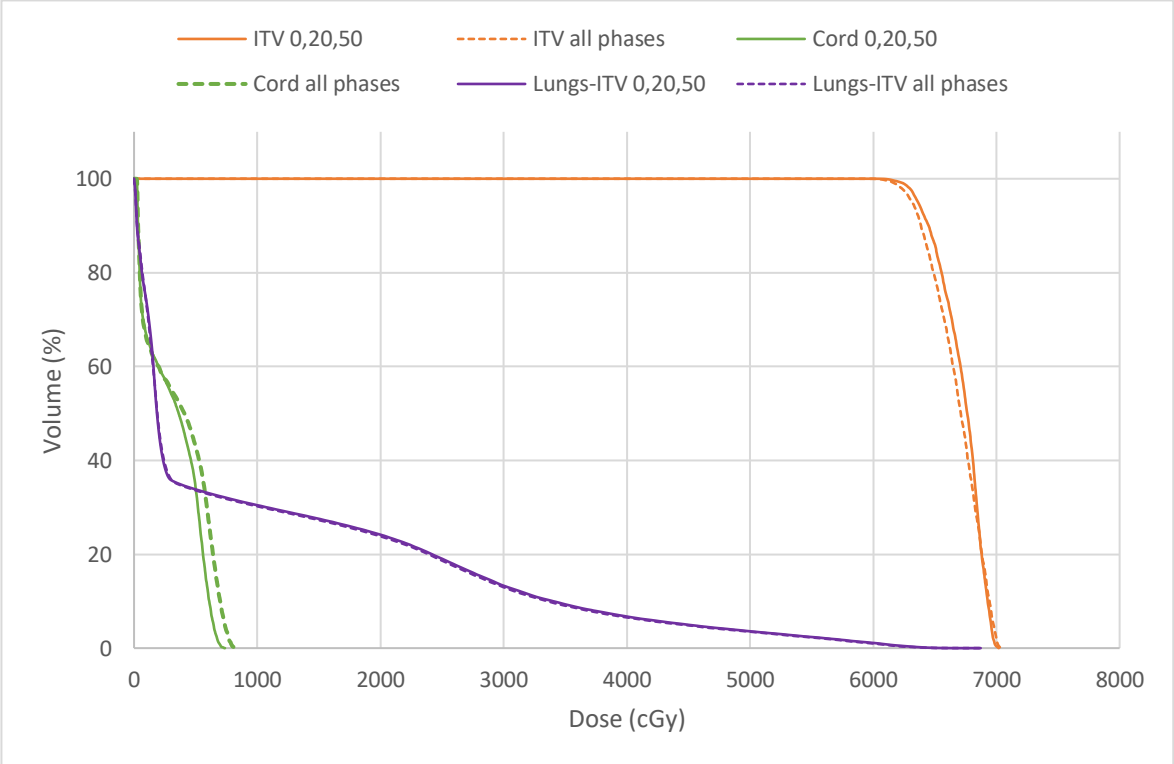

Figure 12.10: Dose-volume histogram for a 4D robust (GTV D99) plan for a lung phantom with moving insert optimised over all phases and optimised over the 0, 20 and 50% phases. Results are for all phases deformed and summed onto the 3DCT.

12.3.3 Pinpoint Measurements

The results from the pinpoint measurements were all within 2.5% except for two 4D robust deliveries with the phantom moving using the RPM trace (Table 12.11). Two pinpoint measurements were taken for each beam and the average dose per beam summed to obtain the measured dose. The repeatability was not explicitly tested but the difference between the two pinpoint readings per beam was up to 3% (1.2% on average). Interplay effects were not tested as measurements were started at an arbitrary point in the breathing cycle. Therefore, the difference between readings could indicate interplay effects.

Table 12.11: Doses for different planning methods for 2 SABR patients (A and B), measured using a pinpoint chamber in a CIRS moving thorax phantom. The phantom was programmed with movement obtained from 4DCBCT or the real-time position management system (RPM) as indicated. Errors were combined in quadrature to obtain the error in pinpoint measurement dose.

Plan	Movement	TPS Dose (Gy)	Measured Dose (Gy)	% Dose Difference (Measured to TPS)
A: Clinical Margin	4DCBCT	15.1	14.9±0.4	-0.8
A: 3D Robust	4DCBCT	14.9	14.6±0.4	-2.1
A: 4D Robust	4DCBCT	16.1	16.0±0.4	-0.6
A: Clinical Margin	RPM	14.5	14.6±0.4	+1.0
A: 4D Robust	RPM	14.8	15.6±0.4	+5.3
B: Clinical Margin	4DCBCT	28.6	28.9±0.7	+1.2
B: 3D Robust	4DCBCT	27.5	28.1±0.7	+2.2
B: 4D Robust	4DCBCT	29.0	29.4±0.8	+1.3
B: Clinical Margin	RPM	28.2	28.9±0.7	+2.3
B: 4D Robust	RPM	28.6	29.7±0.8	+4.1

12.4 Discussion

The 3D robust planning method produced clinically acceptable plans with lung V20Gy and V12.5Gy volumes that were statistically smaller than those from the clinical margin-based plans at the 5% level when compared using a Wilcoxon rank test. The differences in volumes were very small but any reduction in dose could allow for further dose escalation. It has been shown that V20Gy and V12.5Gy are associated with grade ≥2 radiation pneumonitis[12] and that this is one of the main toxicities that limits dose escalation in SABR doses[13]. All other differences in OAR doses for this study were not statistically significant. Other studies have found other OARs to be significantly lower with robust optimisation in addition to the lungs. For example, Zhang *et al.* (2018)[7] found the heart and spinal cord doses to be significantly lower but this study was optimising over all phases rather than an ITV on a 3D scan. Leung *et al.* (2020)[10] found the chest wall dose to be significantly lower when optimising over an ITV on a mid-ventilation CT. However, the plans were not re-normalised for GTV D99 coverage so it was found that GTV D98 was also significantly lower.

The OAR doses for the 4D robust plan (GTV D99) were higher than the corresponding margin-based plan. Other studies have found that the OAR doses were lower using robust optimisation[8,10]. However, these studies were optimising so the GTV D99 received the prescription isodose rather than the GTV D99 from the margin-based plan. When the GTV was optimised to achieve the prescription dose (4D robust (PTV)) the OAR doses were more comparable to the margin-based plans with only the dose to 0.5cc of lung being statistically significantly lower. However, when deformed and summed on the 3DCT, the dose to 95% of the PTV was lower than the prescription for 5 of the patients.

The difference in OAR doses between the margin-based plans and robust plans may be lower in this study than other studies due to the method used to optimise the margin-based plans. The margin-based plans were initially optimised with the air in the PTV set to water. This should decrease the multi-leaf collimator margins around the PTV and hence the dose to the surrounding normal tissue. Only one study was found that compared robust optimisation to a density override method. Archibald-Heeren *et al.* (2017)[9] performed a 3D robust optimisation on an Ave-IP, similar to that performed here with a density override and found that the mean and maximum lung doses were higher on average for these robust plans than margin-based plans using an ITV. They also found the maximum lung dose was also higher for the 4D robust plan compared to the density override plan.

The coverage of the GTV in the presence of patients shifts, showed that margin-based planning and 3D robust planning gave comparable levels of robustness. The 3D robust planning gave a higher dose to GTV D99 in the superior direction than the margin-based plan but this was not statistically significant. Although no comparison was made to margin-based plans, both Zhang *et al.* (2018)[7] and Liang *et al.* (2019)[8] found that ITV D99 was greater than 95% of the prescription for all robustly optimised plans when perturbed up to 5 mm. However, only 6 patients were analysed in Zhang *et al*. (2018)[7] and only 9 patients were analysed in Liang *et al*. (2019)[8]. For the study here, only one patient had GTV D99 less than 95% of the prescription upon perturbation of 4 mm.

For the 4D robust (GTV D99) plans, GTV D99 and D50 were higher across all phases than the margin-based plans. Leung *et al*. (2020)[10] found that margin-based plans on the Ave-IP had higher GTV D98, D50 and D2 doses than robustly optimised plans. However, the plans were optimised so the GTV D99 received the prescription dose rather than the GTV D99 dose from the original clinical plan. Hence, the GTV dose will be lower in this case. One reason for the smaller differences in OAR doses observed here may be due to the use of a transition structure in the optimiser for some of the margin-based plans which was a rind around the PTV with a maximum dose in the optimiser. This was not used for the 4D robust plans due to the computation time. For this study with 21 scenarios computed for 4D robust optimisation, an average iteration took approximately 48 s for only the GTV set to be robust. Further work should be carried out creating a transition structure for each GTV on the phases and a robust optimisation performed with this structure also set to be robust across the phases.

The variation of GTV D99, D50 and D2 was found to be lower in the 4D robust plans (GTV D99) plans compared to the margin-based plans and this was statistically significant. The variation of GTV D99 was also lower in the 4D robust (PTV) plans but higher for D50 and D2. Archibald-Heeren *et al.* (2017)[9] found that the robust methods reduced variation in the maximum dose across the breathing cycle and this was most pronounced for larger tumour motion. However, Leung *et al*. (2020)[10] found that the variation was not statistically significant between both datasets and that the interquartile range from robustly optimised plans was more variable. The result for both sets of 4D robust plans here suggests that coverage of the GTV D99 across the phases is more uniform. However, as all values for GTVD99 we above the prescription, then clinically this is not significant.

The normalisation of robust plans varies across literature. Liang *et al*. (2019)[8] optimised to cover the ITV D99 on all error scenarios over a static CT set. This made the plans hotter than

if they had been re-normalised. For this study the 3D robust plans were re-normalised to compare directly with the margin-based plans. The 4D plans were not re-normalised as it is only possible to re-normalise on the nominal scenario and this would not ensure that the worst-case scenario was robust over the phases. This means that there will still be variation across the breathing phases. It has been shown in other studies that re-normalisation of the GTV to D50 can reduce the variation in GTV doses among patients and methods[10,14] and further work should be done to investigate this for the current study.

The monitor units for all robustly optimised plans were lower than the margin-based plans. This was also found by Zhang *et al.* (2018)[7]. The reduction in monitor units could reduce the overall treatment time and there could be fewer breathing cycles during treatment.

The pinpoint measurements showed good agreement (within 2.5%) with the planning system for all plans except two 4D robust plans with no obvious bias towards a better result for margin-based or robust plans. The 2 results that were greater than 3% could suggest that the 4D robust plans were more complex. On further examination, the difference in chamber measurements compared to the TPS dose for patient B was larger for the first arc (7.6%). The average equivalent square for this arc over all segments was 1.3 cm smaller than the margin-based plan, suggesting that this arc was more complex. The majority of results agreeing within 2.5% to the planning system is similar to Archibald-Heeren *et al.* (2017)[9] who measured static geometry and found a difference compared to the treatment planning system dose of +1.8% for 4D robustly optimised plans and +0.9% difference for margin-based plans. It would be beneficial to measure a larger set of plans and use film as this would allow comparison at the edges of the field rather than a point dose in the centre.

The study only optimised robustly over 0%, 20% and 50% breathing phases rather than all of the phases. The comparison for the phantom and one patient showed minimal differences between the 2 methods. Further comparisons should be made for clinical plans to ensure that the optimisation over fewer breathing phases is valid for a larger population.

A limitation of this study is that the GTV contours on the phases were obtained retrospectively and sometimes by different clinicians to those who outlined the original ITV. In addition, some of the contours were created via deformable registration and although contours were reviewed and edited this could cause a bias in the contours produced. However, all of the margin-based plans were re-optimised using a new phase-based PTV so the comparison between margin-based and 4D robustly optimised plans is still valid.

In addition, only a small number of patients have been assessed in the current study with a maximum tumour amplitude of 1.1 cm. It would be beneficial to conduct a larger study to see if the range of tumour motion observed is representative of the population.

12.5 Conclusions

Robust optimisation on a 3D CT scan could be implemented clinically with comparable plans being achieved. Robust optimisation over phases can produce less variable GTV coverage across breathing phases. Care would have to be taken when implementing clinically to ensure adequate coverage of the GTV. The lower monitor units of robust optimisation could be beneficial but the time taken to optimise plans is slow which could limit clinical implementation of this technique.

12.6 References

1. Vansteenkiste, J.; Wauters, E.; Reymen, B.; Ackermann, C. J.; Peters, S.; De Ruysscher, D., (2019) 'Current Status of Immune checkpoint Inhibition in Early-Stage NSCLC',. *Annals of Oncology*, *30*, pp. 1244-1253.
2. SABR UK Consortium., (2019) 'Stereotactic Ablative Body Radiation Therapy (SABR): A Resource Version 6.1' ,. No. January.
3. Lacornerie, T.; Lisbona, A.; Mirabel, X.; Lartigau, E.; Reynaert, N., (2014) 'GTV-Based Prescription in SBRT for Lung Lesions Using Advanced Dose Calculation Algorithms',. *Radiation oncology (London, England)*, *9*, pp. 223 doi: 10.1186/s13014-014-0223-5.
4. Fredriksson, A.; Forsgren, A.; Hårdemark, B., (2011) 'Minimax Optimization for Handling Range and Setup Uncertainties in Proton Therapy' ,. *Medical Physics*, *38* (3), pp. 1672–1684 doi: 10.1118/1.3556559.
5. Ge, S.; Wang, X.; Liao, Z.; Zhang, L.; Sahoo, N.; Yang, J.; Guan, F.; Mohan, R., (2019) 'Potential for Improvements in Robustness and Optimality of Intensity-Modulated Proton Therapy for Lung Cancer with 4-Dimensional Robust Optimization' ,. *Cancers*, *11* (1) doi: 10.3390/cancers11010035.
6. Li, H.; Zhang, X.; Park, P.; Liu, W.; Chang, J.; Liao, Z.; Frank, S.; Li, Y.; Poenisch, F.; Mohan, R.; Gillin, M.; Zhu, R., (2015) 'Robust Optimization in Intensity-Modulated Proton Therapy to Account for Anatomy Changes in Lung Cancer Patients' ,. *Radiotherapy and Oncology*, *114* (3), pp. 367–372 doi: 10.1016/j.radonc.2015.01.017.
7. Zhang, X.; Rong, Y.; Morrill, S.; Fang, J.; Narayanasamy, G.; Galhardo, E.; Maraboyina, S.; Croft, C.; xia, F.; Penagaricano, J., (2018) 'Robust Optimization in Lung Treatment Plans Accounting for Geometric Uncertainty' ,. *Journal of Applied Clinical Medical Physics*, *19* (3), pp. 19–26 doi: 10.1002/acm2.12291.
8. Liang, X.; Zheng, D.; Mamalui-hunter, M.; Flampouri, S.; Hoppe, B. S.; Mendenhall, N., (2019) 'ITV-Based Robust Optimization for VMAT Planning of Stereotactic Body Radiation Therapy of Lung Cancer' ,. *Practical Radiation*

Oncology, *9* (1), pp. 38–48 doi: 10.1016/j.prro.2018.08.005.

9. Archibald-heeren, B. R.; Byrne, M. V; Hu, Y.; Cai, M.; Wang, Y., (2017) 'Robust Optimization of VMAT for Lung Cancer : Dosimetric Implications of Motion Compensation Techniques' ,. No. February, pp. 104–116 doi: 10.1002/acm2.12142.

10. Leung, R. W. K.; Chan, M. K. H.; Chiang, C.; Wong, M.; Blanck, O., (2020) 'On the Pitfalls of PTV in Lung SBRT Using Type-B Dose Engine : An Analysis of PTV and Worst Case Scenario Concepts for Treatment Plan Optimization' ,. pp. 1–16.

11. Walker, Z.; Chuter, R.; Rogers, J., (2021) 'Evaluating Robust Optimisation Using Realistic Breathing Traces' ,. *Chapter 12 of PhD Thesis*,.

12. Saha, A.; Beasley, M.; Hatton, N.; Dickinson, P.; Franks, K.; Clarke, K.; Jain, P.; Teo, M.; Murray, P.; Lilley, J., (2021) 'Clinical and Dosimetric Predictors of Radiation Pneumonitis in Early-Stage Lung Cancer Treated with Stereotactic Ablative Radiotherapy (SABR) – An Analysis of UK's Largest Cohort of Lung SABR Patients' ,. *Radiotherapy and Oncology*, *156*, pp. 153–159 doi: 10.1016/j.radonc.2020.12.015.

13. Yamashita, H.; Nakagawa, K.; Nakamura, N.; Koyanagi, H.; Tago, M.; Igaki, H.; Shiraishi, K.; Sasano, N.; Ohtomo, K., (2007) 'Exceptionally High Incidence of Symptomatic Grade 2-5 Radiation Pneumonitis after Stereotactic Radiation Therapy for Lung Tumors' ,. *Radiation Oncology*, *2* (1), pp. 1–11 doi: 10.1186/1748-717X-2-21.

14. Tanadini-Lang, S.; Wilke, L.; Karava, K.; Andratschke, N.; Ehrbar, S.; Guckenberger, M., (2018) 'EP-2197: Dose Normalization in Lung SBRT Based on ICRU 91 and Comparison to Alterative Normalization Methods' ,. *Radiotherapy and Oncology*, *127*, pp. S1213–S1214 doi: 10.1016/s0167-8140(18)32506-4.

13 Critical Appraisal

13.1 Introduction

The topics of this thesis were selected as they are all applicable to lung treatment planning. With 80% of patients with lung cancer receiving radiotherapy as part of their treatment[3], any time-saving through the use of software such as DLCExpert could free up staff time to perform other tasks and treatment plans could be produced more quickly. This is important for cancer patients in the NHS in England, Scotland and Northern Ireland who should have no more than a 31 day wait from diagnosis/decision to treat to the first definitive treatment or no more than a 62 day wait from urgent GP referral to first treatment[105]. Any time savings could allow staff to work on other planning improvements such as those assessed in this project.

As previously discussed, lung cancer is the leading cause of cancer death[1] so it is imperative that treatments are continuously improved. Although the use of 4DCT is now common in radiotherapy departments, the work in the 3D vs 4D outlining paper has shown the dosimetric benefits of using 4D outlining for treatment planning. Using 4D PTVs lowered lung doses but there is still the consideration of air within the PTV. The paper on robust optimisation suggests that there is less variation over the GTV when robust optimisation over breathing phases is used. There is also the challenge of measuring dose from plans where the target is moving. The paper on breathing trace extraction explored an Amsterdam shroud method for binned data. Although the technique was not satisfactory for 4DCBCT scans, the method showed that the data could potentially be used for breathing trace extraction using 4DCT scans.

All of the topics within the thesis could potentially improve treatments for lung radiotherapy. This paper will appraise the research process used including strengths and limitations of the work carried out, how the project contributes to clinical practice and further work.

13.2 Outlining for lung radiotherapy

The lung study using Mirada was only a small-scale study performed at one site to test if DLCExpert could be applied for this site. The focus of the paper was for prostate and head and neck as these models were available across all sites. A strength of the paper is there is a large set of data from multiple centres. The results contribute to clinical practice as there was

limited multi-centre data in the literature using generic models. This paper allows other centres to see results from clinical implementation across several centres and the potential time-saving benefits. It also provides clinical values for DSC and DTA for different sites using DLCExpert which there is limited assessment of within the literature. This would be useful for centres to benchmark against if they were implementing the system clinically.

Due to the nature of the study where all centres were allowed to perform their own implementation of the system, different methods were used for analysis and this is a limitation of the study. If the same metrics were used then differences in timings could be correlated with metrics as done in other studies[106,107]. Further work could be carried out to assess the surface DSC and added path length. In addition, a comparison of vendors would be useful for other centres who want to implement DLC but in practice this would be difficult to achieve.

The 3D vs 4D paper adds to the literature as there was only one paper found providing a dosimetric analysis of non-SABR patients, which was small-scale assessing only peripheral tumours. A strength of the paper here is the cohort of patients assessed which covered a range of tumour stages and positions due to selection of sequential patients and the 3D and 4D outlines were performed by the same clinician. However, a limitation is that the 4D outline was derived from the 3D outline and may cause bias in the 4D outline. This method was used as it was easy to implement for clinical patients with minimal extra time required and the 3D outline was done as part of the clinical workflow. An alternative, more robust method, would be to have the same clinician outline a 4D GTV for clinical use and then outline the 3D GTV after a period of time had passed without using the 4D GTV for reference.

Inter-observer variation is an important area where further work should be carried out for lung radiotherapy treatment planning. It would be beneficial to investigate if DLC provides increased consistency and to evaluate the inter-observer variability for tumours in addition to OARs. The importance of this has been highlighted by Lo *et al*. (2014)[108] for SABR lung planning who evaluated peer review for 40 patients OARs and tumour contours. Twenty-three percent of contours were recommended to have major changes and 5% of all structures edited had dosimetric violations. There is limited evidence for the use of DLC for lung tumour volumes as there is no commercial system available for this at the moment. However, non-commercial tests indicate promising results and that consistency in contours can be improved and time savings can be made[109,110]. The consistency of tumour outlines is

important as this contributes to PTV margins. The PTV margin, accounting for delineation uncertainty alone, has been shown to be as large as 5.9 mm for early-stage NSCLC[111].

13.3 Extraction of breathing traces

The paper expands on current literature as it tests the potential of binned data for 4DCBCT which has only been reported for 4DCT[24]. It also attempts to extract a breathing trace directly from the tumour volume rather than the diaphragm which is not in the literature as studies are commonly use breathing trace extraction to bin data rather than to extract a trace corresponding to tumour amplitude[100,112,113]. An advantage of extracting the tumour motion is that dose measurements can be performed with realistic breathing traces. This is important when assessing plans that are aiming to improve radiotherapy for moving targets such as robust optimisation.

The Amsterdam shroud method was chosen for this study as this was used by Elekta to create the 4DXVi and the ITK software was available to do part of the analysis. The use of individual projections was investigated but were not able to be extracted without purchasing a new license file so binned data was used instead. The advantage of this is that clinics can easily obtain and export binned data. However, as shown in the paper the results for 4DCBCT were not acceptable. An alternative method would be to use the individual projections as previously discussed in the literature[100] or investigate the LPCA[114] and Fourier[115] methods that have also been presented using individual projections.

It was decided to run the script for each visible slice of the tumour and then pick the result which gave the maximum displacement. This was to ensure that the worst-case scenario was considered for any subsequent measurements taken using the breathing trace. It is difficult to know if an average should be used as this would be more representative of the whole tumour volume and would reduce the effect from any slices where the tumour deforms. A limitation of the study is the lack of testing on scans with a known amplitude. A phantom with one amplitude was only available at the time of testing. Further tests with different amplitudes should be carried out to obtain whether the method overestimates or underestimates movement depending on the amplitude.

The profiles from the Amsterdam shroud were matched to the profile from the first phase to obtain the offset for each phase. This was chosen as it was the method applied in Zijp *et al*. (2004)[112] with Amsterdam shroud images. However, any error in the first phase would then

manifest in other offsets. It would be useful to investigate the use of adjacent profile matching.

13.4 Robust Optimisation

This paper adds to the literature as there is currently limited evidence of the use of commercial treatment planning systems for robust photon lung planning. Four papers were found that investigated the use for lung SABR and 3 of these created plans on patient CT scans and only included 3, 9 and 13 patients[89,91,92]. Some of the papers carried out robust optimisation for a static geometry[54,89,91] but these all used an average intensity projection image rather than a 3DCT scan as used in the project. The 3D scan was chosen to test robust optimisation as this is used clinically at the centre.

In addition, none of the papers made a comparison of perturbed patient margin-based plans to robust plans for a static geometry. This was performed in the paper, totaling 260 shift scenarios. It was chosen to perturb up to 5 mm as this was the PTV margin used for clinical plans.

All of the robust plans in the current study were compared to clinical plans that had initial optimisations with the air in the PTV set to water. Only one study within the literature compared robust plans to a density override plan but this was for a phantom rather than clinical plans[54]. The current study allows centres to see a clinical implementation of robust optimisation for patients receiving SABR treatment. A further extension of the work would be to compare to margin-based plans with no density override.

The work also extends the current literature as measurements were made of the robustly optimised plans which has only been carried out for patient plans in one conference paper[92]. The measurements from the project indicate that the robustly optimised plans are deliverable, with the dose difference to the treatment planning system being no worse than that from clinical plans in the majority of cases tests. An inaccuracy in the method used is that the scans of the chamber had a 2.5 mm slice width and the chamber volume is small (0.015 cm^3). This means that the outline of the chamber on the CT scan will not be as accurate as if a narrower slice width was used. The 2.5 mm slice width was used as this was the protocol used for clinical patients and a new protocol would need to be created for a different slice width. A limitation is that only a pinpoint measurement was performed, not allowing the

edge of the field to be assessed, where there is likely to be more variation. However, the phantom used did not allow for film measurements to be made.

The 3D plans were normalised to match the GTV D99 of the clinical margin-based plan. This was decided upon to allow direct dosimetric comparison with the clinical margin-based plans. An alternative approach of not normalising was considered but this could make the robust plans hotter as the optimisation is ensuring coverage in the worst-case scenario. It would be useful to assess the doses for the 3D robust plans before re-normalisation to see if the plans were hotter but OAR goals were still met.

The 4D plans were not re-normalised as any re-normalisation would have to be done on the nominal scan, and the plan robustness to ensure the coverage of the GTV over each breathing phase would be therefore be lost. However, Leung *et al*. (2020)[91] tested re-normalising plans so that GTV 50 received the prescription dose on the nominal scan. They found that doing this improved the consistency in doses between the GTVs. Further work could be carried out for the current study to also perform this normalisation.

As previously mentioned, the 4D plans were only optimised over 3 phases as this would cover the extremes of motion and a mid-phase tumour position which was theorised should be enough to cover the tumour motion over all phases. The advantage of this method is time-saving as there are 21 scenarios computed rather than 70 if all of the phases are used. One iteration of a margin-based plan took approximately 2.5 s compared with 48 s for a 4D robust plan over 3 phases. The comparisons to optimising over all 10 for a phantom and for one patient showed minimal differences. Although there are only 2 comparisons these covered a small amplitude of motion (0.6 cm) and a large amplitude of motion (1.5 cm). Further work should be carried out to assess the differences for a larger cohort as any time saving would be beneficial in a clinical setting.

All robust plans ensured the GTV D99 achieved that of the original clinical plan over all scenarios. This was to allow comparison with the margin-based plans. Although the value was slightly different between the clinical plan and the margin-based plan using the phases PTV, the GTV D99 dose exceeded that of both types of margin-based plans. The 4D robust plans were also re-planned to ensure the GTV D99 achieved the prescription dose over all phases. This was done to compare to other studies.

A limitation of the paper is that the outlines for the 4D robust plans came from retrospective GTV outlines only contoured on the 0% and 50% phases. The retrospective nature meant that a different clinician may have been outlining and in addition, the PET scan was not always available to them. The deformable registration between phases could also cause a bias as outlines on the other phases were reviewed rather than drawn from scratch. A more robust method would be to create a GTV outline on all phases at the time of outlining the patient for treatment. However, this was not feasible due to time pressures when outlining as 130 outlines would need to be produced using this method. The DSC and DTA for the combined phases GTV outlines compared to the 4D ITV were calculated (Table 13.1). They were compared to values in the literature for inter-observer variability for lung ITVs (DSC values of 0.84 and 0.802 were found[116,117]). As 8 patients had values lower than the average from these studies, it was decided to re-plan all patients using an ITV from the phases. This allowed direct comparison with the 4D robust plans as any changes in OAR does would not be attributed to differences in outline.

Table 13.1: Dice similarity coefficient (DSC) and distance to agreement (DTA) values for 15 lung cancer SABR patient GTV outlines using 4DCT. Clinical outlines have been compared to a summed outline obtained from deforming outlines from the 0% and 50% breathing phases.

Patient	DSC	DTA (mm)
1	0.842	0.45
2	0.549	1.27
3	0.905	0.62
4	0.868	0.85
5	0.808	1.13
6	0.905	0.73
7	0.85	1.16
8	0.81	1.08
9	0.739	0.91
10	0.773	1.05
11	0.735	0.93
12	0.857	1.18
13	0.743	1.17
14	0.722	0.66

Another limitation of the study is the small cohort of patients. Although, the patients have different prescriptions unlike other robust lung SABR studies within the literature. Further plans should be produced for more patients to ensure the results are representative of a larger patient population.

14 Thesis Conclusions

The work presented in this thesis has focused on aspects of improving lung radiotherapy treatment planning. All papers have demonstrated how these can be applied in a clinical setting with potential benefits being investigated.

It was found that Mirada's generic DLC model for lung OAR outlining shows good agreement with clinical contours for the lungs, heart and cord. DLCExpert was shown to provide time-savings for other sites with the potential of reducing inter-observer variability and this could also be beneficial for lung outlining. Further work is needed to assess these aspects for lung OARs.

For lung tumour outlining, the 3D vs 4D paper showed the benefits of using 4DCT for a variety of tumour stages. Outlining the tumour using the 4DCT reduced doses to the OARs which could reduce radiation induced toxicity or allow for dose escalation.

Robust optimisation of lung SABR plans showed that a 3D method could be implemented clinically with comparable results to margin-based plans and lower lung doses. Robust optimisation over breathing phases was found to produce less variation in GTV coverage across breathing phases. Further work would be needed to demonstrate the best method to use before implementing clinically. Due to the number of scenarios, robust optimisation can be very slow and time-savings from DLCExpert could be beneficial in the lung planning process.

A method of extracting breathing traces from 4D images of a lung tumour was developed and tested using clinical data that would be available in other centres. This performed well for theoretical data and better than a centroid method using 4DCT images. However, this was not adequate for 4DCBCT data and further development is required.

Overall, this work has demonstrated that OAR and tumour outlining can be improved using DLC and 4DCT. These accurate outlines are important for new planning technqiues such as robust optimisation which can use GTV outlines over the breathing phases for optimisation. There are many methods that can be used for robust optimisation and these should be assessed before clinical implementation. It is important to assess the delivery of new lung planning techniques and using the movement of the tumour from images when delivering plans would allow for measurements in a realistic scenario.

15 References

1. Sung, H.; Ferlay, J.; Siegel, R. L.; Laversanne, M.; Soerjomataram, I.; Jemal, A.; Bray, F., (2021) 'Global Cancer Statistics 2020: GLOBOCAN Estimates of Incidence and Mortality Worldwide for 36 Cancers in 185 Countries' ,. *CA: A Cancer Journal for Clinicians*, *71* (3), pp. 209–249 doi: 10.3322/caac.21660.

2. Ferlay J, Ervik M, Lam F, Colombet M, Mery L, P. M., (2020) Global Cancer Observatory: Cancer Today. Lyon: International Agency for Research on Cancer; 2020 https://gco.iarc.fr/today.

3. Diwanji, T. P.; Mohindra, P.; Vyfhuis, M.; Snider, J. W.; Kalavagunta, C.; Mossahebi, S.; Yu, J.; Feigenberg, S.; Badiyan, S. N., (2017) 'Advances in Radiotherapy Techniques and Delivery for Non-Small Cell Lung Cancer: Benefits of Intensity-Modulated Radiation Therapy, Proton Therapy, and Stereotactic Body Radiation Therapy' ,. *Translational Lung Cancer Research*, *6* (2), pp. 131–147 doi: 10.21037/tlcr.2017.04.04.

4. Potters, L.; Steinberg, M.; Rose, C.; Timmerman, R.; Ryu, S.; Hevezi, J. M.; Welsh, J.; Mehta, M.; Larson, D. A.; Janjan, N. A., (2004) 'American Society for Therapeutic Radiology and Oncology and American College of Radiology Practice Guideline for the Performance of Stereotactic Body Radiation Therapy' ,. *International Journal of Radiation Oncology Biology Physics*, *60* (4), pp. 1026–1032 doi: 10.1016/j.ijrobp.2004.07.701.

5. Vorwerk, H.; Zink, K.; Schiller, R.; Budach, V.; Böhmer, D.; Kampfer, S.; Popp, W.; Sack, H.; Engenhart-Cabillic, R., (2014) 'Protection of Quality and Innovation in Radiation Oncology: The Prospective Multicenter Trial the German Society of Radiation Oncology (DEGRO-QUIRO Study): Evaluation of Time, Attendance of Medical Staff, and Resources during Radiotherapy with IMRT' ,. *Strahlentherapie und Onkologie*, *190* (5), pp. 433–443 doi: 10.1007/s00066-014-0634-0.

6. Vinod, S. K.; Jameson, M. G.; Min, M.; Holloway, L. C., (2016) 'Uncertainties in Volume Delineation in Radiation Oncology : A Systematic Review and Recommendations for Future Studies' ,. *Radiotherapy and Oncology*, *121* (2), pp. 169–179 doi: 10.1016/j.radonc.2016.09.009.

7. Lo, A. C.; Liu, M.; Chan, E., (2013) 'The Impact of Peer Review of Volume Delineation in Stereotactic Body Radiation Therapy Planning for Primary Lung Cancer : A Multicenter Quality Assurance Study' ,. *Journal of Thoracic Oncology*, *9* (4), pp. 527–533 doi: 10.1097/JTO.0000000000000119.

8. Zabel, W. J.; Conway, J. L.; Gladwish, A.; Skliarenko, J.; Didiodato, G.; Goorts-matthews, L.; Mrt, T.; Michalak, A.; Mrt, T.; Reistetter, S.; Mrt, T.; King, J.; Nakonechny, K.; Malkoske, K.; Tran, M. N.; Mcvicar, N., (2021) 'Clinical Evaluation of Deep Learning and Atlas-Based Auto-Contouring of Bladder and Rectum for Prostate Radiation Therapy' ,. *Practical Radiation Oncology*, *11* (1), pp. e80–e89 doi: 10.1016/j.prro.2020.05.013.

9. Young, A. V.; Wortham, A.; Wernick, I.; Evans, A.; Ennis, R. D., (2011) 'Atlas-Based Segmentation Improves Consistency and Decreases Time Required for Contouring Postoperative Endometrial Cancer Nodal Volumes' ,. *International Journal of Radiation Oncology Biology Physics*, *79* (3), pp. 943–947 doi: 10.1016/j.ijrobp.2010.04.063.

10. La Macchia, M.; Fellin, F.; Amichetti, M.; Cianchetti, M.; Gianolini, S.; Paola, V.;

Lomax, A. J.; Widesott, L., (2012) 'Systematic Evaluation of Three Different Commercial Software Solutions for Automatic Segmentation for Adaptive Therapy in Head-and-Neck, Prostate and Pleural Cancer' ,. *Radiation Oncology*, *7* (1), pp. 1 doi: 10.1186/1748-717X-7-160.

11. Simmat, I.; Georg, P.; Georg, D.; Birkfellner, W.; Goldner, G.; Stock, M., (2012) 'Assessment of Accuracy and Efficiency of Atlas-Based Autosegmentation for Prostate Radiotherapy in a Variety of Clinical Conditions' ,. *Strahlentherapie und Onkologie*, *188* (9), pp. 807–813 doi: 10.1007/s00066-012-0117-0.

12. Daisne, J. F.; Blumhofer, A., (2013) 'Atlas-Based Automatic Segmentation of Head and Neck Organs at Risk and Nodal Target Volumes: A Clinical Validation' ,. *Radiation Oncology*, *8* (1), pp. 1–11 doi: 10.1186/1748-717X-8-154.

13. Sharp, G.; Fritscher, K. D.; Pekar, V.; Peroni, M.; Shusharina, N.; Veeraraghavan, H.; Yang, J., (2014) 'Vision 20/20: Perspectives on Automated Image Segmentation for Radiotherapy' ,. *Medical Physics*, *41* (5), pp. 1–13 doi: 10.1118/1.4871620.

14. Gambacorta, M. A.; Boldrini, L.; Valentini, C.; Dinapoli, N.; Mattiucci, G. C.; Chiloiro, G.; Pasini, D.; Manfrida, S.; Caria, N.; Minsky, B. D.; Valentini, V., (2016) 'Automatic Segmentation Software in Locally Advanced Rectal Cancer: READY (REsearch Program in Auto Delineation SYstem)-RECTAL 02: Prospective Study' ,. *Oncotarget*, *7* (27), pp. 42579–42584 doi: 10.18632/oncotarget.9938.

15. Kim J, Han J, Ailawadi S, Baker J, Hsia A, Xu Z, R. S., (2016) 'SU-F-J-113: Multi-Atlas Based Automatic Organ Segmentation for Lung Radiotherapy Planning' ,. *Medical Physics*, *45* (6), pp. 3433–3433.

16. Zhong, H.; Kim, J.; Chetty, I. J., (2010) 'Analysis of Deformable Image Registration Accuracy Using Computational Modeling' ,. *Medical Physics*, *37* (3), pp. 970–979 doi: 10.1118/1.3302141.

17. Larrue, A.; Gujral, D.; Nutting, C.; Gooding, M., (2015) 'The Impact of the Number of Atlases on the Performance of Automatic Multi-Atlas Contouring' ,. *Physica Medica*, *31* (2015), pp. e30 doi: 10.1016/j.ejmp.2015.10.020.

18. Meyer, P.; Noblet, V.; Mazzara, C.; Lallement, A., (2018) 'Survey on Deep Learning for Radiotherapy' ,. *Computers in Biology and Medicine*, *98* (March), pp. 126–146 doi: 10.1016/j.compbiomed.2018.05.018.

19. Dijk, L. V. Van; Bosch, L. Van Den; Aljabar, P.; Peressutti, D.; Both, S.; Steenbakkers, R. J. H. M.; Langendijk, J. A.; Gooding, M. J.; Brouwer, C. L., (2020) 'Improving Automatic Delineation for Head and Neck Organs at Risk by Deep Learning Contouring' ,. *Radiotherapy and Oncology*, *142*, pp. 115–123 doi: 10.1016/j.radonc.2019.09.022.

20. Wong, J.; Fong, A.; Mcvicar, N.; Smith, S.; Giambattista, J.; Wells, D.; Kolbeck, C.; Giambattista, J.; Gondara, L.; Alexander, A., (2020) 'Comparing Deep Learning-Based Auto-Segmentation of Organs at Risk and Clinical Target Volumes to Expert Inter-Observer Variability in Radiotherapy Planning' ,. *Radiotherapy and Oncology*, *144*, pp. 152–158 doi: 10.1016/j.radonc.2019.10.019.

21. Lustberg, T.; Soest, J. Van; Gooding, M.; Peressutti, D.; Aljabar, P.; Stoep, J. Van Der; Elmpt, W. Van; Dekker, A., (2018) 'Clinical Evaluation of Atlas and Deep Learning Based Automatic Contouring for Lung Cancer' ,. *Radiotherapy and Oncology*, *126* (2), pp. 312–317 doi: 10.1016/j.radonc.2017.11.012.

22. Rietzel, E.; Liu, A. K.; Doppke, K. P.; Wolfgang, J. A.; Chen, A. B.; Chen, G. T. Y.;

Choi, N. C., (2006) 'Design of 4D Treatment Planning Target Volumes' ,. *International Journal of Radiation Oncology Biology Physics*, *66* (1), pp. 287–295 doi: 10.1016/j.ijrobp.2006.05.024.

23. Underberg, R. W. M.; Lagerwaard, F. J.; Slotman, B. J.; Cuijpers, J. P.; Senan, S., (2005) 'Use of Maximum Intensity Projections (MIP) for Target Volume Generation in 4DCT Scans for Lung Cancer' ,. *International Journal of Radiation Oncology Biology Physics*, *63* (1), pp. 253–260 doi: 10.1016/j.ijrobp.2005.05.045.

24. Wolthaus, J. W. H.; Schneider, C.; Sonke, J. J.; van Herk, M.; Belderbos, J. S. A.; Rossi, M. M. G.; Lebesque, J. V.; Damen, E. M. F., (2006) 'Mid-Ventilation CT Scan Construction from Four-Dimensional Respiration-Correlated CT Scans for Radiotherapy Planning of Lung Cancer Patients' ,. *International Journal of Radiation Oncology Biology Physics*, *65* (5), pp. 1560–1571 doi: 10.1016/j.ijrobp.2006.04.031.

25. McWilliam, A.; Lee, L.; Harris, M.; Sheikh, H.; Pemberton, L.; Faivre-Finn, C.; van Herk, M., (2018) 'Benefit of Using Motion Compensated Reconstructions for Reducing Inter-Observer and Intra-Observer Contouring Variation for Organs at Risk in Lung Cancer Patients' ,. *Radiotherapy and Oncology*, *126* (2), pp. 333–338 doi: 10.1016/j.radonc.2017.11.021.

26. Bradley, J. D.; Nofal, A. N.; El Naqa, I. M.; Lu, W.; Liu, J.; Hubenschmidt, J.; Low, D. A.; Drzymala, R. E.; Khullar, D., (2006) 'Comparison of Helical, Maximum Intensity Projection (MIP), and Averaged Intensity (AI) 4D CT Imaging for Stereotactic Body Radiation Therapy (SBRT) Planning in Lung Cancer' ,. *Radiotherapy and Oncology*, *81* (3), pp. 264–268 doi: 10.1016/j.radonc.2006.10.009.

27. Li, F. X.; Li, J. Bin; Zhang, Y. J.; Liu, T. H.; Tian, S. Y.; Xu, M.; Shang, D. P.; Ma, C. S., (2011) 'Comparison of the Planning Target Volume Based on Three-Dimensional CT and Four-Dimensional CT Images of Non-Small-Cell Lung Cancer' ,. *Radiotherapy and Oncology*, *99* (2), pp. 176–180 doi: 10.1016/j.radonc.2011.03.015.

28. Li, F.; Li, J.; Zhang, Y.; Xu, M.; Dongping, S.; Tingyong, F.; Liu, T.; Shao, Q., (2013) 'Geometrical Differences in Gross Target Volumes between 3dct and 4dct Imaging in Radiotherapy for Non-Small-Cell Lung Cancer' ,. *Journal of Radiation Research*, *54* (5), pp. 950–956 doi: 10.1093/jrr/rrt017.

29. Ahmed, N.; Venkataraman, S.; Johnson, K.; Sutherland, K.; Loewen, S. K., (2017) 'Does Motion Assessment with 4-Dimensional Computed Tomographic Imaging for Non-Small Cell Lung Cancer Radiotherapy Improve Target Volume Coverage?' ,. *Clinical Medicine Insights: Oncology*, *11* doi: 10.1177/1179554917698461.

30. Callahan, J.; Kron, T.; Siva, S.; Simoens, N.; Edgar, A.; Everitt, S.; Schneider, M. E.; Hicks, R. J., (2014) 'Geographic Miss of Lung Tumours Due to Respiratory Motion: A Comparison of 3D vs 4D PET/CT Defined Target Volumes' ,. *Radiation Oncology*, *9* (1), pp. 1–8 doi: 10.1186/s13014-014-0291-6.

31. Wang, L.; Hayes, S.; Paskalev, K.; Jin, L.; Buyyounouski, M. K.; Ma, C. C. M.; Feigenberg, S., (2009) 'Dosimetric Comparison of Stereotactic Body Radiotherapy Using 4D CT and Multiphase CT Images for Treatment Planning of Lung Cancer: Evaluation of the Impact on Daily Dose Coverage' ,. *Radiotherapy and Oncology*, *91* (3), pp. 314–324 doi: 10.1016/j.radonc.2008.11.018.

32. Hof, H.; Rhein, B.; Haering, P.; Kopp-Schneider, A.; Debus, J.; Herfarth, K., (2009) '4D-CT-Based Target Volume Definition in Stereotactic Radiotherapy of Lung

Tumours: Comparison with a Conventional Technique Using Individual Margins' ,. *Radiotherapy and Oncology*, *93* (3), pp. 419–423 doi: 10.1016/j.radonc.2009.08.040.

33. Bai, T.; Zhu, J.; Yin, Y.; Lu, J.; Shu, H.; Wang, L.; Yang, B., (2014) 'How Does Four-Dimensional Computed Tomography Spare Normal Tissues in Non-Small Cell Lung Cancer Radiotherapy by Defining Internal Target Volume?' ,. *Thoracic Cancer*, *5* (6), pp. 537–542 doi: 10.1111/1759-7714.12126.

34. Van Herk, M.; Remeijer, P.; Rasch, C.; Lebesque, J. V., (2000) 'The Probability of Correct Target Dosage: Dose-Population Histograms for Deriving Treatment Margins in Radiotherapy' ,. *International Journal of Radiation Oncology Biology Physics*, *47* (4), pp. 1121–1135 doi: 10.1016/S0360-3016(00)00518-6.

35. T. Landberg, J. Chavaudra, J. Dobbs, G. Hanks, K.-A. Johansson, T. Möller, J. P., (1993) 'ICRU Report 50–Prescribing, Recording and Reporting Photon Beam Therapy' ,. *Journal of the ICRU*, *26* (1), pp. 1–72.

36. Wambersie, A.; T. Landberg, J. Chavaudra, J. Dobbs, J. -P. Gerard, G. Hanks, J. -C. Horiot, K. -A. Johansson, T. Möller, J. Purdy, N. Suntharalingam, H. S., (1999) 'ICRU Report 62: Prescribing, Recording and Reporting Photon Beam Therapy' ,. *Journal of tHE ICRU*, *32* (1), pp. 1–52.

37. Chan, C.; Lang, S.; Rowbottom, C.; Guckenberger, M.; Faivre-Finn, C., (2014) 'Intensity-Modulated Radiotherapy for Lung Cancer: Current Status and Future Developments' ,. *Journal of Thoracic Oncology*, *9* (11), pp. 1598–1608 doi: 10.1097/JTO.0000000000000346.

38. Sheng, K.; Cai, J.; Brookeman, J.; Molloy, J.; Christopher, J.; Read, P., (2006) 'A Computer Simulated Phantom Study of Tomotherapy Dose Optimization Based on Probability Density Functions (PDF) and Potential Errors Caused by Low Reproducibility of PDF' ,. *Medical Physics*, *33* (9), pp. 3321–3326 doi: 10.1118/1.2222331.

39. Chan, T. C. Y.; Mišić, V. V., (2013) 'Adaptive and Robust Radiation Therapy Optimization for Lung Cancer' ,. *European Journal of Operational Research*, *231* (3), pp. 745–756 doi: 10.1016/j.ejor.2013.06.003.

40. Panakis, N.; McNair, H. A.; Christian, J. A.; Mendes, R.; Symonds-Tayler, J. R. N.; Knowles, C.; Evans, P. M.; Bedford, J.; Brada, M., (2008) 'Defining the Margins in the Radical Radiotherapy of Non-Small Cell Lung Cancer (NSCLC) with Active Breathing Control (ABC) and the Effect on Physical Lung Parameters' ,. *Radiotherapy and Oncology*, *87* (1), pp. 65–73 doi: 10.1016/j.radonc.2007.12.012.

41. McNair, H. A.; Brock, J.; Symonds-Tayler, J. R. N.; Ashley, S.; Eagle, S.; Evans, P. M.; Kavanagh, A.; Panakis, N.; Brada, M., (2009) 'Feasibility of the Use of the Active Breathing Co Ordinator™ (ABC) in Patients Receiving Radical Radiotherapy for Non-Small Cell Lung Cancer (NSCLC)' ,. *Radiotherapy and Oncology*, *93* (3), pp. 424–429 doi: 10.1016/j.radonc.2009.09.012.

42. Rosenzweig, K. E.; Hanley, J.; Mah, D.; Mageras, G.; Hunt, M.; Toner, S.; Burman, C.; Ling, C. C.; Mychalczak, B.; Fuks, Z.; Leibel, S. A., (2000) 'The Deep Inspiration Breath-Hold Technique in the Treatment of Inoperable Non-Small-Cell Lung Cancer' ,. *International Journal of Radiation Oncology Biology Physics*, *48* (1), pp. 81–87 doi: 10.1016/S0360-3016(00)00583-6.

43. Lutz, C. M.; Poulsen, P. R.; Fledelius, W.; Offersen, B. V.; Thomsen, M. S., (2016) 'Setup Error and Motion during Deep Inspiration Breath-Hold Breast Radiotherapy

Measured with Continuous Portal Imaging' ,. *Acta Oncologica*, *55* (2), pp. 193–200 doi: 10.3109/0284186X.2015.1045625.

44. Bartlett, F. R.; Colgan, R. M.; Carr, K.; Donovan, E. M.; McNair, H. a.; Locke, I.; Evans, P. M.; Haviland, J. S.; Yarnold, J. R.; Kirby, A. M., (2013) 'The UK HeartSpare Study: Randomised Evaluation of Voluntary Deep-Inspiratory Breath-Hold in Women Undergoing Breast Radiotherapy' ,. *Radiotherapy and Oncology*, *108* (2), pp. 242–247 doi: 10.1016/j.radonc.2013.04.021.

45. Boda-Heggemann, J.; Knopf, A. C.; Simeonova-Chergou, A.; Wertz, H.; Stieler, F.; Jahnke, A.; Jahnke, L.; Fleckenstein, J.; Vogel, L.; Arns, A.; Blessing, M.; Wenz, F.; Lohr, F., (2016) 'Deep Inspiration Breath Hold - Based Radiation Therapy: A Clinical Review' ,. *International Journal of Radiation Oncology Biology Physics*, *94* (3), pp. 478–492 doi: 10.1016/j.ijrobp.2015.11.049.

46. Mampuya, W. A.; Nakamura, M.; Matsuo, Y.; Ueki, N.; Iizuka, Y.; Fujimoto, T.; Yano, S.; Monzen, H.; Mizowaki, T.; Hiraoka, M., (2013) 'Interfraction Variation in Lung Tumor Position with Abdominal Compression during Stereotactic Body Radiotherapy' ,. *Medical Physics*, *40* (9) doi: 10.1118/1.4819940.

47. Bouilhol, G.; Ayadi, M.; Rit, S.; Thengumpallil, S.; Schaerer, J.; Vandemeulebroucke, J.; Claude, L.; Sarrut, D., (2013) 'Is Abdominal Compression Useful in Lung Stereotactic Body Radiation Therapy? A 4DCT and Dosimetric Lobe-Dependent Study' ,. *Physica Medica*, *29* (4), pp. 333–340 doi: 10.1016/j.ejmp.2012.04.006.

48. Inoue, T.; Katoh, N.; Onimaru, R.; Shimizu, S.; Tsuchiya, K.; Suzuki, R.; Sakakibara-Konishi, J.; Shinagawa, N.; Oizumi, S.; Shirato, H., (2013) 'Stereotactic Body Radiotherapy Using Gated Radiotherapy with Real-Time Tumor-Tracking for Stage I Non-Small Cell Lung Cancer' ,. *Radiation Oncology*, *8* (1), pp. 1 doi: 10.1186/1748-717X-8-69.

49. Chin, E.; Loewen, S. K.; Nichol, A.; Otto, K., (2013) '4D VMAT, Gated VMAT, and 3D VMAT for Stereotactic Body Radiation Therapy in Lung' ,. *Physics in Medicine and Biology*, *58* (4), pp. 749–770 doi: 10.1088/0031-9155/58/4/749.

50. Lacornerie, T.; Lisbona, A.; Mirabel, X.; Lartigau, E.; Reynaert, N., (2014) 'GTV-Based Prescription in SBRT for Lung Lesions Using Advanced Dose Calculation Algorithms' ,. *Radiation oncology (London, England)*, *9*, pp. 223 doi: 10.1186/s13014-014-0223-5.

51. Fu, H Perera, S Rudoler, Y. Y., (2013) 'SU-E-T-480: Can PTV Density Be Overridden for SBRT Lung Planning?' ,. *Medical Physics*, *40* (6), pp. 316.

52. Wiant, D.; Yount, C.; Pursley, J.; Terrell, J.; Maurer, J.; Sintay, B., (2013) 'TH-A-137-08: On the Validity of Target Density Overrides for RapidArc Lung SBRT Treatment Planning' ,. *Medical Physics*, *40* (6), pp. 518 doi: 10.1118/1.4815690.

53. Healy, G. E. A.; Marsh, S. H.; Cousins, A. T., (2018) 'The Dosimetric Effect of Electron Density Overrides in 3DCRT Lung SBRT for a Range of Lung Tumor Dimensions' ,. *J Appl Clin Med Phys*, *19* (6), pp. 79–87 doi: 10.1002/acm2.12446.

54. Archibald-heeren, B. R.; Byrne, M. V; Hu, Y.; Cai, M.; Wang, Y., (2017) 'Robust Optimization of VMAT for Lung Cancer : Dosimetric Implications of Motion Compensation Techniques' ,. No. February, pp. 104–116 doi: 10.1002/acm2.12142.

55. Byrne, M.; Hu, Y.; Archibald-Heeren, B., (2016) 'Evaluation of RayStation Robust Optimisation for Superficial Target Coverage with Setup Variation in Breast IMRT' ,. *Australasian Physical and Engineering Sciences in Medicine*, *39* (3), pp. 705–716

doi: 10.1007/s13246-016-0466-6.

56. Unkelbach, J.; Alber, M.; Bangert, M.; Bokrantz, R.; Chan, T. C. Y.; Deasy, J. O.; Fredriksson, A.; Gorissen, B. L.; Van Herk, M.; Liu, W.; Mahmoudzadeh, H.; Nohadani, O.; Siebers, J. V.; Witte, M.; Xu, H., (2018) 'Robust Radiotherapy Planning' ,. *Physics in Medicine and Biology*, *63* (22) doi: 10.1088/1361-6560/aae659.

57. Bortfeld, T.; Chan, T. C. Y.; Trofimov, A.; Tsitsiklis, J. N., (2008) 'Robust Management of Motion Uncertainty in Intensity-Modulated Radiation Therapy' ,. *Operations Research*, *56* (6), pp. 1461–1473 doi: 10.1287/opre.1070.0484.

58. Heath, E.; Unkelbach, J.; Oelfke, U., (2009) 'Incorporating Uncertainties in Respiratory Motion into 4D Treatment Plan Optimization' ,. *Medical Physics*, *36* (7), pp. 3059–3071 doi: 10.1118/1.3148582.

59. Fredriksson, A.; Forsgren, A.; Hårdemark, B., (2011) 'Minimax Optimization for Handling Range and Setup Uncertainties in Proton Therapy' ,. *Medical Physics*, *38* (3), pp. 1672–1684 doi: 10.1118/1.3556559.

60. Goitein, M., (1985) 'Calculation of Dose Uncertianity in Radiation Therapy' ,. *Medical Physics*, *12* (5), pp. 608–612.

61. Lowe, M.; Albertini, F.; Aitkenhead, A.; Lomax, A. J.; Mackay, R. I., (2016) 'Incorporating the Effect of Fractionation in the Evaluation of Proton Plan Robustness to Setup Errors' ,. *Physics in Medicine and Biology*, *61* (1), pp. 413–429 doi: 10.1088/0031-9155/61/1/413.

62. Unkelbach, J.; Chan, T. C. Y.; Bortfeld, T., (2007) 'Accounting for Range Uncertainties in the Optimization of Intensity Modulated Proton Therapy' ,. *Physics in Medicine and Biology*, *52* (10) doi: 10.1088/0031-9155/52/10/009.

63. Fredriksson, A.; Bokrantz, R., (2016) 'The Scenario-Based Generalization of Radiation Therapy Margins' ,. *Physics in Medicine and Biology*, *61* (5), pp. 2067–2082 doi: 10.1088/0031-9155/61/5/2067.

64. Bokrantz, R.; Fredriksson, A., (2017) 'Scenario-Based Radiation Therapy Margins for Patient Setup, Organ Motion, and Particle Range Uncertainty' ,. *Physics in Medicine and Biology*, *62* (4), pp. 1342–1357 doi: 10.1088/1361-6560/aa524d.

65. Gu, W.; Ruan, D.; O'Connor, D.; Zou, W.; Dong, L.; Tsai, M. Y.; Jia, X.; Sheng, K., (2019) 'Robust Optimization for Intensity-Modulated Proton Therapy with Soft Spot Sensitivity Regularization' ,. *Medical Physics*, *46* (3), pp. 1408–1425 doi: 10.1002/mp.13344.

66. Liu, W.; Zhang, X.; Li, Y.; Mohan, R., (2012) 'Robust Optimization of Intensity Modulated Proton Therapy' ,. *Medical Physics*, *39* (2), pp. 1079–1091 doi: 10.1118/1.3679340.

67. Li, H.; Zhang, X.; Park, P.; Liu, W.; Chang, J.; Liao, Z.; Frank, S.; Li, Y.; Poenisch, F.; Mohan, R.; Gillin, M.; Zhu, R., (2015) 'Robust Optimization in Intensity-Modulated Proton Therapy to Account for Anatomy Changes in Lung Cancer Patients' ,. *Radiotherapy and Oncology*, *114* (3), pp. 367–372 doi: 10.1016/j.radonc.2015.01.017.

68. Ge, S.; Wang, X.; Liao, Z.; Zhang, L.; Sahoo, N.; Yang, J.; Guan, F.; Mohan, R., (2019) 'Potential for Improvements in Robustness and Optimality of Intensity-Modulated Proton Therapy for Lung Cancer with 4-Dimensional Robust Optimization' ,. *Cancers*, *11* (1) doi: 10.3390/cancers11010035.

69. Mahmoudzadeh, H.; Lee, J.; Chan, T. C. Y.; Purdie, T. G., (2015) 'Robust Optimization Methods for Cardiac Sparing in Tangential Breast IMRT' ,. *Medical Physics*, *42* (5), pp. 2212–2222 doi: 10.1118/1.4916092.

70. Nguyen, D.; Corbet, C.; Largeron, G.; Josserand-Pietri, F.; Yossi, S.; Khodri, M., (2018) 'EP-1896: Is Robust Optimization Better than Virtual Bolus Method to Achieve Skin Flash in Breast VMAT Plans?' ,. *Radiotherapy and Oncology*, *127*, pp. S1027 doi: 10.1016/s0167-8140(18)32205-9.

71. Chu, M.; Zinchenko, Y.; Henderson, S. G.; Sharpe, M. B., (2005) 'Robust Optimization for Intensity Modulated Radiation Therapy Treatment Planning under Uncertainty' ,. *Physics in Medicine and Biology*, *50* (23), pp. 5463–5477 doi: 10.1088/0031-9155/50/23/003.

72. Baum, C.; Alber, M.; Birkner, M.; Nüsslin, F., (2006) 'Robust Treatment Planning for Intensity Modulated Radiotherapy of Prostate Cancer Based on Coverage Probabilities' ,. *Radiotherapy and Oncology*, *78* (1), pp. 27–35 doi: 10.1016/j.radonc.2005.09.005.

73. Bohoslavsky, R.; Witte, M. G.; Janssen, T. M.; Van Herk, M., (2013) 'Probabilistic Objective Functions for Margin-Less IMRT Planning' ,. *Physics in Medicine and Biology*, *58* (11), pp. 3563–3580 doi: 10.1088/0031-9155/58/11/3563.

74. Miura, H.; Ozawa, S.; Nagata, Y., (2017) 'Efficacy of Robust Optimization Plan with Partial-Arc VMAT for Photon Volumetric-Modulated Arc Therapy: A Phantom Study' ,. *Journal of Applied Clinical Medical Physics*, *18* (5), pp. 97–103 doi: 10.1002/acm2.12131.

75. Fontanarosa, D.; Van Der Laan, H. P.; Witte, M.; Shakirin, G.; Roelofs, E.; Langendijk, J. A.; Lambin, P.; Van Herk, M., (2013) 'An in Silico Comparison between Margin-Based and Probabilistic Target-Planning Approaches in Head and Neck Cancer Patients' ,. *Radiotherapy and Oncology*, *109* (3), pp. 430–436 doi: 10.1016/j.radonc.2013.07.012.

76. 'NCT03552965: Margin-Based Vs. Robust Photon Radiotherapy Planning in IMRT of HN-SQCC' ,. doi: Available from https://clinicaltrials.gov/ct2/show/NCT03552965NCT03552965.

77. Zhang, T.; Jeraj, R.; Keller, H.; Lu, W.; Olivera, G. H.; McNutt, T. R.; Mackie, T. R.; Paliwal, B., (2004) 'Treatment Plan Optimization Incorporating Respiratory Motion' ,. *Medical Physics*, *31* (6), pp. 1576–1586 doi: 10.1118/1.1739672.

78. Trofimov, A.; Rietzel, E.; Lu, H. M.; Martin, B.; Jiang, S.; Chen, G. T. Y.; Bortfeld, T., (2005) 'Temporo-Spatial IMRT Optimization: Concepts, Implementation and Initial Results' ,. *Physics in Medicine and Biology*, *50* (12), pp. 2779–2798 doi: 10.1088/0031-9155/50/12/004.

79. Chan, T. C. Y.; Bortfeld, T.; Tsitsiklis, J. N., (2006) 'A Robust Approach to IMRT Optimization' ,. *Physics in Medicine and Biology*, *51* (10), pp. 2567–2583 doi: 10.1088/0031-9155/51/10/014.

80. Vrancic, C.; Trofimov, A.; Chan, T.; Sharp, G.; Bortfeld, T., (2007) 'Experimental Evaluation of a Robust Optimization Method for IMRT of Moving Targets' ,. *Medical Physics*, *34* (6), pp. 2453.

81. Fayad, H.; Pan, T.; Franois Clement, J.; Visvikis, D., (2011) 'Technical Note: Correlation of Respiratory Motion between External Patient Surface and Internal Anatomical Landmarks' ,. *Medical Physics*, *38* (6), pp. 3157–3164 doi: 10.1118/1.3589131.

82. Bortfeld, T.; Jokivarsi, K.; Goitein, M.; Kung, J.; Jiang, S. B., (2002) 'Effects of Intra-Fraction Motion on IMRT Dose Delivery: Statistical Analysis and Simulation' ,. *Physics in Medicine and Biology*, *47* (13), pp. 2203–2220 doi: 10.1088/0031-9155/47/13/302.

83. Nohadani, O.; Seco, J.; Bortfeld, T., (2010) 'Motion Management with Phase-Adapted 4D-Optimization' ,. *Physics in Medicine and Biology*, *55* (17), pp. 5189–5202 doi: 10.1088/0031-9155/55/17/019.

84. Zhang, X.; Rong, Y.; Morrill, S.; Fang, J.; Narayanasamy, G.; Galhardo, E.; Maraboyina, S.; Croft, C.; xia, F.; Penagaricano, J., (2018) 'Robust Optimization in Lung Treatment Plans Accounting for Geometric Uncertainty' ,. *Journal of Applied Clinical Medical Physics*, *19* (3), pp. 19–26 doi: 10.1002/acm2.12291.

85. Timmerman, R. D.; Hu, C.; Michalski, J.; Straube, W.; Galvin, J.; Johnstone, D.; Bradley, J.; Barriger, R.; Bezjak, A.; Videtic, G. M.; Nedzi, L.; Werner-Wasik, M.; Chen, Y.; Komaki, R. U.; Choy, H., (2014) 'Long-Term Results of RTOG 0236: A Phase II Trial of Stereotactic Body Radiation Therapy (SBRT) in the Treatment of Patients with Medically Inoperable Stage I Non-Small Cell Lung Cancer' ,. *International Journal of Radiation Oncology*Biology*Physics*, *90* (1), pp. S30 doi: 10.1016/j.ijrobp.2014.05.135.

86. Videtic, G. M. M.; Hu, C.; Singh, A. K.; Chang, J. Y.; Parker, W.; Olivier, K. R.; Schild, S. E.; Komaki, R.; Urbanic, J. J.; Choy, H., (2015) 'A Randomized Phase 2 Study Comparing 2 Stereotactic Body Radiation Therapy Schedules for Medically Inoperable Patients with Stage i Peripheral Non-Small Cell Lung Cancer: NRG Oncology RTOG 0915 (NCCTG N0927)' ,. *International Journal of Radiation Oncology Biology Physics*, *93* (4), pp. 757–764 doi: 10.1016/j.ijrobp.2015.07.2260.

87. Liu, H. H.; Balter, P.; Tutt, T.; Choi, B.; Zhang, J.; Wang, C.; Chi, M.; Luo, D.; Pan, T.; Hunjan, S.; Starkschall, G.; Rosen, I.; Prado, K.; Liao, Z.; Chang, J.; Komaki, R.; Cox, J. D.; Mohan, R.; Dong, L., (2007) 'Assessing Respiration-Induced Tumor Motion and Internal Target Volume Using Four-Dimensional Computed Tomography for Radiotherapy of Lung Cancer' ,. *International Journal of Radiation Oncology Biology Physics*, *68* (2), pp. 531–540 doi: 10.1016/j.ijrobp.2006.12.066.

88. McGowan, S. E.; Albertini, F.; Thomas, S. J.; Lomax, A. J., (2015) 'Defining Robustness Protocols: A Method to Include and Evaluate Robustness in Clinical Plans' ,. *Physics in Medicine and Biology*, *60* (7), pp. 2671–2684 doi: 10.1088/0031-9155/60/7/2671.

89. Liang, X.; Zheng, D.; Mamalui-hunter, M.; Flampouri, S.; Hoppe, B. S.; Mendenhall, N., (2019) 'ITV-Based Robust Optimization for VMAT Planning of Stereotactic Body Radiation Therapy of Lung Cancer' ,. *Practical Radiation Oncology*, *9* (1), pp. 38–48 doi: 10.1016/j.prro.2018.08.005.

90. Liu, G.; Hu, F.; Ding, X.; Li, X.; Shao, Q.; Wang, Y.; Yang, J.; Quan, H., (2019) 'Simulation of Dosimetry Impact of 4DCT Uncertainty in 4D Dose Calculation for Lung SBRT' ,. *Radiation Oncology*, *14* (1), pp. 1–12 doi: 10.1186/s13014-018-1191-y.

91. Leung, R. W. K.; Chan, M. K. H.; Chiang, C.; Wong, M.; Blanck, O., (2020) 'On the Pitfalls of PTV in Lung SBRT Using Type-B Dose Engine : An Analysis of PTV and Worst Case Scenario Concepts for Treatment Plan Optimization' ,. pp. 1–16.

92. Fusella, M.; Loi, G.; Oronzio, M.; Puricelli, F.; Secco, C., (2016) 'Robust VMAT Optimization in Lung SBRT with a Commercial System' ,. *Physica Medica*, *32* (2016), pp. 24 doi: 10.1016/j.ejmp.2016.01.085.

93. Ruben, J. D.; Seeley, A.; Panettieri, V.; Ackerly, T., (2016) 'Variation in Lung Tumour Breathing Motion between Planning Four-Dimensional Computed Tomography and Stereotactic Ablative Radiotherapy Delivery and Its Dosimetric Implications: Any Role for Four-Dimensional Set-up Verification?' ,. *Clinical Oncology*, *28* (1), pp. 21–27 doi: 10.1016/j.clon.2015.08.010.

94. Kang, K. H.; Okoye, C. C.; Patel, R. B.; Siva, S.; Biswas, T.; Ellis, R. J.; Yao, M.; Machtay, M.; Lo, S. S., (2015) 'Complications from Stereotactic Body Radiotherapy for Lung Cancer' ,. *Cancers*, *7* (2), pp. 981–1004 doi: 10.3390/cancers7020820.

95. Kong, F. M.; Ten Haken, R. K.; Schipper, M. J.; Sullivan, M. A.; Chen, M.; Lopez, C.; Kalemkerian, G. P.; Hayman, J. A., (2005) 'High-Dose Radiation Improved Local Tumor Control and Overall Survival in Patients with Inoperable/Unresectable Non-Small-Cell Lung Cancer: Long-Term Results of a Radiation Dose Escalation Study' ,. *International Journal of Radiation Oncology Biology Physics*, *63* (2), pp. 324–333 doi: 10.1016/j.ijrobp.2005.02.010.

96. Belderbos, J. S. A.; Heemsbergen, W. D.; De Jaeger, K.; Baas, P.; Lebesque, J. V., (2006) 'Final Results of a Phase I/II Dose Escalation Trial in Non-Small-Cell Lung Cancer Using Three-Dimensional Conformal Radiotherapy' ,. *International Journal of Radiation Oncology Biology Physics*, *66* (1), pp. 126–134 doi: 10.1016/j.ijrobp.2006.04.034.

97. Brower, J. V.; Amini, A.; Chen, S.; Hullett, C. R.; Kimple, R. J.; Wojcieszynski, A. P.; Bassetti, M.; Witek, M. E.; Yu, M.; Harari, P. M.; Baschnagel, A. M., (2016) 'Improved Survival with Dose-Escalated Radiotherapy in Stage III Non-Small-Cell Lung Cancer: Analysis of the National Cancer Database' ,. *Annals of Oncology*, *27* (10), pp. 1887–1894 doi: 10.1093/annonc/mdw276.

98. Guckenberger, M.; Baier, K.; Polat, B.; Richter, A.; Krieger, T.; Wilbert, J.; Mueller, G.; Flentje, M., (2010) 'Dose-Response Relationship for Radiation-Induced Pneumonitis after Pulmonary Stereotactic Body Radiotherapy' ,. *Radiotherapy and Oncology*, *97* (1), pp. 65–70 doi: 10.1016/j.radonc.2010.04.027.

99. Sweeney, R. A.; Seubert, B.; Stark, S.; Homann, V.; Müller, G.; Flentje, M.; Guckenberger, M., (2012) 'Accuracy and Inter-Observer Variability of 3D versus 4D Cone-Beam CT Based Image-Guidance in SBRT for Lung Tumors' ,. *Radiation Oncology*, *7* (1), pp. 1–8 doi: 10.1186/1748-717X-7-81.

100. Sonke, J. J.; Zijp, L.; Remeijer, P.; Van Herk, M., (2005) 'Respiratory Correlated Cone Beam CT' ,. *Medical Physics*, *32* (4), pp. 1176–1186 doi: 10.1118/1.1869074.

101. Thengumpallil, S.; Smith, K.; Monnin, P.; Bourhis, J.; Bochud, F.; Moeckli, R., (2016) 'Difference in Performance between 3D and 4D CBCT for Lung Imaging: A Dose and Image Quality Analysis' ,. *Journal of Applied Clinical Medical Physics*, *17* (6), pp. 97–106 doi: 10.1120/jacmp.v17i6.6459.

102. Tan, Z.; Liu, C.; Zhou, Y.; Shen, W., (2017) 'Preliminary Comparison of the Registration Effect of 4D-CBCT and 3D-CBCT in Image-Guided Radiotherapy of Stage IA Non-Small-Cell Lung Cancer' ,. *Journal of Radiation Research*, *58* (6), pp. 854–861 doi: 10.1093/jrr/rrx040.

103. Lu, J.; Guerrero, T. M.; Munro, P.; Jeung, A.; Chi, P. C. M.; Balter, P.; Zhu, X. R.; Mohan, R.; Pan, T., (2007) 'Four-Dimensional Cone Beam CT with Adaptive Gantry Rotation and Adaptive Data Sampling' ,. *Medical Physics*, *34* (9), pp. 3520–3529 doi: 10.1118/1.2767145.

104. Nakagawa, K.; Haga, A.; Kida, S.; Masutani, Y.; Yamashita, H.; Takahashi, W.;

Sakumi, A.; Saotome, N.; Shiraki, T.; Ohtomo, K.; Iwai, Y.; Yoda, K., (2013) '4D Registration and 4D Verification of Lung Tumor Position for Stereotactic Volumetric Modulated Arc Therapy Using Respiratory-Correlated Cone-Beam CT' ,. *Journal of Radiation Research*, *54* (1), pp. 152–156 doi: 10.1093/jrr/rrs058.

105. Pearson, J.; Doherty, K., (2020) 'National Cancer Waiting Times Monitoring Dataset Guidance' ,. No. September.

106. Vaassen, F.; Hazelaar, C.; Vaniqui, A.; Gooding, M.; van der Heyden, B.; Canters, R.; van Elmpt, W., (2020) 'Evaluation of Measures for Assessing Time-Saving of Automatic Organ-at-Risk Segmentation in Radiotherapy' ,. *Physics and Imaging in Radiation Oncology*, *13* (November 2019), pp. 1–6 doi: 10.1016/j.phro.2019.12.001.

107. Gooding, M.; Smith, A.; Peressutti, D.; Aljabar, P.; Evans, E.; Gwynne, S.; Hammer, C.; Meijer, H. J. M.; Speight, R.; Welgemoed, C.; Lustberg, T.; Van Soest, J.; Dekker, A.; Van Elmpt, W., (2018) 'PV-0531: Multi-Centre Evaluation of Atlas-Based and Deep Learning Contouring Using a Modified Turing Test' ,. *Radiotherapy and Oncology*, *127*, pp. S282–S283 doi: 10.1016/s0167-8140(18)30841-7.

108. Lo, A. C.; Liu, M.; Chan, E.; Lund, C.; Truong, P. T.; Loewen, S.; Cao, J.; Schellenberg, D.; Carolan, H.; Berrang, T.; Wu, J.; Berthelet, E.; Olson, R., (2014) 'The Impact of Peer Review of Volume Delineation in Stereotactic Body Radiation Therapy Planning for Primary Lung Cancer: A Multicenter Quality Assurance Study' ,. *Journal of Thoracic Oncology*, *9* (4), pp. 527–533 doi: 10.1097/JTO.0000000000000119.

109. Wang, J.; Zhang, T.; Chen, X.; Xia, W.; Miao, J.; Zhou, Z.; Dai, J.; Bi, N., (2019) 'Deep-Learning Based Automatic Delineation Improves CTV Contouring Quality and Efficiency for Pathological N2 (PN2) Non-Small Cell Lung Cancer (NSCLC) Receiving Post-Operation Radiation Therapy' ,. *International Journal of Radiation Oncology*Biology*Physics*, *105* (1), pp. S46 doi: 10.1016/j.ijrobp.2019.06.473.

110. Cui, Y.; Arimura, H.; Nakano, R.; Yoshitake, T.; Shioyama, Y.; Yabuuchi, H., (2021) 'Automated Approach for Segmenting Gross Tumor Volumes for Lung Cancer Stereotactic Body Radiation Therapy Using CT-Based Dense V-Networks' ,. *Journal of radiation research*, *62* (2), pp. 346–355 doi: 10.1093/jrr/rraa132.

111. Peulen, H.; Belderbos, J.; Guckenberger, M.; Hope, A.; Grills, I.; Herk, M. Van; Sonke, J., (2015) 'Target Delineation Variability and Corresponding Margins of Peripheral Early Stage NSCLC Treated with Stereotactic Body Radiotherapy' ,. *Radiotherapy and Oncology*, *114* (3), pp. 361–366 doi: 10.1016/j.radonc.2015.02.011.

112. Zijp, L.; Sonke, J.-J.; van Herk, M., (2004) 'Extraction of the Respiratory Signal from Sequential Thorax Cone-Beam X-Ray Images' ,. *International Conference on the Use of Computers in Radiation Therapy*, pp. 507–509.

113. Vedam, S. S.; Keall, P. J.; Kini, V. R.; Mostafavi, H.; Shukla, H. P.; Mohan, R., (2003) 'Acquiring a Four-Dimensional Computed Tomography Dataset Using an External Respiratory Signal' ,. *Physics in Medicine and Biology*, *48* (1), pp. 45–62 doi: 10.1088/0031-9155/48/1/304.

114. Yan, H.; Wang, X.; Yin, W.; Pan, T.; Ahmad, M.; Mou, X.; Cerviño, L.; Jia, X.; Jiang, S. B., (2013) 'Extracting Respiratory Signals from Thoracic Cone Beam CT Projections.' ,. *Physics in medicine and biology*, *58* (5), pp. 1447–1464 doi: 10.1088/0031-9155/58/5/1447.

115. Vergalasova, I.; Maurer, J.; Yin, F. F., (2011) 'Potential Underestimation of the Internal Target Volume (ITV) from Free-Breathing CBCT' ,. *Medical Physics*, *38* (8), pp. 4689–4699 doi: 10.1118/1.3613153.

116. Tsang, Y.; Hoskin, P.; Spezi, E.; Landau, D.; Lester, J.; Miles, E.; Conibear, J., (2019) 'Assessment of Contour Variability in Target Volumes and Organs at Risk in Lung Cancer Radiotherapy' ,. *Technical Innovations and Patient Support in Radiation Oncology*, *10*, pp. 8–12 doi: 10.1016/j.tipsro.2019.05.001.

117. Louie, A. V.; Rodrigues, G.; Olsthoorn, J.; Palma, D.; Yu, E.; Yaremko, B.; Ahmad, B.; Aivas, I.; Gaede, S., (2010) 'Inter-Observer and Intra-Observer Reliability for Lung Cancer Target Volume Delineation in the 4D-CT Era' ,. *Radiotherapy and Oncology*, *95* (2), pp. 166–171 doi: 10.1016/j.radonc.2009.12.028.

16 Appendices

16.1 Appendix – List of AMBS A units and Medical Physics B units together with assignments

AMBS – A Units

Unit title	Credits	Assignment wordcount
A1: Professionalism and professional development in the healthcare environment	30	Practice paper – 2000 words A1 – assignment 1 – 1500 words A1 – assignment 2 – 4000 words
A2: Theoretical foundations of leadership	20	A2 – assignment 1 – 3000 words A2 – assignment 2 – 3000 words
A3: Personal and professional development to enhance performance	30	A3 – assignment 1 – 1500 words A3 – assignment 2 – 4000 words
A4: Leadership and quality improvement in the clinical and scientific environment	20	A4 – assignment 1 – 3000 words A4 – assignment 2 – 3000 words
A5: Research and innovation in health and social care	20	A5 – assignment 1 – 3000 words A5 – assignment 2 – 3000 words

Medical Physics – B Units

B1: Medical Equipment Management	10	2000 word assignment
B2: Clinical and Scientific Computing	10	2000 word assignment
B3: Dosimetry	10	Group presentation 1500 word assignment
B4: Optimisation in Radiotherapy and Imaging	10	Group presentation 1500 word assignment
B6: Medical statistics in medical physics	10	3000 word assignment
B8: Health technology assessment	10	3000 word assignment
B9: Clinical applications of medical imaging technologies in radiotherapy physics	20	Group presentation 2000 word assignment
B10a: Advanced Radiobiology	10	Virtual experiment + 1500 word report
B10c: Novel and Specialised External Beam Radiotherapy	10	1500 word report/piece of evidence for portfolio
B10d: Advanced Brachytherapy	10	1500 word report/piece of evidence for portfolio

Generic B Units

B5: Contemporary issues in healthcare science	20	1500 word assignment + creative project

B7: Teaching Learning Assessment	20	20 minute group presentation
Section C		
C1: Innovation Project	70	4000-5000 word Literature Review Lay Presentation